Differentiation of asteroids in the early solar system from Hf-W systematics

Inauguraldissertation

zur Erlangung des Doktorgrades

der Naturwissenschaften im Fachbereich Geowissenschaften

der Mathematisch-Naturwissenschaftlichen Fakultät

der Albertus-Magnus Universität Köln

vorgelegt von

Toni Schulz

aus Dinslaken

- Köln 2008 -

Prüfer: Prof. H. Palme

Zweiter Referent: Prof. C. Münker

Vorsitzender der Prüfungskomission: Prof. L. Bohatý

Beisitzer: Dr. G. Witt-Eickschen

Tag der mündlichen Prüfung: 23.06.2008

Abstract

The first major differentiation in primitive planetesimals is the formation of metal- or metal-sulfide cores. To constrain the time of asteroidal differentiation, meteoritic metals and silicates coexisting with metals were analyzed for W-isotopes and Hf and W concentrations. The study focused on silicate inclusions in non-magmatic IAB iron meteorites and the corresponding metal phases as well as on winonaites and acapulcoites were analyzed.

IAB iron meteorites formed by crystallization of metal ponds under low pressure conditions at or near the surface of their asteroidal parent body. The presence of abundant silicate inclusions reflects either incomplete metal-silicate separation or mixing of metal and silicates by impacts. Hafnium-W measurements were performed on magnetic and non-magnetic separates from seven IAB iron meteorites to constrain the exact timing of metal separation, silicate differentiation and metamorphism. IAB metals have a deficit in ^{182}W of -3.1 ± 0.2 ε-units (relative to terrestrial standard materials). The silicate fractions in IAB iron meteorites have εW values ranging from -3 to +35, indicating that the exchange of W between metals and silicates ceased within the lifetime of ^{182}Hf. Based on a combined IAB silicate isochron defined by three different bulk inclusions, silicate differentiation in the mantle-like reservoir of the IAB parent body must have occurred 2.9 ± 2.2 Myr after the formation of Ca,Al-rich inclusions (CAIs), the oldest objects known from the solar nebula. This event therefore occurred contemporaneously with the main metal segregation event on the IAB parent body at 3.5 ± 2.3 Myr after CAI formation, which is obtained from the W isotope composition of the metal phase (assuming evolution in a chondritic Hf/W ratio before metal separation). Hence, metal segregation and silicate differentiation occurred early enough, so that ^{26}Al was responsible for

parent body heating causing differentiation. On the other hand, internal isochrones for silicates of the two IAB-iron meteorites El Taco and Lueders yield ages 11.3 ± 2.3 Myr and ~12 Myr after CAI formation, reflecting impact induced heating and redistribution of radiogenic W. Additional later metal-silicate equilibration on the IAB parent body is also found in Mundrabilla (-2.6 ± 0.5 ε-units). Therefore, a prolonged epoch of most likely impact-controlled W re-equilibration on the IAB parent body can be inferred. In contrast to the combined IAB silicate isochron, most of the analyzed Winonaites define a combined isochron with an age that postdates CAI formation by 14.5 ± 2.8 Myr. This age is apparently too young for heating and melting of the parent body by an internal heat-source and indistinguishable within uncertainty from the internal El Taco and Lueders isochrones. Assuming a common origin for IABs and winonaites these ages could be related to a single impact-controlled W re-equilibration on the Winonaite/IAB parent body. A combined isochron defined by different Acapulcoite separates yields an age of 4.6 ± 1.3 Myr after CAI formation. This is within the range of Hf-W ages of ordinary chondrites, although Acapulcoites were heated to significantly higher temperatures than ordinary chondrites, implying a higher level of ^{26}Al. Other chronometers indicate fast cooling of acapulcoites, which is difficult to reconcile with similar cooling rates as those of ordinary chondrites.

A comparison with Hf-W literature data shows that asteroidal differentiation on the IAB parent body occurred after the segregation of most magmatic iron meteorites and contemporaneously with the accretion of chondrite parent bodies, lending further support for a revised solar system chronology where chondrites cannot be the precursor of most differentiated asteroids. Chondritic meteorites with higher equilibration temperatures, such as winonaites and acapulcoites have even younger ages. They are certainly no precursor

material for iron meteorites and their comparatively younger ages probably reflect an impact origin after accretion of chondrite parent bodies.

Zusammenfassung

Das erste Hauptdifferntiationsereignis in primitiven Planetesimalen ist die Bildung eines Metall- oder Metall/Sulfid-kerns. Um die Zeit für asteroidale Differentiation herauszubekommen, wurden meteoritische Metalle und Silikate die mit diesen Metallen koexistieren im Hinblick auf die W Isotopie und die Konzentrationen von Hf und W untersucht. In dieser Studie wurden Metalle und Silikat-Inklusionen in nicht-magmatischen IAB Eisenmeteoriten, Winonaite und Acapulcoite untersucht.

IAB Eisenmeteorite haben sich gebildet durch Kristallisation von Metall-Schmelzen unter niedrigen Druckbedingungen an der Oberfläche ihres asteroidalen Mutterkörpers. Das Vorkommen von Silikat-Inklusionen zeugt entweder von inkompletter Metall-Silikat Separation oder von einer impaktbedingten Mischung von Metall und Silikat. Um die genaue Zeit der Metallseparation, Silikatdifferentiation und Metamorphose herauszubekommen wurden Hf-W Messungen an magnetischen und nicht-magnetischen Separaten von sieben IAB Eisenmeteoriten vorgenommen. IAB Metalle haben ein Defizit in ^{182}W von -3.1 ± 0.2 ε-Einheiten (relativ zu terr. Standardmaterial). Silikatfraktionen in IAB Eisenmeteoriten haben εW Signaturen zwischen -3 to +35. Der Austausch von W zwischen Metallen und Silikaten endete somit innerhalb der Lebenszeit von ^{182}Hf. Basierend auf einer kombinierten IAB isochrone, welche durch drei verschiedene bulk Inklusionen definiert ist, konnte ein Zeitpunkt der Silikatdifferentiation in einem mantelähnlichen Reservoir des IAB Mutterkörpers herausgefunden werden, welcher die Bildung von Ca,Al-reichen Inklusionen (CAIs) um 2.9 ± 2.2 Ma postdatiert. Die Silkatdifferenzierung ereignete sich gleichzeitig mit der Metallsegregation im IAB Mutterkörper (3.5 ± 2.3 Ma nach CAI-Bildung). Dieses Alter konnte aus der

Wolframisotopie der IAB Metalle gewonnen werden (unter der Annahme eines chondritischen Hf/W Verhältnisses im IAB Mutterkörper vor der Metallseparation). Metallsegregation und Silikatdifferentiation ereigneten sich somit früh genug um ^{26}Al als eigentliche Wärmequelle anzunehmen. Interne Isochronen für Silikate der IAB Eisenmeteorite El Taco und Lueders ergeben Alter 11.3 ± 2.3 Ma and ~12 Ma nach CAI Bildung. Diese Alter reflektieren eine impaktinduzierte Aufheizung und Umverteilung von radiogenem Wolfram. Die Wolframisotopie der Metallphase von Mundrabilla (-2.6 ± 0.5 ε-Einheiten) bezeugt eine weitere Metall-Silikat Equilibrierung im IAB Mutterkörper. Somit kann ein längerfristiges Zeitintervall von impaktkontrollierter Wolframequilibrierung abgeleitet werden.

Im Gegensatz zur kombinierten IAB Silkatisochrone liegen die meißten der analysierten Winonaitseparate auf einer Isochrone, welche ein Alter von 14.5 ± 2.8 Ma nach CAI-Bildung ergibt. Die so datierte Equilibrierung ist zu jung um durch interne Hitzequellen erklärt warden zu können. Ferner ist das so erhaltene Alter ununterscheidbar von den El Taco und Lueders isochronen. Einen gemeinsamen Ursprung von IAB Eisenmeteoriten und Winonaiten annehmend, könnten diese Alter auf ein distinktes Impaktereignis auf dem gemeinsamen IAB/Winonait Mutterkörper zurückgeführt werden.

Eine Isochrone definiert durch verschiedene Acapulcoitseparate ergibt ein Alter 4.6 ± 1.3 Ma nach CAI-Bildung. Dieses Alter ist vergleichbar mit Hf-W Altern gewöhnlicher Chondrite, obwohl Acapulcoite auf höhere Temperaturen erhitzt wurden, was einen höhere Konzentration an 26Al impliziert. Andere Chronometer zeugen von einer rapiden Abkühlung der Acapulcoite, was schlecht erklärbar ist eingedenk der ähnlichen Abkühlungsraten für gewöhnliche Chondrite.

Ein Vergleich mit allen verfügbaren Hf-W Literaturdaten zeigt, daß asteroidale Differentiation im IAB Mutterkörper nach der Segregation der meißten magmatischen Eisenmeteorite und gleichzeitig mit der Akkretion der Chondritmutterkörper stattfand. Dies unterstützt die neue Sonnensystemchronologie, welche besagt, daß Chondrite nicht das Ursprungsmaterial der meißten differenzierten Asteroiden sein kann. Chondritische Meteorite mit höheren Equilibrierungstemperaturen, wie etwa Winonaite und Acapulcoite haben noch jüngere Alter. Diese Meteoriten können somit nicht das Ursprungsmaterial der magmatischen Eisenmeteorite sein. Außerdem zeugen derart junge Alter von einer impaktbedingten Bildung nach der Akkretion chondritischer Mutterkörper.

Contents

Chapter 1

1. Introduction and research objectives

1.1 Classification of meteorites

There are two different types of meteorites. Undifferentiated meteorites are chunks of disrupted planetesimals that never reached temperatures for global melting and differentiation. Undifferentiated meteorites are also designated chondritic meteorites, as most of them contain chondrules, mm-sized once molten spherules. Chondrules are aggregates of dust particles that formed most likely in the solar nebula, before accretion of material to larger planetesimals. The source of the energy for melting of chondrules is unknown. Undifferentiated meteorites, in particular those that have not, or only slightly been heated in their parent body (minimal thermal metamorphism) provide evidence for the origin of the earliest formed matter in the solar system. The chemical composition of undifferentiated meteorites is very similar to that of the Sun, except for all elements heavier than oxygen and except rare gases. Differentiated meteorites on the other hand come from planetesimals that were more or less completely molten and thus differentiated into a metal core and a silicate mantle. Iron meteorites are differentiated meteorites, but also stony-iron meteorites, material from the boundary between core and mantle. The non-chondritic stony meteorites are collectively called achondrites. They have chemical compositions very different from that of the Sun, representing melts or residues from melt extraction, obvious from their igneous textures. Achondrites are assumed to be remnants of the silicate parts of differentiated asteroids (e.g. eucrites, ureilites). Meteorites that retain the primitive chemical signature of the chondritic precursor material but exhibit igneous or recrystallized textures are referred to as primitive achondrites (e.g. acapulcoites, winonaites). They were not heated to temperatures allowing complete melting and differentiation.

1.2   Asteroidal differentiation

One of the most fundamental processes that occurred shortly after the onset of solar system formation was the transformation of condensed nebular particles into asteroids and planets with cores, mantles and crusts. Once the parent body formed by successive stages of accretion, extensive heating of the parent body induces asteroidal differentiation. Potent heat sources that could contribute the adequate thermal energy for triggering asteroidal differentiation are provided by the decay of short-lived radionuclides like ^{26}Al or ^{60}Fe (e.g. Urey, 1955; Ghosh and McSween, 1998; Merk et al., 2002; Bizzarro et al., 2005). However, energy for heating of planetesimals could also have been delivered by impacts. Although it is unlikely that impacts caused global melting of asteroids, they may well have caused localized heating, including melting.

A major asteroidal differentiation event is the formation of a metallic core by segregation and later crystallization of (Fe-Ni)$_{metal}$-FeS melts from the bulk chondrite (Taylor et al., 1993; Hewins and Newsom, 1988; McCoy et al., 2006). The temperature where segregation of the (Fe-Ni)$_{metal}$-FeS melt occurred is still a matter of debate. Although the temperature of the Fe-FeS eutectic (980°C) is significantly below the silicate solidus (~1150°C) it is unclear if the first S-rich melt is able to separate from silicates. This depends on the viscosity of the melt and the wetting angle with silicate minerals. Also the sulfur content determines the amount of liquid with eutectic composition. Some scenarios deal with core formation prior to silicate melting (Ghosh and McSween, 1998), whereas in other cases the core formation commenced subsequent to silicate melting (Taylor 1992; Taylor et al., 1993). However, in all cases the segregated metal-core incorporates essentially the entire inventory of highly siderophile elements (e.g. Ir, Pt) and a large fraction of moderately siderophile elements (e.g. W, Co).

Constraints on the timescales involved in core formation (segregation of the $(Fe-Ni)_{metal}$-FeS melt and its crystallization) can be obtained from chronological investigations of iron meteorites. Most of them are assumed to represent remnants of asteroidal cores and formed by fractional crystallization of a slowly cooling magma (Haack and Scott, 1993; Wasson and Richardson, 2001). Any segregation of a metal melt from a silicate residue (e.g. core formation) can be dated using the extinct ^{182}Hf-^{182}W chronometer, because parent- and daughter nuclides fractionate during metal segregation (see section 1.4). The siderophile W partitions into the metal-liquid while the lithophile Hf remains in the silicates. During the last decade many research groups have applied this chronometer to a variety of iron meteorite groups and found them to have segregated within less than 5 Myr after the formation of the solar system (Masarik, 1997; Horan et al., 1998; Leya et al., 2000, 2003a,b; Kleine et al., 2002; Yin et al., 2002; Yin and Jacobsen, 2003; Quitté and Birck, 2004; Kleine et al., 2005a, 2005b; Markowski et al., 2006; Schersten et al., 2006; Qin et al., 2006). Core crystallization on the other hand can be dated using the ^{107}Pd-^{107}Ag, ^{187}Re-^{187}Os and ^{190}Pt-^{190}Os chronometers. Here all involved elements are siderophile, i.e. they enter the metallic core more or less quantitatively (Carlson et al., 2001; Sugiura et al., 2003). The necessary fractionations between parent and daughter nuclides thus occur during crystallization of the metal mass depending on partitioning between solid iron and liquid S-containing melt. Consequently, these radionuclide systems date the crystallization history of the core rather than metal segregation itself. Timescales of core crystallization determined from ^{187}Re-^{187}Os chronometry show that isotopic closure for Re-Os spanned a period of ~30 Myr for most iron meteorites, beginning with the oldest ages of ~4557 Myr for group IIIAB irons (Shen et al., 1996; Smoliar et al., 1996; Horan et al., 1998; Cook et al., 2004).

Additional steps of asteroidal differentiation involve the formation of the source reservoirs in the mantle that subsequently produced crustal materials and corresponding residues during partial melting. Whole-rock isochrones of achondritic silicate meteorites based on short-lived chronometers have the potential for precisely constraining the timing of global silicate differentiations. Such isochrones have recently been reported for the eucrite and aubrite parent bodies (Lugmair and Galer S.J.G, 1998; Quitté et al., 2000; Kleine et al., 2004; Shukolyukov and Lugmair, 2004). Global silicate differentiation on the parent body of the eucrites occurred 3-4 Myr after CAI formation (Kleine et al., 2004) and ~2 Myr earlier than mantle differentiation on the aubritic parent body (Shukolyukov and Lugmair, 2004).

Primary crystallization ages based on internal mineral isochrones from basaltic achondrites on the other hand provide the best estimates of the timescales of asteroidal crust formation. Based on the application of several extinct and extant chronometers most groups of basaltic achondrites are shown to be emplaced within the first ~3 Myr after CAI formation (e.g. Nyquist et al., 1994; Wadhwa and Lugmair, 1996). This process is likely to have continued until ~10 Myr after CAI formation based on data for non-cumulate eucrites and basaltic angrites. Figure 1.1 summarizes the timescales for asteroidal differentiation.
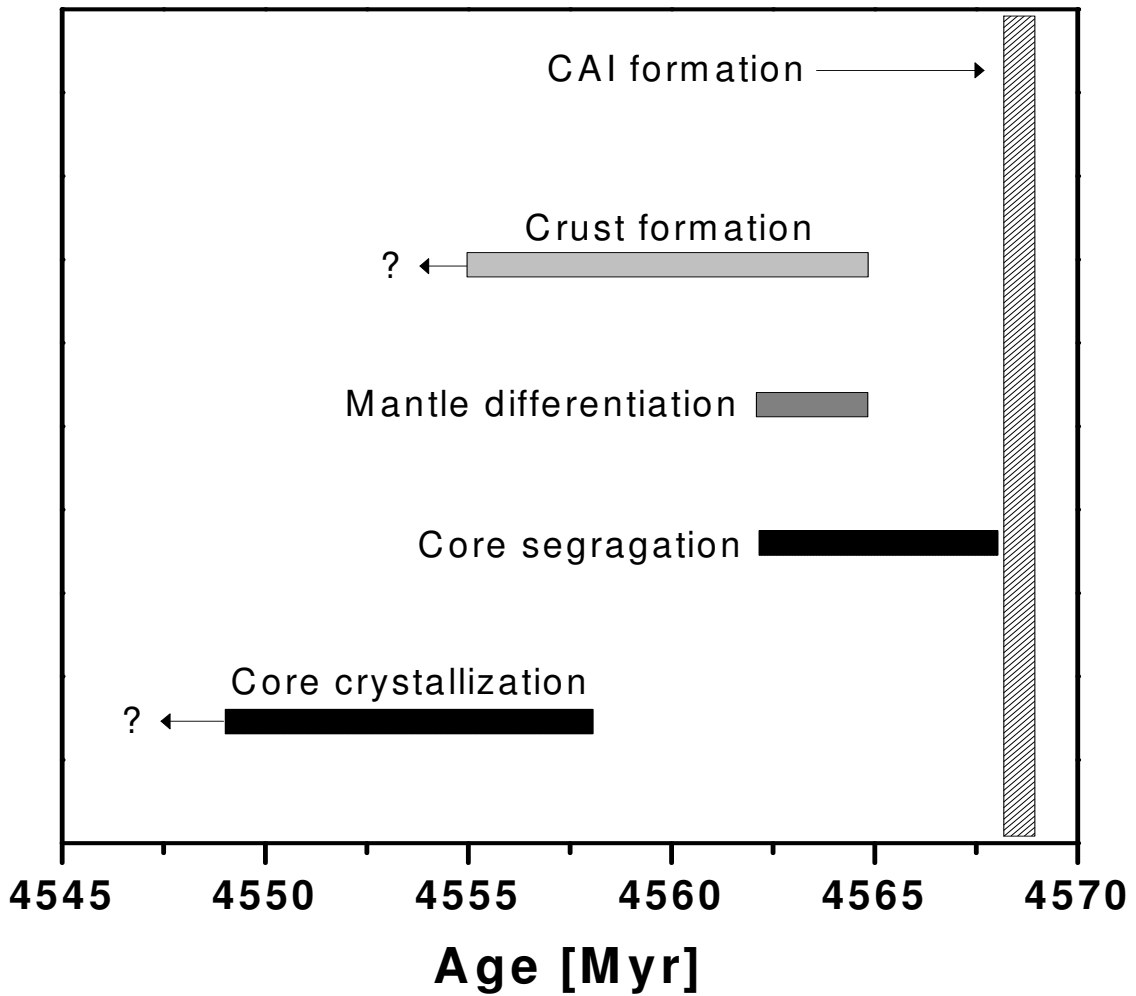
Figure 1.1: Timescales for asteroidal differentiation as inferred from extinct and extant radionuclide systems. The vertical dashed line represents the formation of CAIs, the first solids that condensed from the cooling protosolar cloud. For references see text.

1.3   Magmatic- versus Non-magmatic iron meteorites

Based on petrological and mineralogical evidence four large groups of iron meteorites can be identified. There seems to be a general agreement that three of these groups formed by fractional crystallization of a slowly cooling metal melt (Haack and Scott, 1993; Wasson and Richardson, 2001). These are magmatic iron meteorites. A fourth large group, the IAB iron meteorites were initially assumed to have originated during condensation from the solar nebular. Wasson (1972) therefore introduced the term "non-magmatic". However, this theory was later rejected because of difficulties in explaining the huge crystal sizes in the metal phase that are only insufficiently explained by condensation processes and the abundance of numerous silicate inclusions that are dispersed throughout the metal-host in a pore-free assemblage (Fig. 1.2). Instead, Wasson et al. (1980) and Choi et al. (1995) concluded that the IAB group of iron meteorites formed by the crystallization of impact generated melts. A second model for the IAB origin involves inefficient fractional crystallization of magmas (Kracher, 1982; Benedix et al., 2000) or successive extractions of partial melts from a chondritic source (Kelly and Larimer, 1977). Although, the term "non-magmatic" for this iron meteorite group is now obsolete, it is in use.
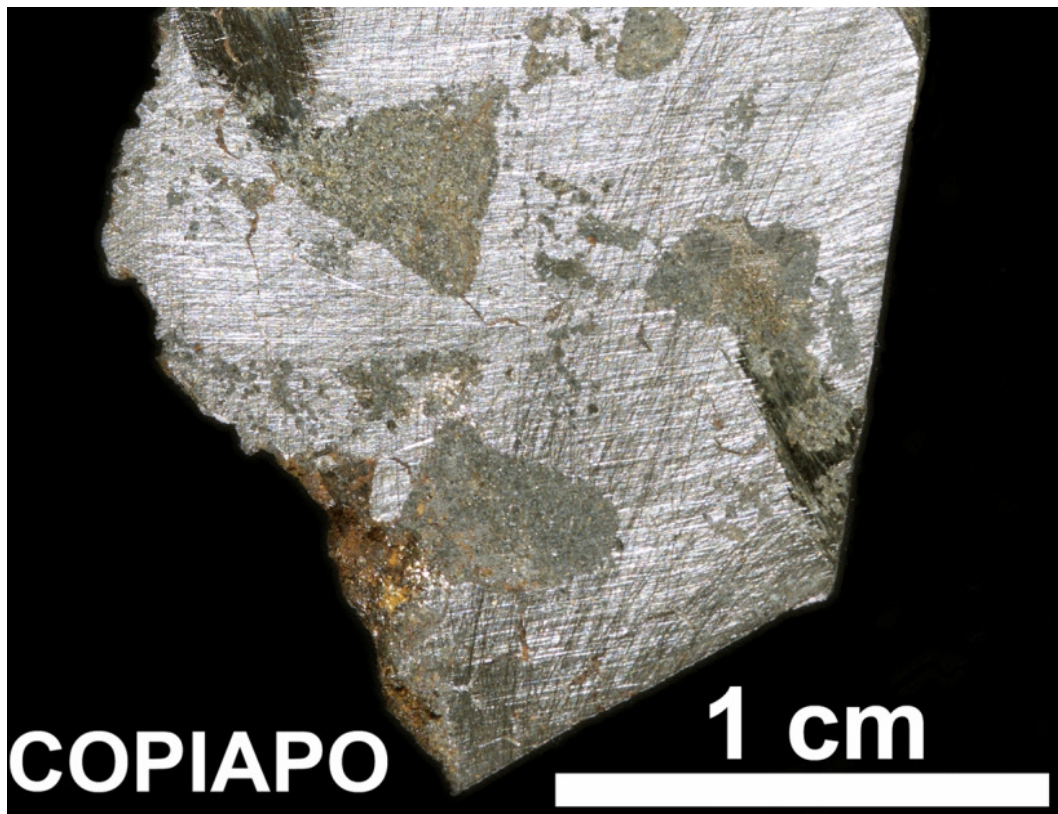
Figure 1.2: Polished slice of the Copiapo specimen of the non-magmatic IAB iron meteorite group. Silicate domains (silicate inclusions) are dispersed throughout the Fe-Ni host (matrix-metal).

1.4   The Hf-W chronometer

The Hf-W chronometer is based on the decay of ^{182}Hf into ^{182}W. The corresponding half-live of 8.9 Myr (Vockenhuber et al., 2004) is sufficiently short to resolve the timescales of asteroidal differentiation processes within the first ~50 Myr of solar system history.

Hafnium and W can be assumed to occur in chondritic proportions in undifferentiated solar system matter because both elements are refractory

(both elements condensed at nearly the same temperatures during cooling of the proto- solar cloud). During metal-silicate separation the lithophile, silicate loving Hf preferentially partitions into the silicates, whereas the siderophile, metal-loving W is enriched in the metal phase (Fig. 1.3). The extinct ^{182}Hf-^{182}W isotope system therefore provides a unique opportunity for the relative timing of metal-silicate separation (e.g. segregation of a metal core). Metals separated early in asteroids will have a relatively unradiogenic tungsten composition (low in ^{182}W), depending on the exact timing of the metal-silicate differentiation (Fig. 1.4). Tungsten is only moderately siderophile and is therefore partly retained in the mantle (Palme et al., 1981). Silicate melts produced by subsequent internal differentiation of the silicate mantle are enriched in W relative to the residue, because W- oxides are more
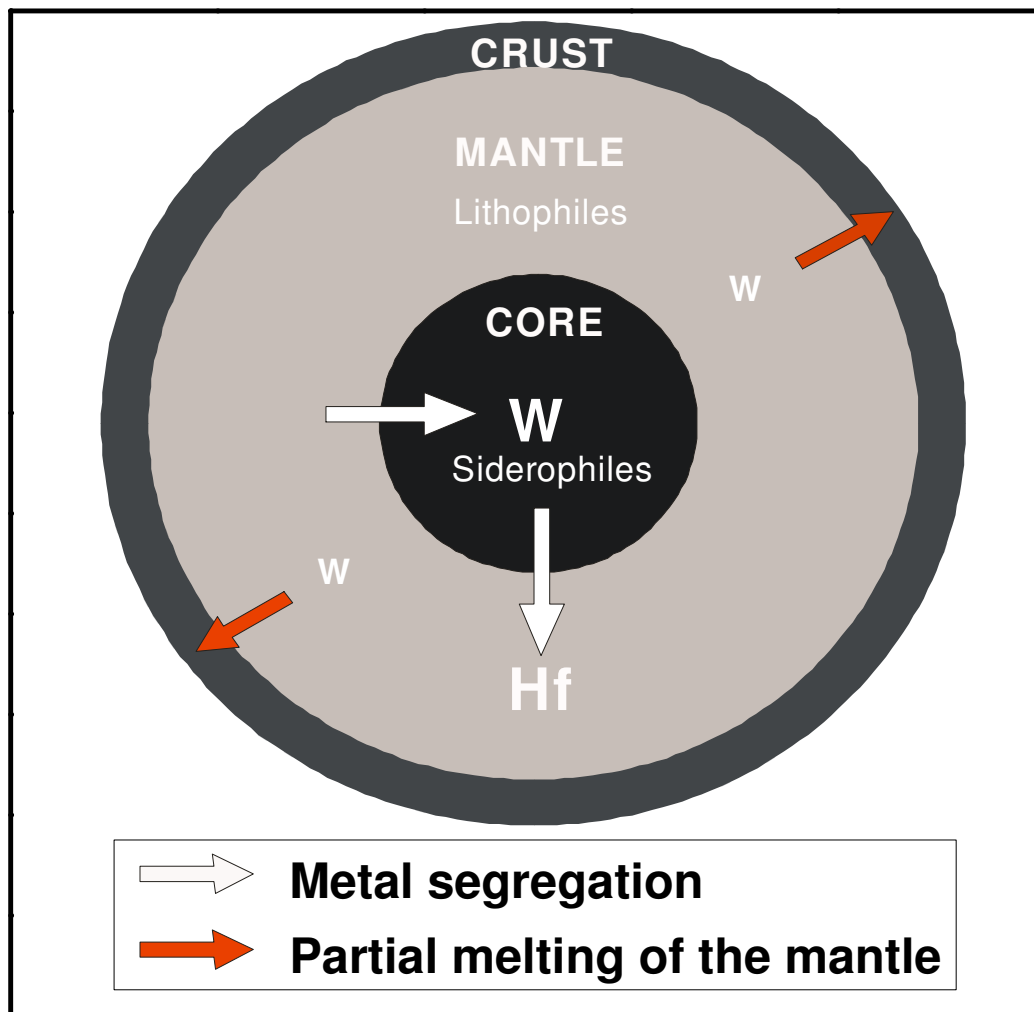
Figure 1.3: Partitioning of Hf and W under oxidizing conditions during asteroidal differentiation. Tungsten is moderately siderophile and therefore partitions strongly into the core, whereas the lithophile Hf partitions into silicates. The W remaining in the mantle (WO_2 and WO_3) will be enriched in the crust during partial mantle melting as a result of its incompatible properties. Enrichments in W in crustal rocks so obtained can even exceed the W concentration of the bulk asteroid (Palme et al., 1981).

incompatible than Hf during silicate melting. If segregation of Hf from W occurs during the parent nuclides life-time, the differentiated materials will have a time dependent excess or deficit in their ^{182}W abundances.
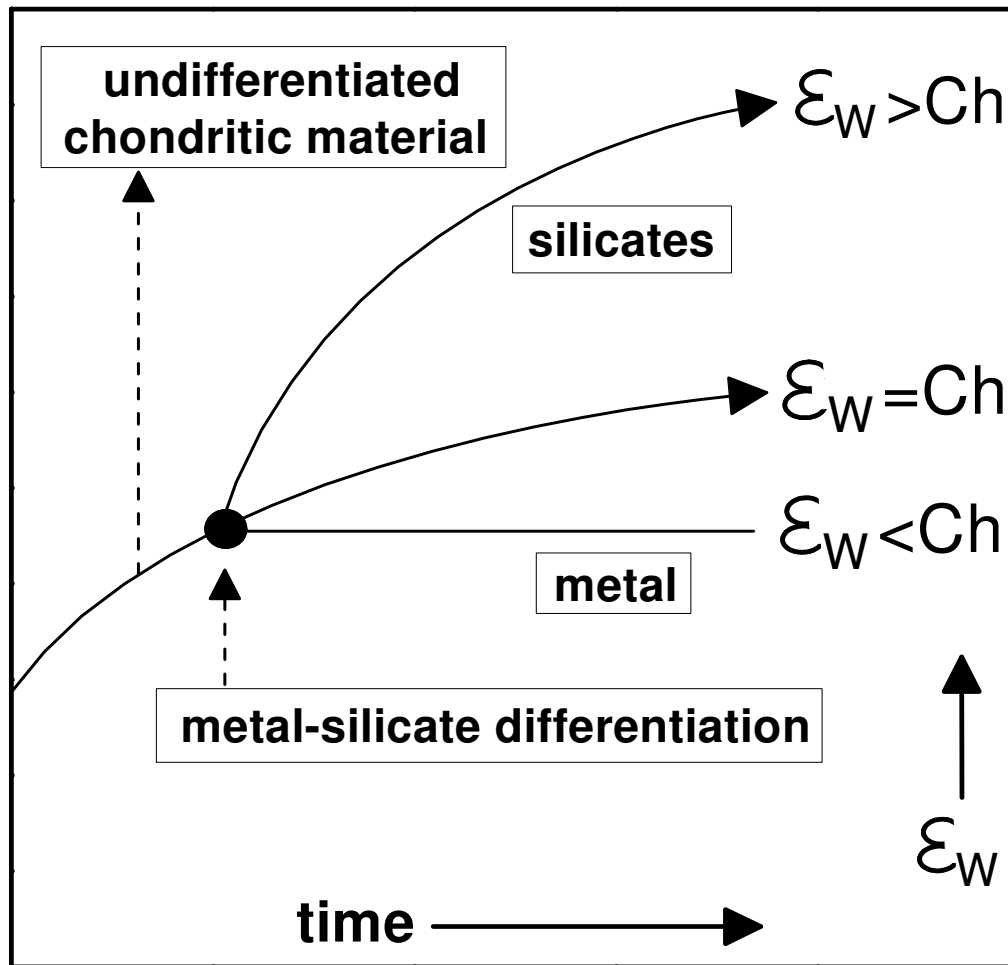
Figure 1.4: Radiogenic ingrowth of ^{182}W during asteroidal differentiation. Metals that segregate from a chondritic precursor during the lifetime of ^{182}Hf (approximately the first 30 Myr of solar system history) have a time-dependent ^{182}W depletion relative to chondrites. In contrast, silicates evolve to highly radiogenic W isotope compositions depending on the time of the metal-silicate separation event. The Epsilon notation is defined as the deviation of the ^{182}W/^{184}W ratio in a specific reservoir relative to a terrestrial standard (εW = 0) in parts per 10.000. Ch = chondritic.

The advantage of this chronometer therefore is that it can be applied to define the time of metal separation by determining the W isotope composition of metal and to silicate differentiation by constructing internal isochrones (Fig. 1.5).

Hf/W

Figure 1.5: ^{182}Hf-^{182}W isochron diagram, showing two reservoirs (Res.1 + Res.2) with different Hf/W ratios and a single initial tungsten isotope composition. During the parent nuclides lifetime the two reservoirs evolve to different radiogenic tungsten compositions. After
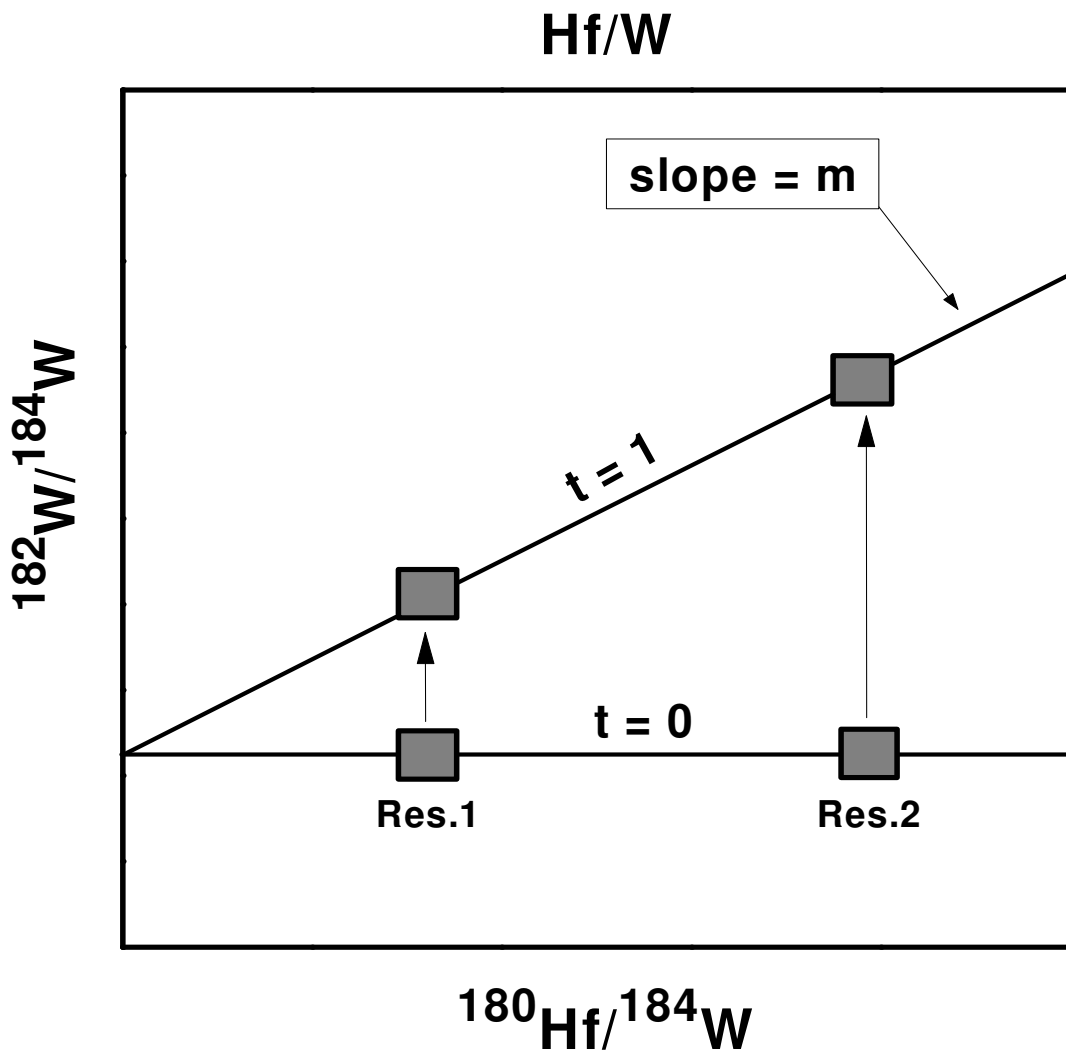
the complete decay of ^{182}Hf these reservoirs define an isochron with the slope m (m =

$$\left(\frac{^{182}W}{^{184}W}\right) = \left(\frac{^{182}W}{^{184}W}\right)_i + \left(\frac{^{182}Hf}{^{180}Hf}\right)_i \times \left(\frac{^{180}Hf}{^{184}W}\right)).$$

Age calculations

Age differences between Hf-W fractionation events in any two reservoirs can be calculated from their initial ^{182}Hf/^{180}Hf ratios as determined from the slope of the isochron in the ^{182}W/^{184}W versus ^{180}Hf/^{184}W space (Fig. 1.5):

$$\Delta t_{A-B} = \frac{1}{\lambda} \ln \frac{\left(^{182}Hf/^{180}Hf\right)_A}{\left(^{182}Hf/^{180}Hf\right)_B} \qquad (1)$$

where λ is the decay constant of ^{182}Hf and (^{182}Hf/^{180}Hf)$_A$ and (^{182}Hf/^{180}Hf)$_B$ designate the initial concentrations of the parent nuclide in reservoirs A and B.

An important requirement in cosmochronology is to combine the relative time informations derived from short-lived radionuclides with informations derived from long-lived chronometers. The best way to anchor an extinct chronometer in the absolute time-scale is the comparison of the initial concentration extinct parent nuclide (determined from the slope of an internal meteorite isochron) with the absolute ^{207}Pb-^{206}Pb age of the same material. The different accumulation of radiogenic lead from the decay of the long-lived radionuclides ^{238}U and ^{235}U provides the best achievable resolution for early solar system events using extant radionuclide systems. Several well dated meteorites

were used in the last years to anchor the ^{182}Hf-^{182}W chronometer onto an absolute time-scale.

Kleine et al. (2004) obtained an internal Hf-W isochron for the H chondrite Ste Marguerite corresponding to an initial ^{182}Hf/^{180}Hf ratio of (0.85 ± 0.05) x 10^{-4}. They anchored this value by using the ^{53}Mn/^{53}Cr age of 4565.0 ± 0.7 Myr for this meteorite (Polnau and Lugmair, 2001). This age is indistinguishable from the whole rock Ste Marguerite ^{207}Pb-^{206}Pb age of 4566.7 ± 1.6 Myr (Göpel et al., 1994). The ^{53}Mn-^{53}Cr radionuclide system is a short-lived chronometer which itself is related to an absolute time-scale by comparison of the ^{53}Mn-^{53}Cr systematics for the angrite Lewis Cliff 86010 to the also measured ^{207}Pb-^{206}Pb age for this meteorite (which is 4557.8 ± 0.5 Myr; Lugmair and Gailer, 1992). The advantage of this indirect approach is an additional cross calibration of two short-lived chronometers. Most recently, the angrite D`Orbigny with a ^{207}Pb-^{206}Pb age of 4564.48 ± 0.24 Myr (Amelin et al., 2007) and an initial ^{182}Hf/^{180}Hf ratio of (0.72 ± 0.02) x 10^{-4} (Markowski et al., 2007) as well as CAIs with a ^{207}Pb-^{206}Pb age of 4568.5 ± 0.5 Myr (Bouvier et al., 2008) and an initial ^{182}Hf/^{180}Hf ratio of (1.01 ± 0.05) x 10^{-4} (Burkhardt et al., 2007) were used as additional anchors for the ^{182}Hf-^{182}W chronometer. Angrites are among the oldest igneous meteorites of roughly basaltic composition which cooled rapidly (Baker et al., 2005; Wadhwa et al., 2005). This makes possible differences in blocking temperatures of the Hf-W and U-Pb systems negligible. Amelin (2008) reported precise ^{207}Pb-^{206}Pb ages for several angrites and found an age dispersion among these meteorites of several million years, which makes an intercalibration of the Hf-W and U-Pb chronometer possible. Figure 1.6 shows a correlation between measured initial ^{182}Hf/^{180}Hf ratios for different meteorites and their respective ^{207}Pb-^{206}Pb ages. NWA 4590 and D`Orbigny define a line that passes through the point defined by Allende CAIs (CAI-2), which have a ^{207}Pb-^{206}Pb age of 4568.5 ± 0.5 Myr

(Bouvier et al., 2008) and an initial ^{182}Hf/^{180}Hf of $(1.01 \pm 0.05) \times 10^{-4}$ (Burkhardt et al., 2007). The calibration of the Hf-W chronometer to an absolute timescale therefore yields consistent results regardless which of these samples (Angrites or CAI-2) is used as an anchor. The H-chondrite Ste. Marguerite plots slightly above the line defined by angrites and Allende CAIs (CAI-2) which most likely reflects a slight disturbance of the Hf-W system in
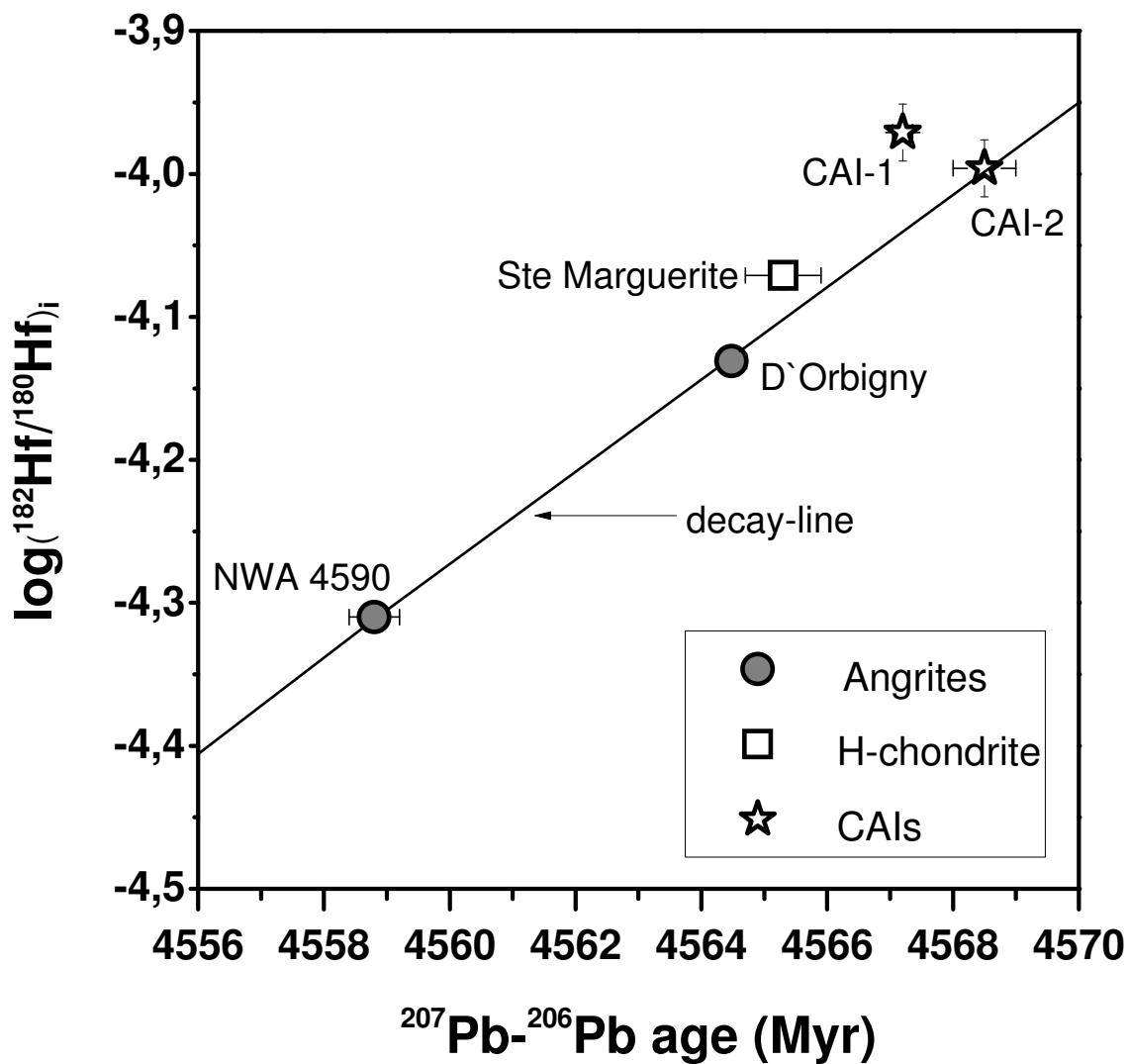

Figure 1.6: Initial ^{182}Hf/^{180}Hf versus ^{207}Pb-^{206}Pb ages. Data are from Amelin et al. (2006),

Amelin (2008), Kleine et al. (2004), Kleine et al. (2008), Burkhardt et al. (2007), Bouvier et al. (2007).

this sample (Kleine et al., 2008). A point defined by Allende CAIs (CAI-1) with a ^{207}Pb-^{206}Pb age of 4567.2 ± 0.5 Myr (Amelin et al., 2006) and an initial ^{182}Hf/^{180}Hf ratio of (1.07 ± 0.10) x 10^{-4} (Kleine et al., 2005) also plots off the line defined by the Angrites. In this study all ages are calculated relative to an initial (^{182}Hf/^{180}Hf) of (1.01 ± 0.05) x 10^{-4} (Burkhardt et al., 2007). Absolute ages are anchored on CAIs dated at 4568.5 ± 0.5 Myr (Bouvier et al., 2008), using the following equation:

$$T = \frac{1}{\lambda} \ln \frac{\left(^{182}Hf/^{180}Hf\right)_1}{\left(^{182}Hf/^{180}Hf\right)_{CAI-2}} + T_{CAI-2} \qquad (2)$$

(λ = decay constant of ^{182}Hf; (^{182}Hf/^{180}Hf)$_1$ = initial ^{182}Hf/^{180}Hf of reservoir 1; (^{182}Hf/^{180}Hf)$_{CAI-2}$ = initial ^{182}Hf/^{180}Hf of Allende CAIs; T_{CAI-2} = ^{207}Pb-^{206}Pb age for CAIs; T = time before present). Age uncertainties can be calculated employing the general formula for error-propagation:

$$\sigma_T^2 = \left(\sigma_m \frac{\partial T}{\partial m}\right)^2 + \left(\sigma_{m_{CAI-2}} \frac{\partial T}{\partial m_{CAI-2}}\right)^2 + \left(\sigma_{T_{CAI-2}} \frac{\partial T}{\partial T_{CAI-2}}\right)^2 + \left(\sigma_\lambda \frac{\partial T}{\partial \lambda}\right)^2 \qquad (3)$$

This results in the following equation:

$$\sigma_t^2 = \left(\frac{1}{\lambda m} \Delta m\right)^2 + \left(\frac{-1}{\lambda m_{CAI-2}} \Delta m_{CAI-2}\right)^2 + \left(\frac{1}{\lambda} \ln \frac{m}{m_{CAI-2}} \Delta t_{CAI-2}\right)^2 + \left(\frac{-\ln\left(\frac{m}{m_{CAI-2}}\right)}{\lambda^2}\right)^2$$

$$(4)$$

(m$_{CAI-2}$ = slope of the CAI-2 isochron; Δi = 2σ error of value i). For metals (phases with very low Hf/W ratios) it is also possible to calculate a model-age. The time difference between metal-silicate separation events in two objects from an initially chondritic parent body (Hf/W=1.2) can be calculated according to the following equation:

$$\Delta t_{A-B} = \frac{1}{\lambda} \ln \left(\frac{\varepsilon_W(A) - \varepsilon_W(C)}{\varepsilon_W(B) - \varepsilon_W(C)} \right)$$

(5)

εW(i) is the deviation of the ^{182}W/^{184}W ratio in reservoir i relative to a terrestrial standard in parts per 10.000; εW(C) is the present day value for carbonaceous chondrites of -1.9 ± 0.1 (Kleine et al., 2004).

Cosmogenic effects on W isotopes

In general is the W-isotopic composition of terrestrial and extraterrestrial material identical with the exception of ^{182}W. There is, in particular, no evidence for nucleosynthetic anomalies of the r- and s-process, because all non-radiogenic tungsten isotopes occur in terrestrial ratios in all types of meteorites (p-process anomalies of ^{180}W are so far not detectable). Only in rare cases small deviations from the terrestrial ^{184}W /^{183}W ratios have been observed in meteorites that must be of nucleogenic origin (e.g. Tlacotepec and Cranbourne; Markowski et al., 2006).

Spallation reactions during exposure of the meteorite to cosmic rays may have a large effect on W-isotopes, primarily because of the high cross section of ^{182}W for thermal neutron capture and the often long irradiation records of iron

meteorites in space. Particularly important is the thermal neutron capture of ^{182}W, ^{182}W(n,γ)^{183}W. The duration of the exposure to cosmic rays, the position of the sample within the meteorite, isotope abundances as well as the capture cross section of ^{182}W have to be taken into account to precisely determine this effect (Leya et al., 2003; Masarik, 1997; Markowski et al., 2006). An exact quantification of neutron capture induced ^{182}W depletions in meteorites with long exposure histories (>100 Myr) is therefore crucial for obtaining precise age informations. The problem is here that the relevant reactions are neutron induced reactions. But neutrons are secondary particles produced by spallation reactions of primary high energy protons and the slowing down of neutrons in an iron meteorite parent body is not well understood and thus there is an inherent uncertainty in the effect of thermal neutron capture that cannot precisely calculated.

1.5   Objectives of this study

The goal of this study is to apply the Hf-W chronometer to metals and silicates from different achondritic meteorite groups to better understand their parent body histories and to better resolve the succession of asteroidal differentiation in the early solar system (metal segregation, silicate differentiation and metamorphism). In this study we analyzed metal phases and silicates from IAB iron meteorites and two groups of primitive achondrite groups (winonaites and acapulcoites).

Chapter 2

Methods

2.1 Sample preparation

Several 200 mg to 1 g pieces of silicate material were separated from all analyzed meteorites. The silicate samples were subsequently cleaned with steel-free abrasives and leached in 0.5 M HNO_3 in an ultra-sonic bath for 15 min to remove potential terrestrial contaminants before they were finally powdered in an agate mortar. For IAB iron meteorites it was necessary to extract silicate inclusions from the Fe-Ni host (matrix-metal). Silicates from the Landes and Lueders meteorite are mm-sized and vein-like, therefore it was possible to obtain a mixture of different inclusions. For the IAB iron meteorites Copiapo and El Taco cm-sized ovoidal inclusions were extracted using diamond-saw blades. For Caddo County, two different silicate-inclusions could be analyzed originating from the masses kept at Universität Bonn and Universität Mainz. All silicate samples were gently crushed in an agate mortar. Additionally, metal-pieces of IAB iron meteorites were analyzed. They were free of any visible silicate inclusions and were cut into pieces weighing between 0.2 and 0.4 g using diamond saw blades. To remove potential terrestrial contamination, fusion crusts and rust were removed from the surface of the metal samples by polishing with steel-free abrasives. The metals were then cleaned in an ultrasonic bath and then leached in hot aqua regia for 10-20 min. Silicates from all analyzed winonaites, acapulcoites and IAB iron meteorites contain at least some weight percent metal and sulfides. The separation of these components from the silicates was achieved using a hand-magnet. For the IAB silicate inclusion from El Taco it was possible to extract separates of pure inclusion metals that were visibly unrelated to the matrix-metal. Silicate dust adhering to the metal grains was removed by repeated crushing of the fractions in ethanol. All IAB silicate separates are assigned to a specific inclusion or inclusion-mix (marked A or B) and were distinguished in weakly-magnetic (WM) and non-magnetic (NM) separates. The non-magnetic

fractions represent metal-free separates consisting of silicates and oxides, whereas the weakly-magnetic fractions represent mixtures of silicates, sulfides and metal. We also analyzed bulk fractions from inclusions that represent a mixture of silicates, sulfides and oxides as well as inclusion metal. Procedures for sample digestions and ion exchange separation follow those of Kleine et al. (2004). About 100-700 mg of the bulk silicate and non-magnetic fractions and 50-250 mg of the magnetic separates were dissolved in Savillex® vials at 180°C on a hotplate using HF-HNO_3-$HClO_4$ (5:3:2) for silicates and aqua regia for the metal fractions. After digestion, the samples were dried and re-dissolved in HNO_3-H_2O_2 to remove organic compounds. Subsequently, the samples were completely dissolved in a mixture of 6 M HCl and 0.06 M HF.

2.2   Ion-exchange chromatography

In order to obtain sufficiently clean W cuts for isotope analysis, chemical separation of W from the matrix was performed using a two column anion exchange chemistry (Münker et al., 2001; Kleine et al. 2004). The separation procedure is divided in two separate steps which are outlined in Table 2.1. Both steps involve the use of BIORAD AG 1x8 anion exchange resin (100-200 mesh, chloride form). During the first separation technique W together with Nb and Mo is collected in 16 ml 6 M HNO_3-0.2 HF. After drying down, the W cut is re-dissolved in 0.5 ml 0.5 M HCl - 0.5 M HF and than loaded onto a second set of columns for a final purification of W. Spiked aliquots were loaded onto columns identical to the columns used for the clean-up chemistry (Table 2.2). Hafnium is eluted in 2 ml 9 M HCl-0.01 M HF and W is eluted in 4 ml 6 M HNO_3-0.2 M HF. The average sample yields are 80-90%.

Step	Reservoir volumes	Acid
Column I (BIORAD AG 1 x 8, 4ml)	**[ml]**	
Equilibration	5	0.5 M HCl – 0.5 M HF
Load	10	1 M HCl – 0.5 M HF
Rinse	10	0.5 M HCl – 0.5 M HF
Rinse	3x3	0.5 mM HCl – 0.5 mM HF
Ti	40	3.6MHAc/8mMHNO$_3$/1% H$_2$O$_2$
Rinse	5	9 M HAc
Zr-Hf	8	9 M HCl – 1 M HF
W-Nb-Mo	15	6 M HNO$_3$ – 0.2 M HF
Cleaning	10	1 mM DTPA – 1 M HCl
Cleaning	10	3 M HNO$_3$
Cleaning	2 x 10	6 M HNO$_3$ – 0.2 HF
Column II (BIORAD AG 1 x 8,		
Equilibration	2.5	0.5 M HCl – 0.5 M HF
Load W-Nb-Mo cut	0.5	0.5 M HCl – 0.5 M HF
Rinse	2	0.5 M HCl – 0.5 M HF
Rinse	1	7 M HCl – 1 M HF
W	6	7 M HCl – 1 M HF
Cleaning	5	1 mM DTPA – 1 M HCl
Cleaning	5	3 M HNO$_3$
Cleaning	2 x 5	6 M HNO$_3$ – 0.2 M HF

Table 2.1: Two-step column chemistry for separating W for isotope composition measurements (HAc = acetic acid).

Step	Reservoir volumes	Acid
Column (BIORAD AG 1 x 8, 1 ml)	**[ml]**	
Equilibration	5	0.5 M HCl – 0.5 M HF
Load	1	1 M HCl – 0.5 M HF
Rinse	2.5	0.5 M HCl – 0.5 M HF
Hf	2.5	9 M HCl – 0.01 M HF
W	5	6 M HNO$_3$ – 0.2 M HF
Cleaning	5	1 mM DTPA – 1 M HCl
Cleaning	5	3 M HNO$_3$
Cleaning	2 x 5	6 M HNO$_3$ – 0.2 M HF

Table 2.2: Column chemistry for separating W for isotope dilution measurements.

2.3   Mass Spectrometry

All measurements have been performed on a Micromass IsoProbe multicollector-inductively coupled mass spectrometer (MC-ICPMS) at Universität Münster. The instrument is used in conjunction with a Cetac MCN 6000 desolvating nebuliser. For measurements, all samples were dissolved in 0.5 - 1 ml 0.56 M HNO_3-0.24 M HF.

2.3.1   Isotope dilution measurements

For sufficiently precise and accurate W and Hf concentration measurements a 10 % aliquot of the sample is doped with a mixed ^{180}Hf-^{183}W Spike. For concentration determinations the ratios $^{180}Hf/^{177}Hf$ and $^{183}W/^{184}W$ were measured. External errors on Hf/W ratios were typically better than 1 % (2σ). The main source of error in the Hf-W concentration measurements is the blank correction. The propagated errors from blank corrections were considered in all cases, assuming a blank uncertainty ±50%. Total procedural blanks for W were approximately ~50 pg, total procedural blanks for Hf are ~5pg. Resulting uncertainties in the Hf/W ratios are typically better than ± 1% (2σ).

2.3.2   High precision isotopic measurements of tungsten

Measured $^{182}W/^{184}W$ ratios were normalized to $^{186}W/^{184}W$ = 0.92767 using the exponential law and were corrected for Os interferences using mass 188 as a monitor. Osmium interference corrections for most samples were well within the analytical uncertainty. Isotope compositions were measured with a typical signal intensity of ~1V on ^{182}W, which was obtained for a ~20 ppb W solution. In each

measurement 60 ratios are collected in blocks of 20. The masses from 180 to 188 are measured with Faraday cups and 10^{11} Ω amplifier. External reproducibilities are in the order of $\pm$ 0.3 ε units ($2\sigma_m$) and ranges up to 200 ppm for silicates fraction where only a few ng of W were measured. Total blanks for W isotope measurement were <250pg. If only a few ng of W were analyzed, measured isotope ratios were corrected for blank contributions assuming terrestrial ^{182}W/^{184}W compositions and a blank uncertainty of $\pm$50% for error propagation.

Chapter 3

The evolution of the IAB iron meteorite parent body

from Hf-W systematics

3.1 Introduction

Calcium Aluminium - rich inclusions in chondrites (CAIs) have traditionally been regarded as the oldest dated material formed in the solar system with a U-Pb age of 4568.5 ± 0.5 Myr (Bouvier et al., 2008). Chondrites are the chemically least processed material of the solar system and have, with respect to their refractory element budget, a composition similar to the solar photosphere. They are considered to represent the precursor materials from which asteroidal and planetary bodies accreted and subsequently differentiated to form silicate and Fe-Ni metal. This sequence of events in the early solar system recently had to be modified due to new age constraints obtained with several short lived chronometers on different meteorite classes. Within analytical error, some parent bodies of magmatic iron meteorites were now shown to be at least as old as CAIs (e.g. Kleine et al., 2005, Schersten et al., 2006, Markowski et al., 2006). It also was shown that parent bodies of magmatic iron meteorites and many achondrites accreted and differentiated before or contemporaneously with the chondrite parent bodies. This new chronology of early solar system events indicates that the oldest planetesimals all segregated metal cores most likely due to the presence of [26]Al. Only the younger chondrite parent bodies had the chance to remain undifferentiated or only partly differentiated. The arguments for the new chronology proposed for early solar system events are mostly based on the observation of a strong deficit of [182]W in iron meteorites compared to chondrites. This deficit in [182]W is more pronounced in magmatic iron meteorites compared to non-magmatic iron meteorites (e.g. Markowski et al., 2006). Non-magmatic iron meteorites formed as impact generated melts with only minor solid/liquid partitioning effects (Wasson et al., 1980; Choi et al., 1995) or as successive extractions of partial melts from a chondritic source (Kelly and Larimer, 1977). The most recent models for the evolution of non-magmatic irons involves

fractional crystallization of magmas (e.g. Benedix et al., 2000). The difference in [182]W between the two iron meteorite clans (magmatic and non-magmatic) therefore indicate that the IAB irons with an εW of ~ -3.01 ± 0.25 (Markowski et al. 2006) formed 5 ± 3 Myr after the main core forming event in the parent bodies of magmatic iron meteorites, which have an εW initial close to the CAI initial of -3.51 ± 0.25 (Schersten et al., 2006). IAB iron meteorites formed contemporaneously with or shortly after the accretion of chondrite parent bodies. In spite of their much lower density, silicates in IAB irons are distributed throughout the metal. This could provide evidence for an arrested state of metal-silicate separation, probably due to a decreasing activity of internal heat sources. However, younger silicates have to be enclosed by older metal in order to provide a pore free assemblage of this components (Wasson et al., 2002). Silicate inclusions therefore provide an additional source of information about the chronology of metal-silicate segregation and mantle differentiation as well as metamorphism in the IAB parent body.

Here we present [182]Hf-[182]W systematics for metal phases from seven IAB iron meteorites and separates from different silicate inclusions. Based on the data, a chronology of magmatism and metamorphism on the IAB parent body is proposed and compared to previous genetic models for the IAB iron meteorite parent body.

3.2   Analyzed samples and results

The IAB samples selected for this study include metals and silicate inclusions from the meteorites Landes, Copiapo, Caddo County, Lueders and the El Taco mass of the Campo del Cielo meteorite as well as metal phases from San Cristobal and Mundrabilla (Mundrabilla is sometimes also considered to be a

IIICD iron; e.g. Chen et al., 1990, Petaev et al., 2004; Bizzarro et al., 2006; Markowski et al., 2006). Peak temperatures reached within the silicates determined from the two-pyroxene thermometer are around ~1000°C for Landes (Bunch et al., 1972), ~1067°C for Lueders (McCoy et al., 1996; Benedix et al., 2005), ~1020°C for Caddo County (Palme et al., 1991; Benedix et al., 2005), ~933°C for Copiapo (Benedix et al., 2005) and ~965°C for Campo del Cielo (Benedix et al., 2005). Peak temperatures for these meteorites are thought to be slightly higher. The inclusions in the selected samples include metamorphosed chondritic silicates in Lueders (McCoy et al., 1996; Benedix et al., 2005) and the El Taco mass of Campo del Cielo (Wlotzka et al., 1977; Benedix et al., 2000) as well as basaltic lithologies in Caddo County (e.g. Palme et al., 1991; Benedix et al., 2000) and more peridotitic mineralogies in Landes (Bunch et al., 1972; Luzius-Lange et al., 1985).

Tungsten concentrations in the metal phases range from 0.7 to 1.5 ppm, whereas Hf concentrations range from 0.2 to 40 ppb. The highest Hf concentrations were measured in Lueders, Landes and El Taco metals. This most likely reflects the presence of submicroscopic silicate inclusions within the metal or of silicate grains adhering to the metal. The $^{182}W/^{184}W$ isotope compositions of all analyzed metals overlap within analytical uncertainties and range from -2.9 to -3.4 ε-units, with a weighted average of -3.1 ± 0.2 ε-units. This value agrees with earlier estimates (Kleine et al., 2005; Markowski et al., 2006; Schersten et al., 2006) and provides an important constraint on the time of metal segregation (e.g. core formation) in the IAB parent body. Mundrabilla was excluded from the calculation of the average εW -value for the metals because this meteorite does not strictly belong to the IAB-main group defined by most IAB individuals based on different compositional trends (Wasson et al., 2002). If an origin of the IAB metals in different melt pools of the IAB parent body is warranted (e.g. Wasson

et al., 2002), it is not justifiable to average the εW signatures of metals that belong to different subgroups of the IAB meteorite group. Mundrabilla, an ungrouped member of the IAB clan (Wasson et al., 2002) has a slightly more radiogenic εW -signature (-2.6 ± 0.4 ε-units) compared to the IAB metal average (-3.1 ± 0.2 ε-units) and possibly samples a different melt pool than the samples from the main-group. However, a study of Mundrabilla from Markowski et al. (2006), yields a slightly more unradiogenic value of -3.33 ± 0.16 ε-units, indistinguishable from the IAB metal average. Metal samples extracted from two different El Taco inclusions also display the same εW signatures (-3.3 ± 0.4 ε-units) as the IAB metal average.

Tungsten concentrations range from 12 to 120 ppb in the non-magnetic fractions and from 340 to 530 ppb in the weakly-magnetic fractions, depending on the separation technique applied and the presence of sub-microscopic metal grains in the fractions. Hafnium concentrations in the non-magnetic and weakly magnetic fractions range from 80 to 800 ppb (Table 3.1). Weakly-magnetic fractions are mixtures of silicates, sulfides and oxides and display Hf/W ratios between 0.1 and 1, whereas the non-magnetic fractions are visibly free of metals and display Hf/W ratios between 1 and 41. Most silicates exhibit strong excesses in ^{182}W of up to +35 ε-units. The highest ^{182}W excesses and He/W were measured for a separate from Caddo County, originating from the Mainz Split (we = +34.7 ± 1.3). All other analyzed separates from Caddo County originate from the Bonn Split, a different inclusion that shows excesses between +3 and +6 ε-units. The two splits most likely sample different lithologies. In contrast to the highly radiogenic compositions found in Caddo County inclusions, the Lueders silicates show metal-like εW signatures of around -3, despite their elevated Hf/W ratios of up to 3.5 (the associated uncertainty is 2 ε-units, the largest reported for silicates in this study). All other analyzed fractions from Copiapo, Landes and El Taco

show W isotope signatures between these extremes. Three bulk silicates from Landes (A-bulk), Copiapo (A-bulk) and El Taco (B-bulk) define a combined IAB isochron (Fig. 3.1) with a slope corresponding to $^{182}Hf/^{180}Hf = (8.03 \pm 1.34)$ x 10^{-5} and an initial ratio of -1.5 ± 0.8 εW (MSWD 2.6). A fourth bulk separate from Caddo County plots off the combined isochron. All other measured silicate separates from different meteorites, including the bulk separate from Caddo County, lie below this isochron. Two silicate separates from two distinct Caddo County inclusions and the metal phase define an isochron with a slope of $^{182}Hf/^{180}Hf = (6.86 \pm 0.26)$ x 10^{-5} and an intercept of ~ -3.5 ± 0.5 ε-units (Fig. 3.2). An internal silicate isochron for the El Taco mass of the Campo del Cielo meteorite is defined by three separates from one distinct silicate inclusion (A-NM1-3; Fig. 3.3). Compared to the combined IAB isochron, this isochron has a shallower slope corresponding to an initial $^{182}Hf/^{180}Hf = (4.18 \pm 0.72)$ x 10^{-5} and an intercept at -1.4 ± 0.5 εW. A fourth El Taco separate (B-bulk) is from a different part of the El Taco mass and does not plot on this isochron. Instead, B-bulk plots on the combined IAB isochron. For Lueders it is possible to define a poorly constrained best fit line, defined by three different separates (MM, A-WM and A-NM). The corresponding slope is $^{182}Hf/^{180}Hf = (\sim4.0)$ x 10^{-5} and the intercept of ~3.3 ε-units (Fig. 3.4). Silicate separates from Copiapo and Landes define correlation lines that show steeper slopes than the combined IAB isochron (Fig. 3.5 and 3.6).

Meteorite	separate	$^{182}W/^{184}W$ [6/4]±2σ	εW [6/4]±2σ	W [ppm]	Hf [ppm]	$^{180}Hf/^{184}W$ ±2σ
Copiapo	MM	0.864395 ± 43	-3.3 ± 0.5	0.7588	0.0002	0.0004 ± 2
	A-bulk	0.865164 ± 86	5.6 ± 1.0	0.0303	0.1780	6.9426 ± 4
	B-NM	0.864663 ± 43	-0.2 ± 0.5	0.0570	0.1562	3.2436 ± 1
	B-WM	0.864400 ± 43	-3.3 ± 0.5	0.3442	0.1661	0.5692 ± 3
Landes	MM	0.864429 ± 43	-2.9 ± 0.5	1.3224	0.0096	0.0085 ± 4
	A-bulk	0.864758 ± 43	0.9 ± 0.5	0.0727	0.1821	2.9589 ± 1
	B-WM1	0.864429 ± 43	-2.9 ± 0.5	0.4482	0.1390	0.3657 ± 2
	B-WM2	0.864420 ± 138	-3.0 ± 1.6	0.5314	0.1113	0.2470 ± 1
Caddo County	MM	0.864403 ± 43	-3.2 ± 0.5	0.7904	0.0003	0.0005 ± 2
	A-NM1	0.865164 ± 43	5.6 ± 0.5	0.1161	0.7992	8.1333 ± 4
	A-NM2	0.864983 ± 43	3.5 ± 0.5	0.0689	0.5374	9.2754 ± 5
	B-NM	0.867680 ± 112	34.7 ± 1.3	0.0194	0.7881	48.030 ± 2
El Taco	MM	0.864412 ± 43	-3.1 ± 0.5	1.2688	-	0.0100 ± 5
	A-IM	0.864403 ± 43	-3.2 ± 0.5	1.5159	0.0284	0.0100 ± 5
	B-IM	0.864385 ± 43	-3.4 ± 1.3	0.8933	0.0397	0.0524 ± 3
	A-NM1	0.864698 ± 43	0.2 ± 0.5	0.0463	0.1303	3.3167 ± 1
	A-NM2	0.864749 ± 43	0.8 ± 0.5	0.0741	0.2815	4.5118 ± 2
	A-NM3	0.865251 ± 86	6.6 ± 1.0	0.0067	0.0893	16.538 ± 5
	B-bulk	0.865515 ± 130	9.7 ± 1.5	0.0125	0.1311	12.356 ± 4
Lueders	MM	0.864403 ± 43	-3.2 ± 0.5	0.8241	0.0313	0.0100 ± 5
	A-WM	0.864399 ± 173	-3.3 ± 2.0	0.0344	0.1188	0.0100 ± 5
	A-NM	0.864446 ± 43	-2.7 ± 0.5	0.4957	0.0787	0.0524 ± 3
San Cristobal	MM	0.864415 ± 52	-3.1 ± 0.6	-	-	-
Mundrabilla	MM	0.864512 ± 43	-2.6 ± 0.5	-	-	-

Table 3.1: Hf-W data for metals and inclusion separates. MM = matrix metal, IM = inclusion- metal, WM = weakly magnetic fraction, NM = non-magnetic fraction, bulk = matrix-metal free bulk inclusion. Prefixes "A" and "B" indicate different inclusions. The εW values of each isotope measurement are expressed as the deviations in parts per 10,000 relative to the terrestrial standard value of 0.864680. Uncertainties refer to the last significant digits.
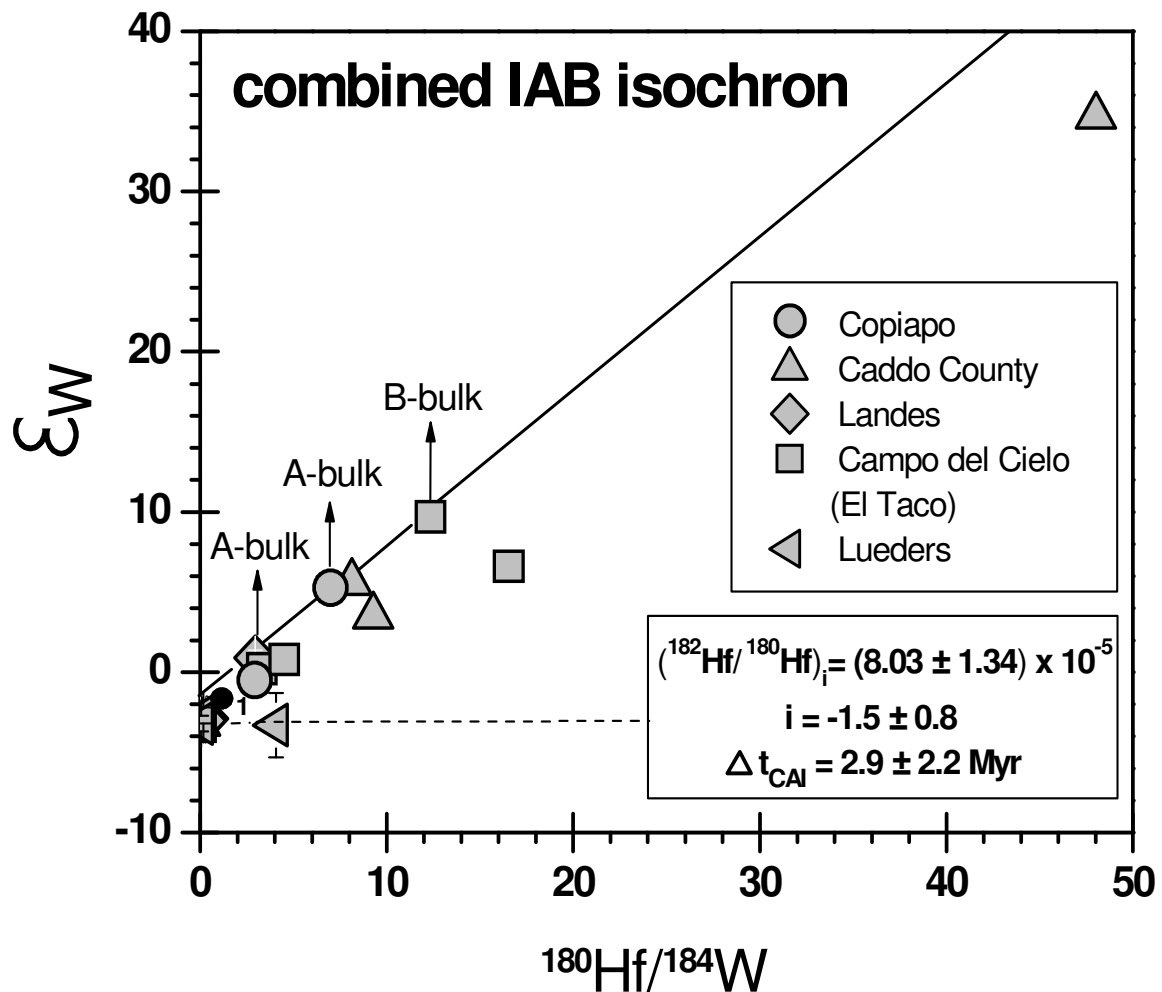
Figure 3.1: Combined IAB silicate isochron defined by three different bulk silicate fractions from three different IAB iron meteorites (Landes A-bulk, Copiapo A-bulk, El Taco B-bulk; MSWD 2.6). This isochron yields an age postdating the formation of the CAIs by 2.9 ± 2.2 Myr. Slopes of all other inclusions lie below the combined IAB silicate isochron. Except for Lueders all quoted errors (Table 3.1) are lower than symbol-size. A point defining carbonaceous chondrites (Kleine et al., 2002) plots off the isochron (1).
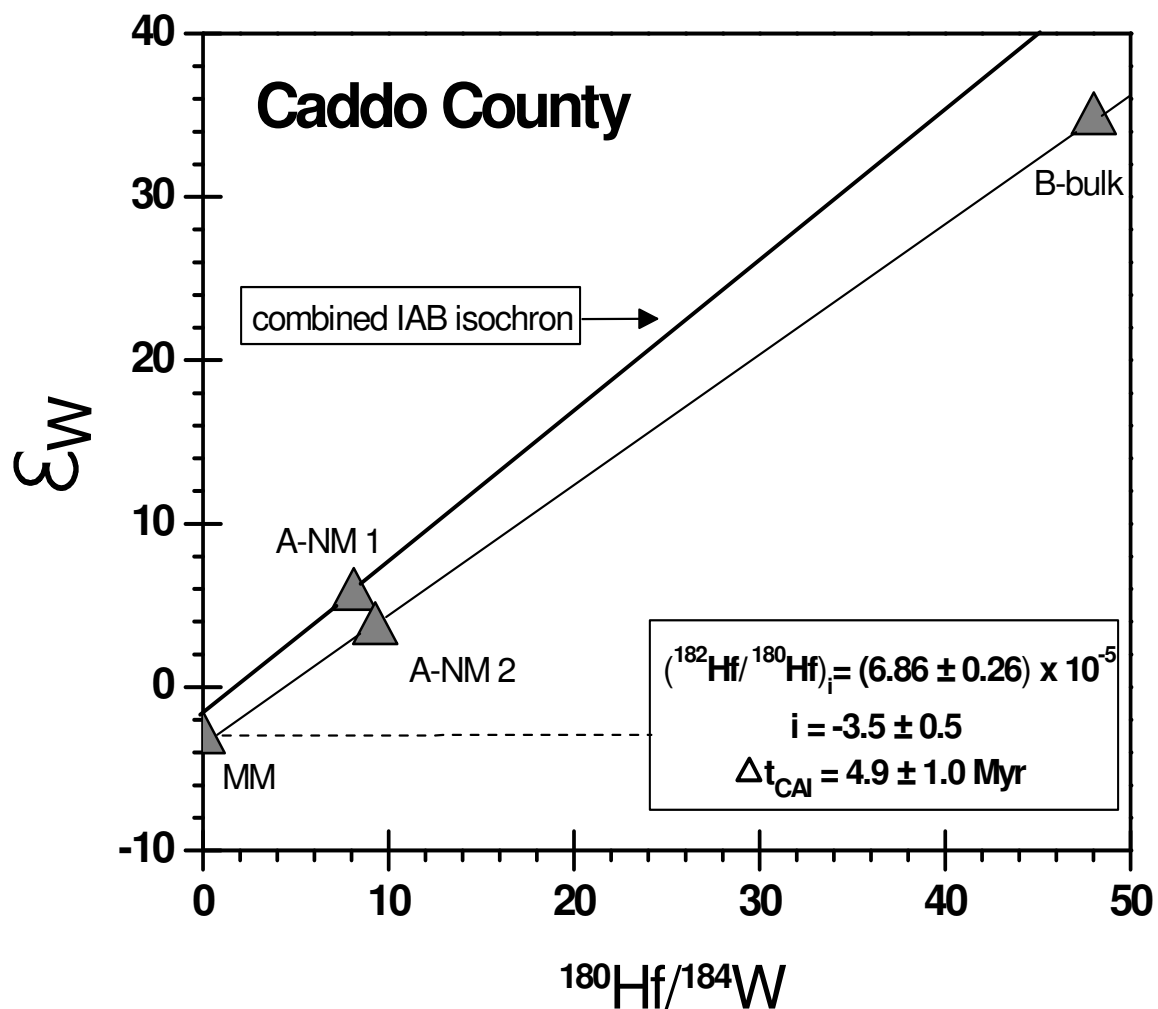
Figure 3.2: Internal silicate isochron for Caddo County, defined by two silicate separates (A-NM2 and B-bulk) and the metal phase (MM), yielding an age 4.9 ± 1.0 Myr after CAIs. Quoted errors (Table 3.1) are smaller than the symbol size.
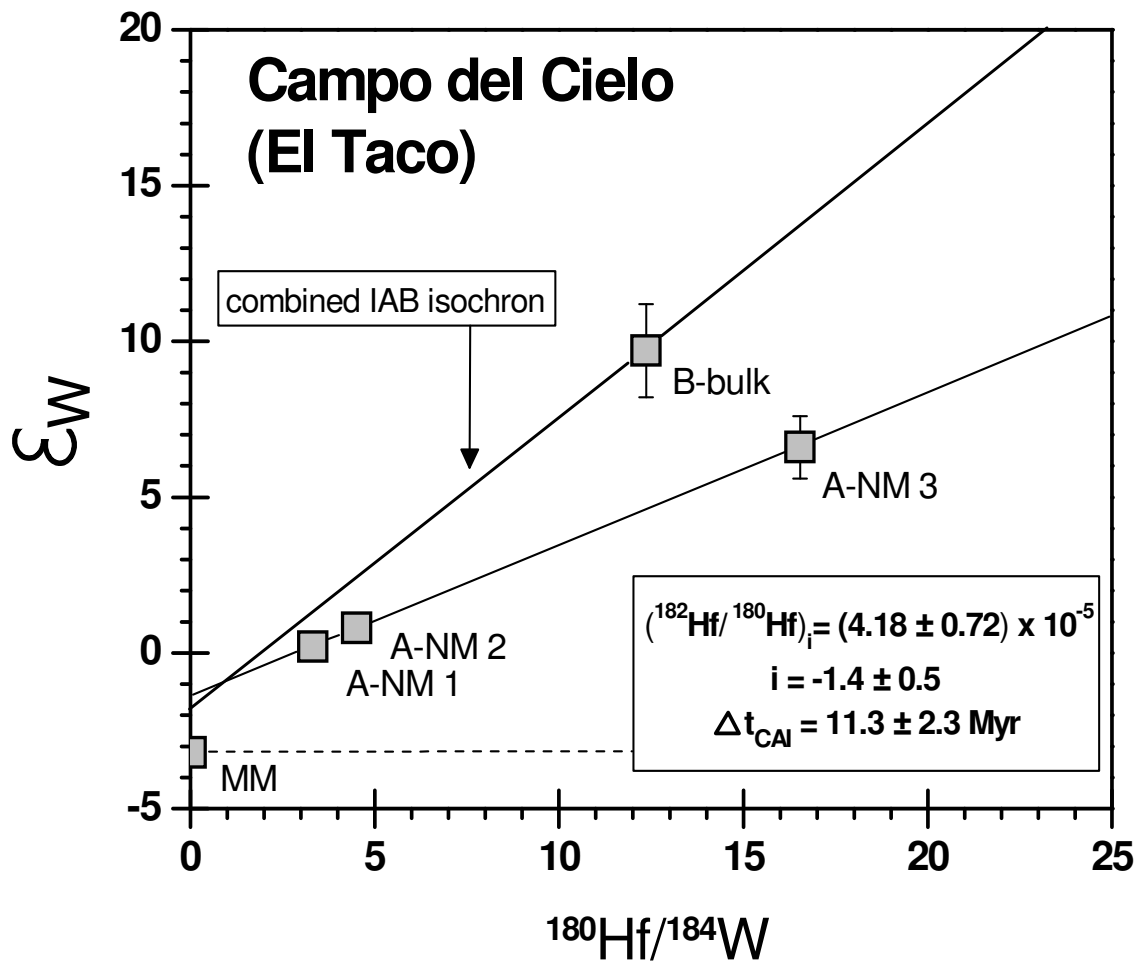
Figure 3.3: Internal silicate isochron for El Taco, defined by three different non-magnetic fractions from one single El Taco inclusion (A-NM1-3), yielding an age of 11.3 ± 2.3 Myr after CAIs (MSWD 0.0032). A bulk sample (B-bulk) from a different El Taco silicate inclusion does not plot on this internal El Taco isochron and most likely represents another lithology.
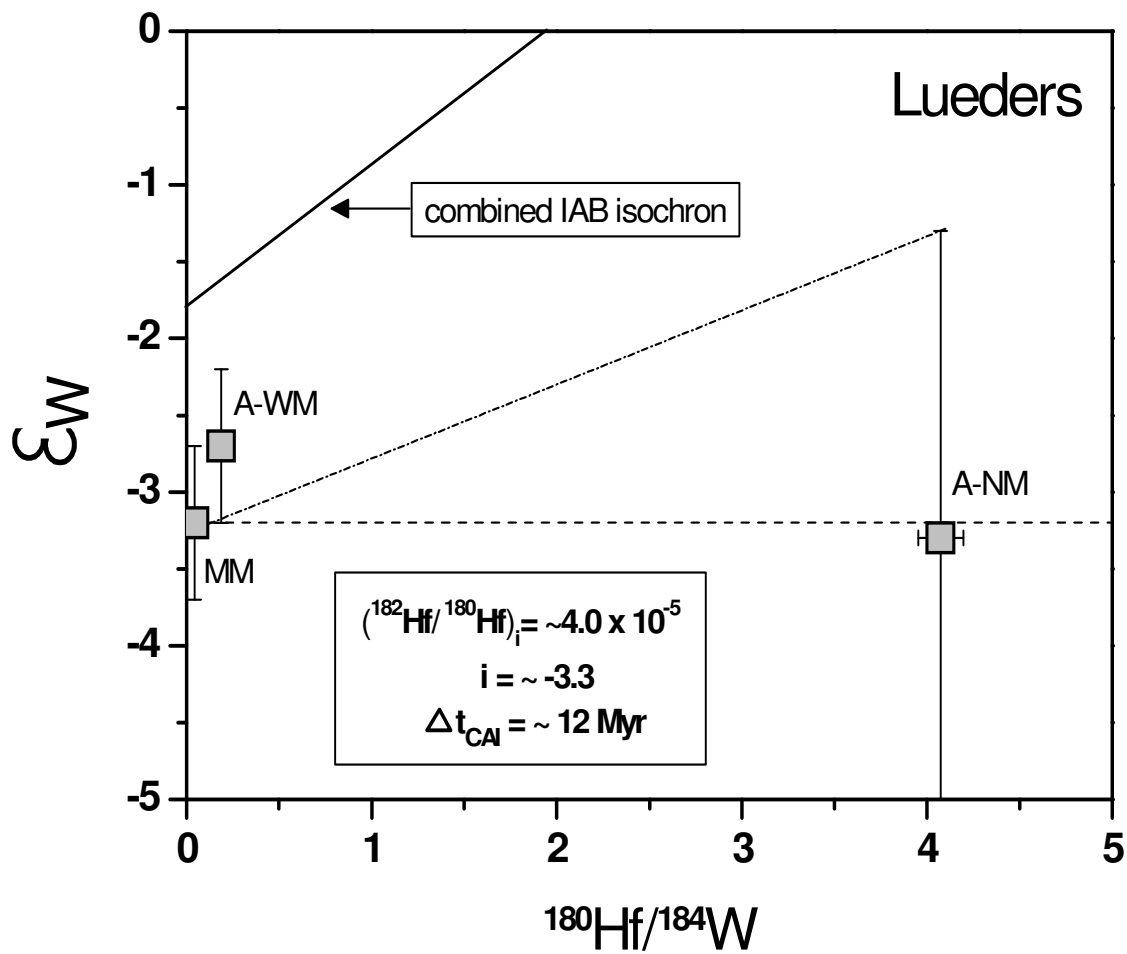
Figure 3.4: Best fit line for Lueders separates defined by the upper limit of the 2σ error for A-NM and the lower limit for A-WM. The corresponding maximum age for Lueders postdates CAI formation by ~12 Myr.
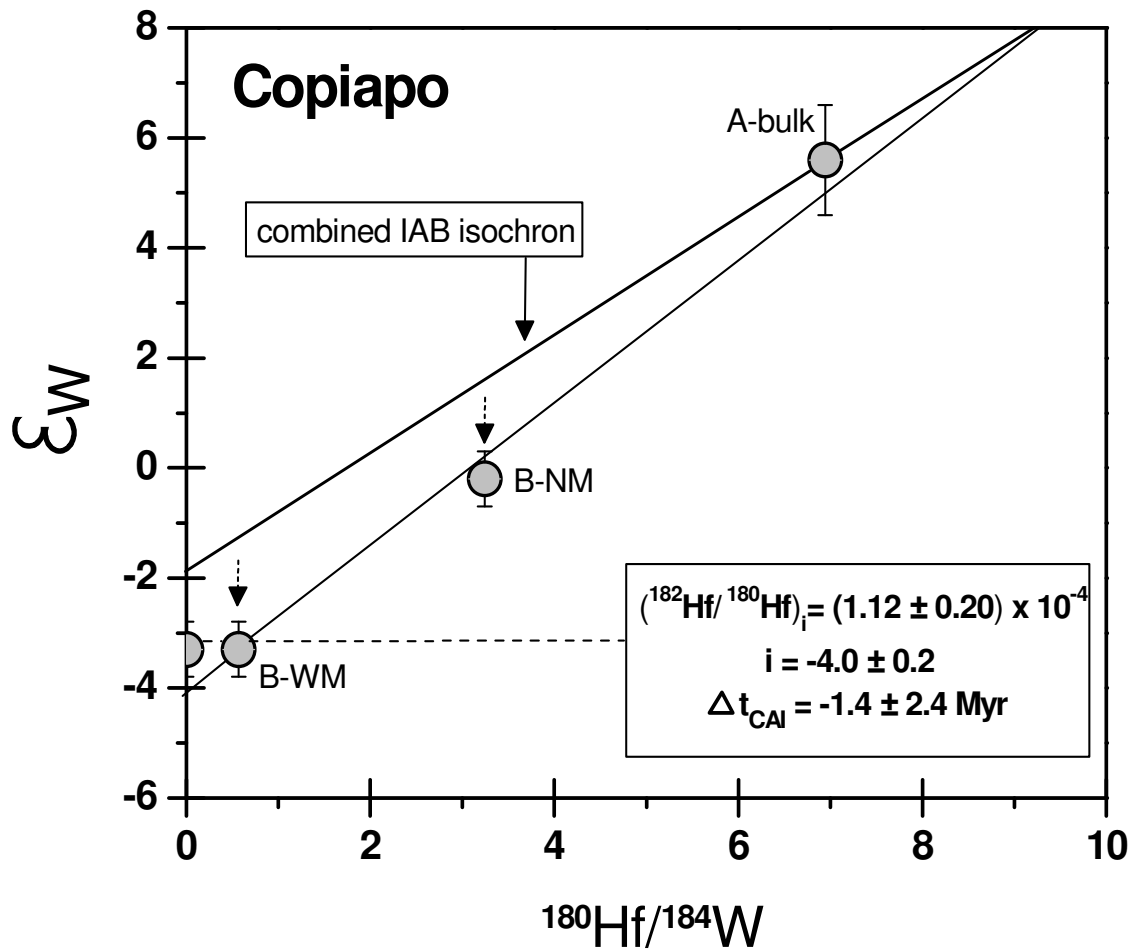
Figure 3.5: Internal silicate isochron for Copiapo, defined by three different bulk and weakly-magnetic fractions (A-bulk, B-WM, B-NM), yielding an age that predates CAI formation by 1.4 ± 2.4 Myr (MSWD 3.8).

Figure 3.6: Internal silicate isochron for Landes, defined by three different bulk and weakly-magnetic fractions (A-bulk, B-WM1-2), yielding an age that predates CAI formation by 2.8 ± 2.3 Myr (MSWD 0.0064).

3.3 The distribution of Hf and W in IAB silicates and metal and parent body evolution

The Hf and W concentrations measured in the IAB silicates allow valuable insights into the process controlling metal segregation and internal mantle differentiation. The parental chondritic material of the IAB parent body closely resembles those of carbonaceous chondrites (Wasson et al., 2002). D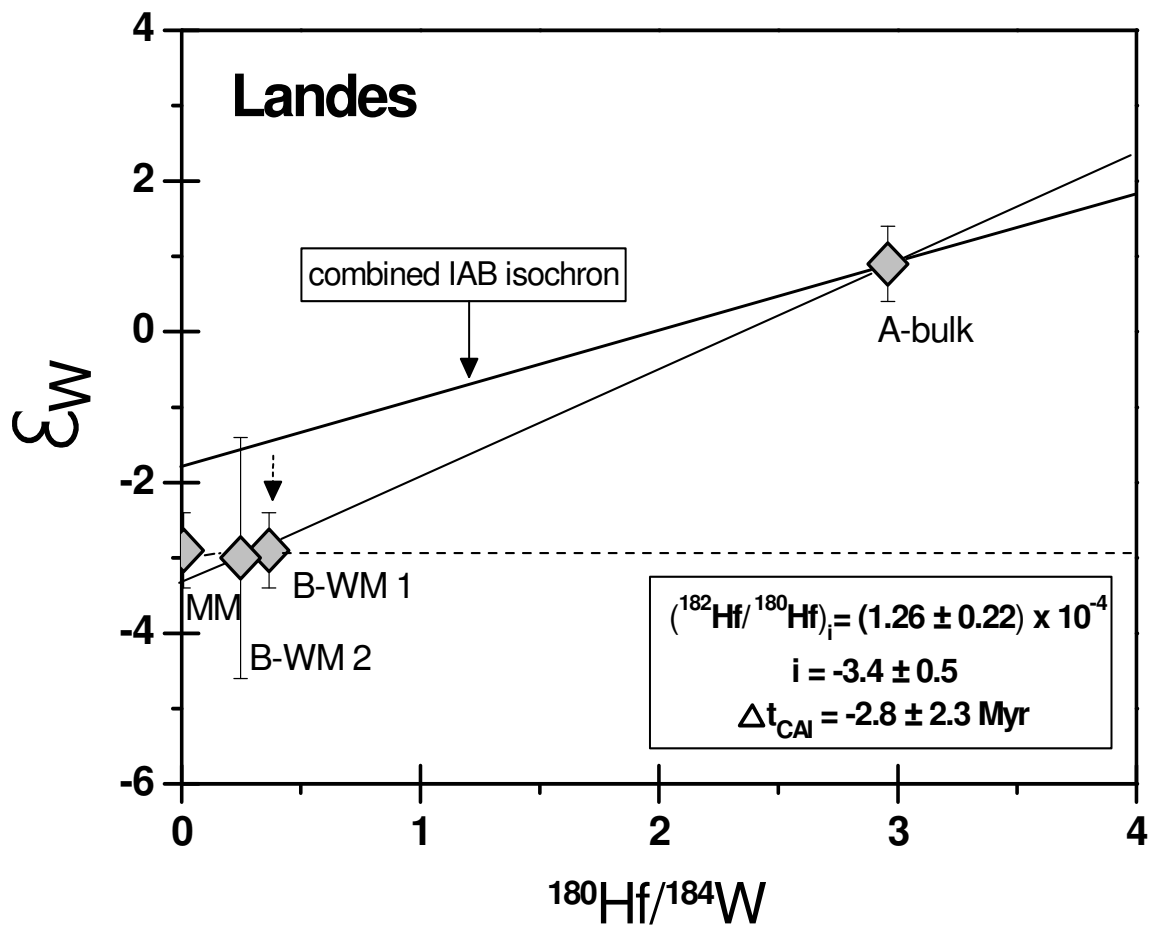uring metal-silicate equilibration the moderately siderophile W partitions into the metal-core, whereas Hf partitions into the silicate- mantle (Palme et al., 1981). As a consequence, the Hf contents of the IAB mantle should be higher than in average chondrites (~120 ppb Hf), whereas the W concentration should be lower than the chondritic value of ~100 ppb. The resulting Hf/W ratio and Hf content of the IAB mantle then depends on conditions during metal-silicate segregation. Particularly important is the oxygen fugacity that prevailed during metal-silicate equilibrium. For example, W will be much more effectively removed from silicates at reducing conditions. The Hf/W ratio in the IAB mantle can be further modified during partial melting and fractional crystallization. Oxidized W (WO_3) is very incompatible and preferentially partitions into partial melts of the mantle. The concentration of W in such a "basaltic melt" may even exceed the W abundance of the bulk planet (Palme et al., 1981). However, in the metal-rich environment of the IAB silicates (a possible result of an inefficient metal-silicate separation and reducing conditions) it is expected that W does not behave as an incompatible element (Palme et al., 1981). If metal is present during a melting event, W is buffered in the melt and the Hf/W ratio in a partial melt is higher, opposite to what is expected for pure silicate systems.

Most of the analyzed non-magnetic fractions show chondritic to superchondritic Hf/W ratios and Hf contents between 120 and 800 ppb. This is

expected, because all non-magnetic fractions are metal-free. To determine the Hf/W ratio and the Hf content of the IAB mantle it is necessary to analyse bulk inclusions with a representative ratio of silicates to inclusion-metal. However, this ratio is difficult to determine because the metal inside a IAB inclusion could be either cogenetic with the silicates (inclusion-metal) or constitute additional contributions of admixed core-material (matrix-metal). The analyzed three bulk samples that define the combined IAB isochron (Landes A-bulk, Copiapo A-bulk and El Taco B-bulk) have superchondritic Hf/W ratios (2.5-12) and Hf contents (130-180 ppb) and a subchondritic W content (10-70 ppb). This can be explained by a metal-silicate separation that depleted the forming IAB mantle (represented by the bulk separates) in W and enriched it in Hf, thereby increasing the Hf/W ratios. We therefore assume that the IAB mantle has Hf concentrations of about 130-180 ppb and Hf/W ratios that lie somewhere between the values measured for the three bulk inclusions (2.5-12). However, a Caddo County bulk separate is not included in this calculation because it represents a partial melt (e.g. Palme et al., 1991; Benedix et al., 2000). An additional Hf enrichment in IAB mantle material to concentrations up to 800 ppb, as found for Caddo County silicates, is then assumed to be achieved by enrichment through subsequent mantle melting, or melting of the chondritic precursor. As Fig. 3.7 reveals, the analyzed metal-free Caddo County bulk silicate inclusion (B-bulk) shows a high Hf/W ratio up to ~41 and a strong enrichment in Hf with respect to the proposed mantle value of 130-180 ppb (Fig. 3.7). The Caddo County inclusions are therefore interpreted as enriched partial melts. This is consistend with their basaltic to andesitic petrology (e.g. Palme et al., 1991; Benedix et al., 2000).

In contrast to Caddo County, the El Taco separate A-NM3 has a subchondritic Hf content even though its Hf/W ratio is ~14. The low Hf

concentration of this matrix-metal-free separate could be due to depletion in modal clinopyroxene (main carrier of Hf), therefore producing a more

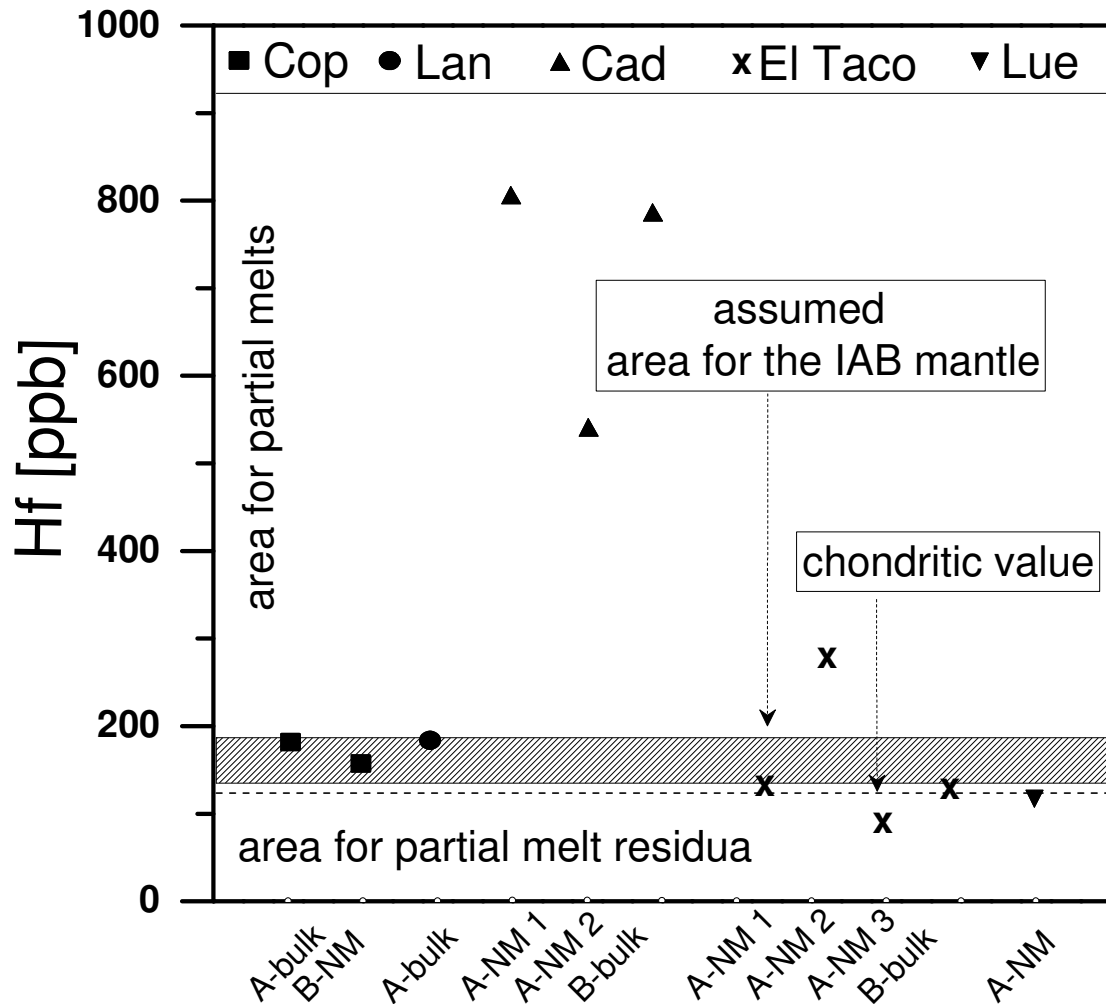Figure 3.7: Comparison of the Hf contents determined for all non-magnetic fractions and bulk inclusions. The silicates are assumed to represent different lithologies in the IAB parent body (residues, partial melts and less processed chondritic material). Solid and grey bar indicate the chondritic Hf content and the assumed Hf concentration of the IAB mantle, as constrained by bulk inclusions from three different IAB meteorites.

residual, Hf depleted mineralogy. The El Taco inclusion therefore is assumed to sample the depleted mantle of the IAB parent body. Hence, the Hf and W budgets in IAB inclusions most likely comprise primitive and depleted mantle compositions as well as enriched partial melts. This petrogenetic interpretation based on Hf and W systematics is also in agreement with previous models.

Some silicates from Caddo County were found to be different from compared to the average IAB lithologies, as they have a basaltic to andesitic bulk chemistry (e.g. Niemeyer, 1979b; Palme et al., 1991; Takeda et al., 1993). These Caddo County lithologies were interpreted as crystallization products of partial melts originating from a chondritic parent body (Takeda et al., 2000). The separates investigated here are possibly part of a more gabbroic lithology. Wlotzka et al. (1977) provided a detailed mineralogical and bulk chemical description of several Campo del Cielo inclusions and reported chemical differences between inclusions. Compositional variations in Ca and Al were interpreted as the result of diopside and/or feldspar removal from a chondritic precursor material through partial melting. Bild et al. (1977) described an inclusion from Campo del Cielo that is highly depleted in siderophile elements compared to the CI composition. Therefore they concluded that the siderophiles in this inclusion were sequestered into the host metal (matrix-metal). Additionally, variable modal amounts of clinopyroxene in Landes inclusions (Luzius-Lange et al., 1985) are possibly also evidence for the evolved nature of the IAB silicates.

Processes that affected the IAB meteorites therefore include siderophile-element depletion, possibly during metal-silicate separation and incompatible-element enrichment and depletion during partial melting of silicates.

3.4   Relationship between matrix- and inclusion-metal

Bild et al. (1977) analyzed several IAB iron meteorites and pointed out that the approximately chondritic abundances of the siderophile elements in most silicate inclusions (except for example in Campo del Cielo) indicate that the metal in these inclusions is native to the silicates. They argued that random addition of matrix-metal to silicates would not result in consistently chondritic abundances of siderophile elements in the bulk-inclusions. Hence, an independent formation of host- and inclusion-metals was proposed. However, the ^{182}Hf-^{182}W isotope system provides no evidence for a separate origin of these metals. Host and inclusion metals overlap in their W contents and ^{182}W signatures (an exception is the metal from Mundrabilla, which seems to have a slightly more radiogenic signature). Identical ^{182}W/^{184}W values in host and inclusion metal indicate a more or less contemporaneous formation. Hence, there is no evidence for the segregation of a radiogenic, late-stage metal phase in the IAB silicates as observed for eucrites (Kleine et al., 2005) and possibly for the winonaites (Schulz et al., 2007). Such second stage metals are generated during late reduction events on their parent bodies and inherit evolved radiogenic W isotope signatures from the high Hf/W silicates in which these metals formed. The lack of a radiogenic metal phase in IAB irons is in agreement with the assumption that the reduced nature of the IAB silicates is an intrinsic property of the precursor material and was not established during later reduction of a more oxidized precursor (Benedix et al., 2005). The two analyzed inclusion metals from El Taco differ in their W contents but the contents are still within the range of concentrations measured in the different matrix-metals. Therefore it can be concluded that the inclusion-metal was left behind in the silicates during incomplete metal-silicate separation on the IAB parent body. The matrix-metal therefore represents asteroidal "core-

like material", whereas the inclusion-metal plus silicates may indicate the presence of trapped "mantle-like material".

3.5   Thermal evolution of the IAB parent body

In the εW versus $^{180}Hf/^{184}W$ space, the silicates show an increase of ^{182}W excesses with Hf/W ratios (Fig. 3.1). A linear regression through three data-points, comprising pure bulk silicate fractions from different IAB meteorites (Copiapo, Landes and El Taco) is interpreted as an isochron and yields an absolute age of 4565.6 ± 2.7 Myr (combined IAB isochron). A point for carbonaceous chondrites plots close but off the isochron (Fig. 3.1). Some IAB inclusions plotting below this isochron may have been reset by later thermal events. During such re-heating events, isotope exchange of ^{182}W by tracer diffusion from silicates into metal is expected to be the dominant diffusion process (Fig. 3.8), whereas changes of the Hf/W ratio due to chemical diffusion should be less significant (Lesher, 1990; Quitté et al., 2004). Hence, radiogenic W produced in silicates may equilibrate with less radiogenic W in the matrix-metal. This isotope diffusion effect shifts the silicates from the combined IAB isochron towards less radiogenic εW signatures until the blocking temperature is reached during cooling (Fig. 3.9). The W isotope composition of the metal remains almost unchanged during this process because all metals are W-rich. If the thermal equilibration ceased within the lifetime of ^{182}Hf, radiogenic W could accumulate again, starting from an initial εW value that depends on the extent and duration of prior metal-silicate equilibration. This results in a new isochron with a slope corresponding to the time of the thermal overprint (internal isochron). The effects of late-stage re-equilibration in the IAB silicates are best illustrated by the internal isochron for El Taco (Fig. 3.3).
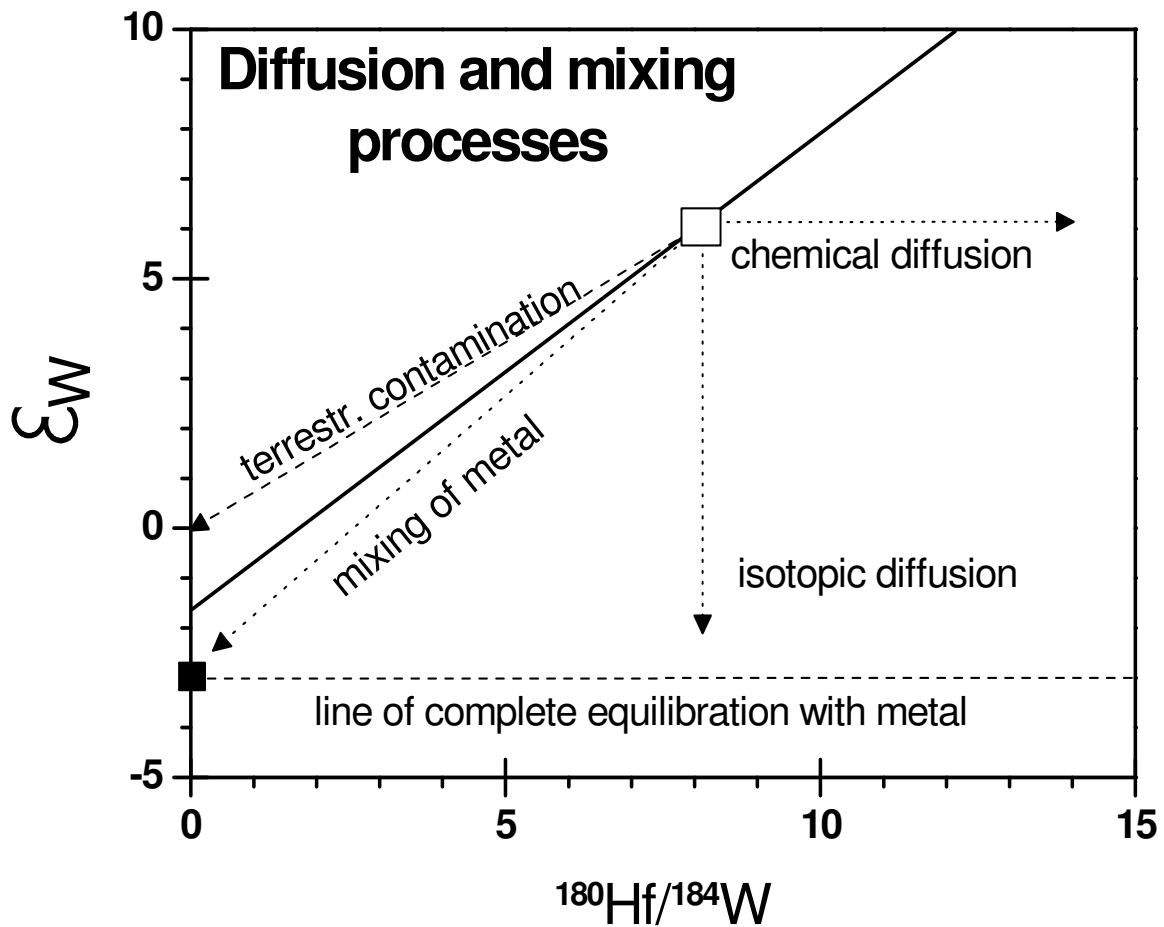
Figure 3.8: Shematic diagram illustrating the principal mechanisms that affected the W budget of the IAB silicates. All samples, whether they define an isochron or not, could be affected by the following processes: (1) local isotopic equilibration between high and low Hf/W reservoirs, changing the [182]W-budget of the silicates towards the value for the matrix metal and acting much faster than (2) chemical diffusion affecting the Hf/W ratio of the respective reservoirs. (3) Mixing of partially equilibrated silicates with matrix-metal can also affect the slope of an isochron.
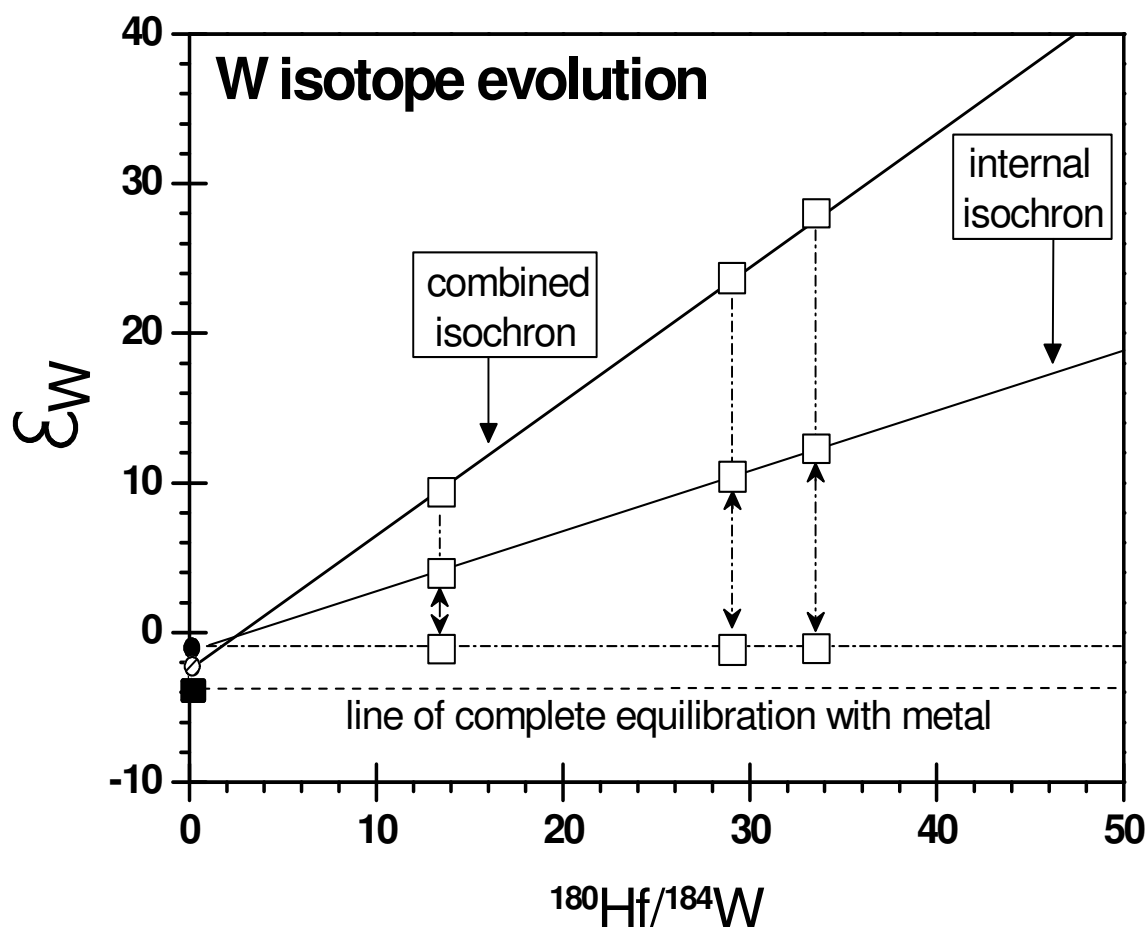
Figure 3.9: Schematic graph illustrating multistage W isotope evolution in IAB silicates. All silicates that remained unaffected from any late-stage equilibration define the combined IAB isochron. Silicates affected by metamorphism might have partially equilibrated with matrix-metal. Hence, they were shifted from their assumed initial position on the combined IAB isochron towards lower [182]W values. During the equilibration, excess [182]W continuously diffused from the silicate inclusions into the matrix-metal. Within the lifetime of [182]Hf, these equilibrated silicate inclusions can accumulate radiogenic [182]W again, finally defining younger internal isochrones.

For this sample, it becomes apparent that late-stage partial equilibration ceased within the life-time of ^{182}Hf. The new internal isochron for El Taco consequently has a shallower slope compared to the combined IAB isochron and dates a thermal event at 11.3 ± 2.3 Myr after CAI formation, which corresponds to ~8 Myr after silicate differentiation on the IAB parent body (as defined by the combined IAB isochron). Contrastingly, Lueders seems to be completely re-equilibrated with matrix-metal (Fig. 3.4), indicating that W re-distribution occurred when ^{182}Hf was nearly extinct. However, the silicate separates are not aligned. Even when considering the large error bars, it is still difficult to draw a regression line through the data points. A regression line defined by the upper limit of the 2σ error for the non-magnetic fraction and the lower limit of the 2σ error for the weakly-magnetic fraction yields a maximum slope that corresponds to a time ~12 Myr after CAIs, indistinguishable from the internal El Taco isochron (11.3 ± 2.3 Myr after CAIs). Either these two events occurred contemporaneously or Lueders was affected at a later time. Samples from inclusions in Copiapo (Fig. 3.5) and Landes (Fig. 3.6) define very steep slopes in εW versus ^{180}Hf/^{184}W space, yielding unrealistically high ages which predate the combined IAB isochron and CAI formation by several million years. A possible reason for this unrealistically old ages could be mixing with matrix-metal (Fig. 3.8). This affected the isochrones, resulting in less radiogenic intercepts (-4.0 ± 0.2 and -3.4 ± 0.5 ε-units) and steeper slopes. The mixing line (between matrix-metal and inclusion-material) therefore provides no time information. Contrastingly, the combined IAB isochron and the internal El Taco isochron have highly radiogenic intercepts (-1.8 ± 0.8 and -1.4 ± 0.5 ε-units) far from the value for the matrix-metal, indicating that the metal-mixing effect is minor or absent. Additionally, two inclusion separates from two different Caddo County splits and the corresponding metal phase define an isochron with an absolute age of 4563.5

± 2.6 Myr, indistinguishable within error from the age of the combined IAB isochron (4565.6 ± 2.7 Myr). However, a fourth separate (A-NM1) plots off the internal Caddo County isochron. Instead, this separate plots on the combined IAB isochron.

A model for the thermal evolution of the IAB parent body based on Hf-W systematics contains the following sequence of events: (1) A major metal segregation on the IAB parent body. Assuming a chondritic bulk composition for the IAB parent body this happened 3.5 ± 2.3 Myr after CAI formation as indicated by the εW signature of the matrix-metal. The metal segregation was most likely incomplete ("arrested core formation") and may not have involved the whole parent body, leaving behind some almost pristine chondritic parts of the asteroid. (2) Silicates cooled through the blocking temperature of the Hf-W system 2.9 ± 2.2 Myr after CAIs (4565.6 ± 2.7 Myr) as indicated by the combined IAB silicate isochron. Within analytical error this age is indistinguishable from the metal segregation event and dates undisturbed cooling of the mantle-like silicate material (left behind after metal segregation) or it marks a distinct differentiation event in a non-chondritic reservoir. However, the fact that the combined IAB silicate isochron has an initial of -1.5 ± 0.8 ε-units, significantly more radiogenic than the metal value of ~ -3.1 ± 0.2 ε-units indicates a distinct silicate re-equilibration event. (3) Partial melting of the mantle-like reservoir or of pristine chondritic material formed basaltic to andesitic lithologies as indicated by an internal Caddo County isochron which yields an age of 4563.5 ± 2.6 Myr, corresponding to 4.9 ± 1.0 Myr after CAIs. (4) A thermal event caused local equilibration of W between metals and silicates 11.3 ± 2.3 Myr after CAIs as indicated by the internal El Taco isochron. The re-equilibration of Lueders silicates at ~ 12 Myr after CAIs is most likely related to this event. Additional metal segregation is indicated by the W isotope

composition obtained for Mundrabilla-metal which is slightly more radiogenic (-2.6 ± 0.5 ε-units) compared to the value of -3.1 ± 0.2 ε-units obtained for all other analyzed IAB metals (the two values are indistinguishable within error, therefore it remains ambiguous if Mundrabilla represents a second generation of metal segregation). Assuming that this metal-segregation occurred in a chondritic reservoir, this age corresponds to ~11 Myr, indistinguishable from the El Taco and Lueders ages Markowski et al. (2007) reported a different value for Mundrabilla of ~ -3.3 ε-units).

3.6   Heat sources

Following current models for differentiation of planetesimals, an internal heat source is likely to have induced core segregation and mantle differentiation in the earliest formed parent bodies in the solar system. Within the first ~5 Myr of the solar system internal heat sources such as the decay of ^{26}Al provided sufficient heat to trigger large scale melting and metal segregation (Urey, 1955). Therefore, metal segregation in the IAB parent body (3.5 ± 2.3 Myr relative to CAIs) is most likely induced by such internal heat sources, but impacts may have contributed heat as well. The fact that bulk silicate inclusions from different IAB iron meteorites define a combined IAB isochron may be the result of a global silicate differentiation on the IAB parent body, which is difficult to reconcile with an impact event that would only have affected the target object locally. The age obtained from the combined IAB silicate isochron is attributed to the decreasing heat supply from such an internal heat source. In this case, the age defines cooling and solidification of the mantle from peak temperatures to the blocking temperature for W diffusion. Alternatively, this age information could mark a separate differentiation event that affected the mantle-like material on the IAB parent body after re-heating, possibly during an impact event. An additional stage in the thermal evolution of the IAB parent body is the partial melting of chondritic or processed silicate material. The production of partial melts on the IAB parent body requires elevated temperatures, which could have been reached contemporaneously with or shortly after the silicate differentiation, possibly triggered by both heat sources (internal and external). This assumption is supported by the age information obtained from the internal Caddo County isochron which yields an age of 4.9 ± 1.0 Myr after CAIs. In contrast to the ages obtained for metal segregation, silicate differentiation and partial melting on the IAB parent body, the prolonged time window for re-equilibrations in the IAB

mantle is difficult to reconcile with an internal heat source model, as radionuclides, like ^{26}Al, would have been extinct at this stage. Probably the "El Taco-event" (internal El Taco isochron; 11.3 ± 2.3 Myr after CAIs) and "Lueders-event" (regression line defining a maximum age of ~ 12 Myr after CAIs) are related to a single impact-event that affected the IAB parent body on a local scale. However, in contrast to El Taco, Lueders seems to be fully equilibrated with matrix-metal, suggesting a deep burial depth in the parent body that resulted in more protracted cooling at higher temperatures, and therefore a more pronounced metal-silicate equilibration.

3.7 Comparison of the Hf/W data with other chronometers and formation models for the IAB parent body

Information on the time interval elapsed between metal-segregation and core crystallization on the IAB parent body can be derived from combined ^{182}Hf/^{182}W and ^{187}Re-^{187}Os chronometry. This interval depends on the size of the parent body and the thickness of a possible regolith cover. For metal phases in IAB iron meteorites Horan et al. (1998) derived a combined ^{187}Re-^{187}Os isochron yielding a core-crystallization age of 4537 ± 21 Myr. This age postdates the metal-silicate separation event, dated by Hf-W chronometry to 4565.0 ± 2.3 Myr, by at least 5 Myr. However, because of the large error of the Re-Os crystallization age, it is impossible to derive a realistic time frame for the interval between metal-segregation and solidification of the IAB core. A detailed discussion of previously reported geochronological data for IAB silicates is given by Bogard et al. (2005) and is updated and summarized in Table 3.2. ^{129}I-^{129}Xe ages for IAB silicates typically range from 4558-4566 Myr, whereas ^{40}Ar-^{39}Ar ages for several IABs and ^{147}Sm-^{143}Nd and ^{87}Rb-^{87}Sr isochron ages for Caddo

County are $\geq$ 30 Myr younger. The Hf-W ages therefore seem to be closely related to the older ^{129}I-^{129}Xe ages. The Hf-W age obtained from the internal El Taco silicate isochron is, within uncertainty, indistinguishable from the ^{129}I-^{129}Xe age (4558.6 ± 0.7 Myr; Podosek, 1970). This indicates that the thermal overprint during the "El Taco –event" also appears to have caused partial degassing of the IAB parent body. Younger Ar-Ar, Sm-Nd and Rb-Sr ages either reflect the protracted cooling history of the IAB parent body, or they indicate additional impact events that did not reset the I-Xe and Hf-W system with their relatively high blocking temperatures (around 900°C; Bogard et al., 2005; Kleine et al., 2005; van Orman et al., 2008). Such late thermal overprints are possibly related to impact events, not accompanied by internal heat sources. They appear to be recorded by all of the other chronometers (Ar-Ar, Sm-Nd and Rb-Sr).

A number of evolutionary models for the origin of the IAB parent body were established in the last decades. Primary models argue for condensation as the main IAB forming process. Wasson (1972) concluded that element trends in the IAB group could be the result of direct condensation from the nebula. Therefore, he introduced the term "non-magmatic". He later rejected this model because of difficulties in explaining the huge crystal sizes in the metal phase of IAB irons, which cannot be caused by condensation from a vapor. Presently, the most widely accepted models involve at least two stages in order to explain the origin of the IAB iron meteorites by metal segregation inside an asteroidal parent body. The hybrid-model of Benedix et al. (2000) divides the IAB evolution into two intervals, a first pre-collisional phase dominated by internal heat-sources and a subsequent period of mixing between disparate lithologies that followed a catastrophic, impact-related gravitational reassembly. Bogard et al. (2005) found that even with the hybrid-model of Benedix et al. (2000), all available age data for IAB iron meteorites are inconsitent with a simple thermal cooling history. Our

new Hf-W data support a more complex cooling history and can also be interpreted in the light of the model proposed by Benedix et al. (2000). The ^{182}Hf/^{182}W ages for metal-segregation and silicate differentiation obtained in the present study record the pre-collisional period. Conversely, the ages for El Taco and Lueders most likely record major collisional and local, less catastrophic impact events. It is then evident that the Hf-W system was not reset during break-up and reassembly of the IAB parent body as recorded by the Ar-Ar, Sm-Nd and Rb-Sr chronometers. This most likely is a result of the high blocking temperatures for the I-Xe and Hf-W systems of > 900°C (Bogard et al., 2005; Kleine et al., 2005; van Orman et al., 2008) compared to the other chronometers.

Meteorite	^{87}Rb/^{87}Sr	^{147}Sm/^{143}Nd	^{39}Ar/^{40}Ar	^{129}I/^{129}Xe
Copiapo	-	-	4.447 (30) [D]	4.5609 (7) [G]
Landes	-	-	4.427 (30) [D]	4.5597 (6) [G]
Caddo County	4.57 (23) [A]	4.53 (2) [C]	4.520 (5) [E]	4.5579 (1) [E]
	4.52 (3) [A]	4.50 (4) [A]	4.506 (10) [F]	
El Taco	~4.66 [B]	-	~4.5 [F]	4.5586 (7) [H]

Table 3.2: Compilation of geochronological data for IAB silicate inclusions. All age data are in Ga. References: A = Liu et al., 2002; B = Burnett et al., 1967; C = Stewart et al., 1996; D = Niemeyer, 1979b; E = Takeda et al., 2000; F = Bogard et al., 2005; G = Niemeyer et al., 1979a; H = Podosek, 1970.

3.8   Conclusions

IAB iron meteorites provide a unique record of early planetesimal differentiation and impact-related bombardment in the early solar system. An evaluation of the Hf-W systematics in silicate and metal phases of seven IAB iron meteorites provides a detailed account of multi-stage melting and metamorphism on the IAB parent body.

The age of 3.5 ± 2.3 Myr after CAIs for the main metal segregation on the IAB parent body slightly postdates the segregation of most magmatic iron meteorites, but is identical to the time of core formation inferred for Vesta at 3.5 ± 2.3 Myr after CAIs (Quitté et al., 2004; Kleine et al., 2005). Core formation on larger planets such as Mars and the Earth occurred significantly later at 12 ± 5 Myr (Quitté et al., 2004; Kleine et al., 2004) and >33 Myr after CAI formation (Kleine et al., 2002; Schoenberg et al., 2002). Hence, metal segregation and silicate differentiation on the IAB parent body occurred contemporaneously with the accretion of chondrites (~3 Myr after CAI formation; Kleine et al., 2005), lending further support to a revised solar system chronology where the presently sampled generation of chondrites is not the precursor material for most differentiated planetesimals. In marked difference to IAB metals, silicate inclusions retain information about later thermal events. The emplacement of silicate inclusions in the metal is most likely a result of an incomplete metal-silicate separation (arrested core formation). The combined IAB isochron defined by bulk silicate inclusions (2.9 ± 2.2 Myr relative to CAIs) yields an age indistinguishable within error from the major metal-segregation age (3.5 ± 2.3 Myr relative to CAIs) and most likely dates a distinct silicate differentiation event in a mantle-like reservoir with a nonchondritic Hf/W ratio. However, it appears plausible that silicate differentiation cannot predate the main metal segregation

on the IAB parent body. Later overprints are local and most likely impact related (Fig. 3.11). The thermal events that affected the IAB parent body lasted at least for ~12 Myr after solar system formation, much too long to have been driven by the decay of short-lived radionuclides such as ^{26}Al. Therefore, we prefer a more continuous evolution model for the IAB parent body, where a larger number of smaller impacts caused brecciation and local re-equilibration of the parent body. Possibly, the effects of this continuous bombardment were initially overprinted by the "straw fire" of ^{26}Al decay that triggered the major metal segregation event and subsequent silicate differentiation.

Accretion

A > 4565 Myr

Differentiation

1

2

ε_W -3.1

B ~ 4565 Myr

Metamorphism

3

ε_W -2.6

ε_W -3.1

C ~ 4556 Myr

ε_W -2.6

ε_W -3.1

4?

D $\leq$ 4556 Myr

Chondritic lithologies   **Silicates**

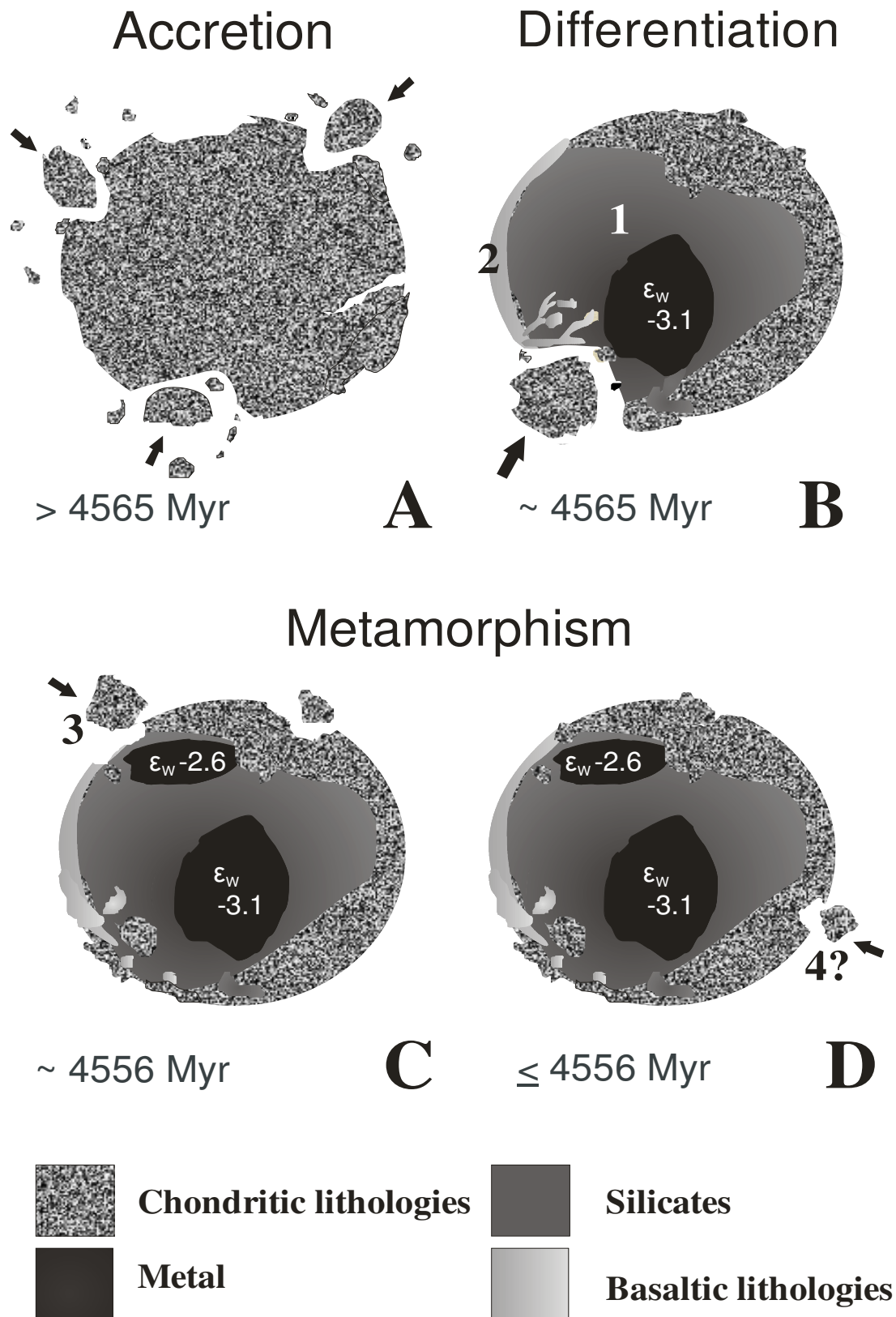**Metal**   **Basaltic lithologies**

Figure 3.11: Possible formation scenario for the IAB parent body. All lithologies are defined by different colours as described in the legend. A: Accretion of the chondritic IAB precursor body. B: Internal heat production as well as impacts supplied heat energy to the growing parent body, triggering major metal segregation at 4563.8 ± 2.3, silicate differentiation at 4565.6 ± 2.7 Myr (1) and partial melting at 4563.5 ± 2.6 Myr (2). All age data are indistinguishable within uncertainty and are assumed to have occurred more or less contemporaneously. These processes probably affected only a major part of the parent body, leaving behind some unaffected pristine chondritic areas. C: Approximately 12 Myr after the start of the solar system a new, impact-generated metal pod is formed (3). Mundrabilla with an εW signature of ~ -2.6 samples this distinct metal pod. At the same time, a thermal event ("El Taco event") affected parts of the IAB mantle, causing local re-equilibration of ^{182}W between silicate and metal. D: A thermal overprint that affected Lueders (4) cannot be dated properly, but a maximum regression-line yields a value indistinguishable from the "El Taco event" and "Mundrabilla event" (~12 Myr), suggesting that re-equilibration of these meteorites could be caused by the same impactor.

Chapter 4

Timing of asteroid differentiation

in the early solar system

from Hf-W systematics

4.1. Introduction

In recent years, advances in the understanding of asteroidal differentiation in the early solar system were made using the short-lived ^{182}Hf-^{182}W radionuclide system. Based on new age constraints on a variety of differentiated and undifferentiated meteorites, a new chronology for early solar system evolution was obtained. Parent bodies of most iron meteorites were now found to have differentiated during a short time-interval of about ~1.5 Myr, contemporaneously with formation of Ca, Al- rich inclusions in carbonaceous chondrites (Kleine et al., 2005; Bizzarro et al., 2005; Schersten et al., 2006). The most remarkable finding was that core formation in the parent asteroids of the oldest iron meteorites slightly predates the formation of chondritic meteorites (~3 Myr; Kleine et al., 2006). This is inconsistent with the general assumption that chondrites, which comprise the major fraction of the world`s meteorite collections, are the precursor material from which the iron meteorites formed. The undifferentiated nature of chondrites is now assumed to be the result of the lower concentrations of the heat producing radionuclide ^{26}Al in their parent bodies compared to the parent bodies of the older iron meteorites. These iron meteorites formed earlier, at a time when more ^{26}Al was available. Residual silicate phases of iron meteorite formation have not been identified.

Acapulcoites and Winonaites are designated as primitive achondrites. Both types of meteorites experienced higher temperatures than chondrites. Silcates and metal were just beginning to melt, but the temperature was not high enough to cause separation of metal on larger scale. Primitive achondrites are therefore transitional between chondrites and fully differentiated meteorite parent bodies. With the Hf-W method it should be possible to date the time of the last metal-silicate equilibration. The timing of differentiation obtained for Acapulcoites and

Winonaites is then compared to existing literature data for different chondritic and achondritic meteorite groups. Based on this comparison, a broader model is developed, describing the timing of the beginning of asteroidal differentiation during the first few million years of solar system history.

4.2 Hf-W chronometry of undifferentiated and differentiated meteorites

Chondrites and their components

Chondrites are the least processed material in the solar system. They have approximately the chemical composition of the Sun for all elements heavier than oxygen and excluding rare gases. Differences in chemistry among chondritic meteorites include variable volatile element contents, variations in Fe-Ni and other siderophile elements and some spread in Mg/Si ratios. Type 1 carbonaceous chondrites fit the solar abundances best.

Dating of individual components in chondrites provides information about the formation interval of chondrite parent bodies. Calcium- aluminium rich inclusions are the oldest components in meteorites. They are believed to have formed by condensation in a hot solar nebula. They display Pb-Pb ages of 4567.2 ± 0.6 Myr based on the E60 CAI from Efremovka (Amelin et al., 2002) and 4568.5 ± 0.5 Myr based on a combined CAI isochron using Allende and Efremovka CAIs (Bouvier et al., 2007). Their formation interval, based on the short-lived ^{26}Al-^{26}Mg chronometer ($T_{1/2}$=0.73 Myr) has recently been found to be extremely short, in the range of 150,000 years (Bizzaro et al., 2004). Determining the initial ^{182}Hf/^{180}Hf and ^{182}W/^{184}W ratios of these inclusions therefore provide a good estimate for the initial ^{182}Hf/^{180}Hf signature of the solar

system. Kleine et al. (2005) has linked a ^{182}Hf/^{180}Hf of (1.07 ± 0.10) x 10^{-4} from a combined CAI isochron to an absolute timescale using Sainte Marguerite as an anchor. An age of 4568.0 ± 1.7 Myr was derived for CAI formation. Burkhardt et al. (2007) re-determined the solar system initial ^{182}Hf/^{180}Hf to (1.01 ± 0.05) x 10^{-5} from an isochron using an expanded dataset including fassaite- and melilite-rich separates from CAIs of the carbonaceous chondrite Allende. Using the angrite D`Orbigny as an anchor they derived an absolute age of 4568.5 ± 0.8 Myr. This age is in remarkable agreement with the Pb-Pb age of 4568.5 ± 0.5 Myr determined for CAIs from Bouvier et al. (2007), but is somewhat older than the CAI age of 4567.2 ± 0.6 Myr determined by Amelin et al. (2002).

Ages of chondrites and their components, determined using several extinct- and extant chronometers provide some time estimate for the earliest stages of solar system evolution. The parent bodies of most chondrites (H and LL groups) are now assumed to have accreted between 1-3 Myr after CAI formation based on absolute Pb-Pb ages of chondrules and on the comparatively low ^{26}Al in chondrules of ordinary chondrites (Bouvier et al., 2007). For the LL-chondrite parent body, a protracted cooling history that lasted for more than ~30 Myr is documented (Bouvier et al., 2007). Kleine et al. (2002) determined the initial ^{182}Hf/^{180}Hf of the solar system from the slope of an isochron defined by separates from the well dated H chondrite Ste Marguerite. These authors obtained a value of (0.85 ± 0.05) x 10^{-4} (see section 1.3), which indicates cooling below Hf-W closure for metal-silicate exchange at 4565.3 ± 0.6 Myr. An isochron for the CH chondrite Acfer 182 yields a similar ^{182}Hf/^{180}Hf initial of (0.89 ± 0.19) x 10^{-4}. The H-chondrite parent body therefore accreted and cooled below the Hf-W blocking temperature within the first ~3 Myr of solar system history. Additionally, Kleine et al. (2002) and Yin et al. (2002) determined the present ^{182}W/^{184}W ratio of

carbonaceous chondrites to be -1.9 ± 0.1 ε–units relative to the terrestrial standard.

Iron- and stony iron meteorites

Most iron meteorites are asteroidal core fragments from differentiated and subsequently disrupted parent bodies. Due to their high W abundances, iron meteorites were among the first extraterrestrial objects that were analyzed for W-isotopes. Iron meteorites show a strong deficit in their $\varepsilon^{182}W$ abundance compared to terrestrial material. This is a result of their early formation by asteroidal metal-silicate segregation events. Measured isotopic compositions range between $\varepsilon^{182}W \sim$ -4.6 and -3.5 (Horan et al., 1998; Kleine et al., 2005; Schersten et al., 2006; Markowski et al., 2007). This is significantly less than the solar system initial of -3.51 ± 0.19 calculated by Schersten et al. (2006) as a weighted average of two independent chondrite Hf-W studies of Yin et al. (2002) and Kleine et al. (2002). A problem in interpreting the W-isotopic composition of iron meteorites is the effect of cosmic ray exposure on the W isotopes. Iron meteorites often have very long exposure ages up to a billion years and more. Galactic cosmic rays produce neutrons through secondary reaction with Fe and Ni, which after thermalization may react with W-isotopes. Since ^{182}W has a high thermal neutron capture cross section, the ^{182}W will be reduced making the metal-silicate separationage older than it is. The effect depends on the exposure age and the secondary neutron flux in the meteorite. However, only considering magmatic iron meteorites with short cosmic ray exposure ages, a formation interval of ~1.5 Myr directly after CAI formation is predicted (Schersten et al., 2006), lending support to the assumption that ^{26}Al is the principal heat source that triggered differentiation of these parent bodies. In contrast to magmatic iron meteorites,

non-magmatic iron meteorites display slightly more radiogenic εW signatures (Markowski et al., 2006; Schersten et al., 2006). Non-magmatic IAB irons formed 5 ± 3 Myr after CAIs and IIE irons within the first 19 Myr of solar system history (Markowski et al., 2006). The variations of $\varepsilon^{182}W$ signature in the non-magmatic iron meteorites possibly reflects an impact control on metal segregation, or an origin triggered by a combination of internal and external heat-sources.

Stony-iron meteorites are intermediate in their compositions between iron meteorites and achondrites. Some groups, such as pallasites, are assumed to originate from the core-mantle boundary of their parent body. They consists mainly of olivine and Fe-Ni metal. In contrast, mesosiderites are very heterogeneous with respect to their silicate textures from metamorphosed to partially molten (Floran, 1978; Hewins, 1983) and the distribution of metal (Wasson et al., 1972). All stony-iron meteorites have similar oxygen isotope compositions (Clayton and Mayeda, 1996). Quitté et al. (2005) applied the Hf-W chronometry to these meteorite groups to evaluate possible genetic relationships between stony-irons and the basaltic eucrites. The analyzed stony-iron metals have a quite variable ^{182}W isotope composition, even within a single meteorite. The values for these metals range between -1.3 to -4.2 ε-units. They concluded that some metals lost their primary ^{182}W signature due to thermally induced isotope exchange. Additionally it was found that some stony-irons have the same ^{182}W composition in their metal portion as that of primary eucrite metal. Arguing that this is not just a random coincidence, they proposed the formation of eucrites, mesosiderites and pallasites on the same parent body, where the stony-irons represent material from the outer portion of the core.

Achondrites

Eucrites are derived from the silicate portion of a differentiated asteroid, most likely the asteroid Vesta with a diameter of several kilometers. Eucrites are products of early mantle melting (e.g., Allegre et al 1975; Shukolyukov and Lugmair 1993; Lugmair and Shukolyukov 1998; Srinivasan et al., 1999, Quitté et al., 2000). As eucrites have a large excess of ^{182}W, reflecting early Hf-W fractionations due to core formation as well as mantle differentiation on their parent body. It is possible to make constrains on the timing of these two differentiation processes on the eucrite parent body (EPB) by detailed analyses of their Hf-W systematics.

Kleine et al. (2004) derived a combined whole-rock isochron for eucrites that defines an ^{182}Hf/^{180}Hf ratio of (7.25 ± 0.50) x 10^{-5}, yielding an age of 4563.2 ± 1.4 Myr. Since core formation cannot postdate mantle differentiation on the eucrite parent body (EPB), this age most likely gives the latest possible time of core formation. The eucrite isochron does, however, not pass through the chondritic value, indicating that this isochron dates silicate mantle differentiation which must then have occurred some time after core formation. Kleine et al. (2004) estimate an age difference of 0.9 ± 0.3 Myr between these two processes.

The first direct dating of the thermal metamorphism on the EPB was provided by Kleine et al. (2005). The analyzed eucritic metals were found to have high W contents and excesses in the abundance of ^{182}W between 2 and 16 ε–units, relative to an initial εW of -0.5 for the combined whole rock isochron, indicating a late re-mobilization of radiogenic W from silicates into metal. Hf-W ages for metal formation/re-equilibration in most of the analyzed eucrites overlap and give a weighted average that postdates the event dated with the combined whole-rock isochron by 16 ± 2 Myr (using Ste Marguerite as an anchor). Because

metal and silicates have not been in complete W isotopic equilibrium, Kleine et al. (2007) concluded that this age corresponds to a metamorphic, rather than a magmatic event.

Acapulcoites and Lodranites represent two groups of highly metamorphosed to partially molten groups of primitive achondrites. Acapulcoites are relatively fine-grained with chondritic proportions of troilite and plagioclase (McCoy et al., 1996), whereas lodranites are relatively coarse grained and tend to be depleted in troilite and plagioclase. Lodranites are residues of partial melting (McCoy et al., 1996). Both meteorite groups have similar oxygen isotope compositions, which resembles those of CR-chondrites. Both groups are therefore believed to form an evolutionary related sequence from a common parent body. Gaffey et al. (1993) support the idea of a possible match of the common Acapulcoite/Lodranite parent body with S asteroids, based on similarities in reflectance spectroscopy. Taking into account different heat-sources, Takeda et al. (1994) concluded that radioactive ^{26}Al and impacts were involved in triggering partial melting of these meteorites. Lee et al. (2006) determined the W isotope composition of a bulk rock sample from the Acapulcoite NWA 725 and of a metal phase from the Lodranite GRA 95209. Both samples exhibit deficits in ^{182}W between -2.6 and -3.3 ε-units, suggesting metal-silicate segregation not later than ~5 Myr since the start of the solar system. Touboul et al. (2007) analyzed metallic and silicate separates from three different Acapulcoites (Dhofar 125, NWA 2627 and NWA 2775) with Hf/W ratios up to ~50. Measured W concentrations in the Acapulcoite metal were found to be similar to those observed for metals in equilibrated ordinary chondrites, indicating transfer of W from silicates into metal during thermal metamorphism. A combined isochron with a slope corresponding to an initial ^{182}Hf/^{180}Hf ratio of 6.50 ± 0.23 x 10^{-5} yields an absolute age of 4562.1 ± 1.4 Myr, using an initial ^{182}Hf/^{180}Hf for

Allende CAIs (Kleine et al., 2005) and the absolute age for CAIs of 4568.5 ± 0.5 Myr (Bouvier et al., 2007). The Hf-W age is older than a Pb-Pb age for phosphates (4557 ± 2 Myr, Zipfel et al., 1995) and a Mn-Cr age from Acapulco oxides and silicates (4555 ± 1 Myr, Lugmair et al., 1998), most likely reflecting the higher blocking temperature of the Hf-W system compared to the other chronometers.

Aubrites (enstatite achondrites) are brecciated meteorites that formed under the most reducing conditions recorded in solar system materials (Keil, 1989; Casanova et al., 1992). They consists mainly of Fe-free enstatite (Lodders et al., 1991). Oxygen isotope ratios for most aubrites plot close to the terrestrial fractionation line (Lorenzetti et al., 2003). Shifts in the isotopic composition of Sm and Gd are in part a result of cosmic-ray irradiation on the regolithic surface of their parent body (Hidaka et al., 2006). Petitat et al. (2008) applied Hf-W chronometry to this meteorite group and found them to be clustered in two age groups. The first group has ages of ~4560 Myr, the second has ages of ~4550 Myr. However, so far it remains unclear if the isochrones provide meaningful ages, because it is not shown whether the different fractions of one meteorite have been in isotopic equilibrium or not.

Angrites represent the oldest igneous rocks that formed in the solar sytem. They formed under oxidizing conditions and are mainly composed of plagioclase, Ca-Ti pyroxene and olivine (Floss et al., 2003). Angrites can be subdivided according to their different cooling-rates. Some angrites cooled very rapidly and have quenched melt textures like skeletal anorthite crystals (Mikouchi et al., 2000; Mikouchi and McKay 2001), whereas some members of this group are metamorphosed and have a more complex cooling history (Mikouchi et al., 2000; Fittipaldo et al., 2005; Irving et al., 2005; Kuehner et al., 2006). Amelin et al.

(2008) applied Pb-Pb chronometry to several angrites and found an age interval of ~7 Myr. All measured ages lie between ~4557 Myr (Angra dos Reis) and ~4564 Myr (D`Orbigny). Markowski et al. (2007) applied the Hf-W chronometry to three meteorites of this group. Using an initial (^{182}Hf/^{180}Hf) for CAIs of (1.07 ± 0.2) x 10^{-5} (Kleine et al., 2005) and a corresponding Pb-Pb age of 4568.5 ± 0.5 Myr (Bouvier et al., 2007) as an anchor, they derived ages of 4563.4 ± 1.4 Myr for Sahara 99555, 4559.0 ± 3.3 Myr for NWA 2999 and 4563.8 ± 1.4 Myr for D`Orbigny. They concluded that two distinct metal-silicate separation events affected the angrite parent body within the first ~5 Myr, resulting in different Hf/W ratios of the mantle, similar to that on Mars (~4, Lee and Halliday, 1997) and much lower than the respective values for the Moon (~27, Jones and Palme, 2000) and the Earth (~20, Newsom et al., 1996). Finally, Kleine et al. (2008) obtained internal Hf-W isochrones for the angrites Northwest Africa 4590 and 4801 and yield corresponding initial ^{182}Hf/^{180}Hf ratios of (4.81 ± 0.17) x 10^{-5} and (4.49 ± 0.24) x 10^{-5}. A comparison of known Pb-Pb ages for the angrites D`Orbigny, Sahara 99555, Northwest Africa 4590 and 4801 led Kleine et al. (2008) conclude that a calibration of the Hf-W system onto an absolute timescale yields consistent results regardless of which of the four angrites is used as an anchor.

4.3   Analyzed samples and results

Acapulcoite samples selected for this study include silicate separates from the Monument Draw and Dhofar 125 specimens. Monument Draw consists of olivine, orthopyroxene, chromian diopside, plagioclase, Fe-Ni metal, troilite and chromite. The presence of numerous 120° triple junctions indicate extensive recrystallization (McCoy et al., 1992). Dhofar 125 has very similar mineralogy. A

two-pyroxene equilibration temperature of 1120°C calculated for Dhofar 125 lies well within the 980-1170°C range that is typical for other Acapulcoites (Greshake et al., 2001). Hafnium-W data for acapulcoites are summarized in Table 1. The W concentration in the metal separate from Dhofar 125 is ~ 0.5 ppm. Tungsten concentrations measured for weakly magnetic fractions vary between ~50 ppb and ~250 ppb. A bulk sample measured from Dhofar 125 shows a slightly superchondritic Hf/W ratio of ~1.9. The $^{182}W/^{184}W$ measurement of the metal phase from Dhofar 125 yielded a value of -2.9 ± 0.4 ε-units. Non-magnetic fractions exhibit excesses in ^{182}W up to +11.7 ε-units at a Hf/W as high as ~14. A weakly magnetic fraction of Monument Draw displays, within uncertainty, the same ^{182}W signature (-2.3 ± 0.4 ε-units) as the metal separate in Dhofar 125. All separates define a linear array with the slope corresponding to $^{182}Hf/^{180}Hf = (7.04 ± 0.66) \times 10^{-5}$ and an initial $^{182}W/^{184}W$ ratio of -3.1 ± 0.3 ε-units (Fig. 4.1). The slope corresponds to an age of 4563.9 ± 1.4 Myr (4.6 ± 1.3 Myr relative to CAIs), using an initial $^{182}Hf/^{180}Hf$ ratio of $(1.01 ± 0.05) \times 10^{-4}$ for Allende CAIs (Burkhardt et al., 2007) and the absolute Pb-Pb age for CAIs of 4568.5 0.5 Ma (Bouvier et al., 2007). Internal isochrones for the analyzed Acapulcoite specimens yield initial $^{182}Hf/^{180}Hf$ ratios of $(6.34 ± 0.96) \times 10^{-5}$ (Dhofar 125) and $(7.64 ± 0.90) \times 10^{-5}$, both indistinguishable from the combined Acapulcoite isochron. A value for carbonaceous chondrites (εW value -1.9 ± 0.1 and a chondritic Hf/W ratio of ~1.2; Kleine et al., 2004) plots on the combined Acapulcoite isochron, reflecting the chondritic bulk composition of the Acapulcoites.

Meteorite	Separate	$^{182}W/^{184}W$ [6/4]±2σ	εW [6/4]±2σ	W [ppm]	Hf [ppm]	$^{180}Hf/^{184}W$ ±2σ
Monument Draw	NM	0.865692 ± 138	11.7 ± 1.6	0.0223	0.3006	16.824 ± 84
	WM	0.864481 ± 35	-2.3 ± 0.4	0.2624	0.2178	0.9803 ± 49
Dhofar 125	M	0.864429 ± 35	-2.9 ± 0.4	0.5377	0.0475	0.1041 ± 5
	WM	0.864749 ± 35	0.8 ± 0.4	0.0520	0.2261	5.1310 ± 257
	bulk	0.864576 ± 35	-1.2 ± 0.4	0.1096	0.2082	2.2400 ± 112

Table 4.1: NM = non-magnetic fraction, WM = weakly magnetic fraction; M = metal; bulk = whole rock. The εW values of each isotope measurement are expressed as the deviations in parts per 10,000 relative to the terrestrial standard value of 0.864680. Uncertainties refers to the last significant digits.
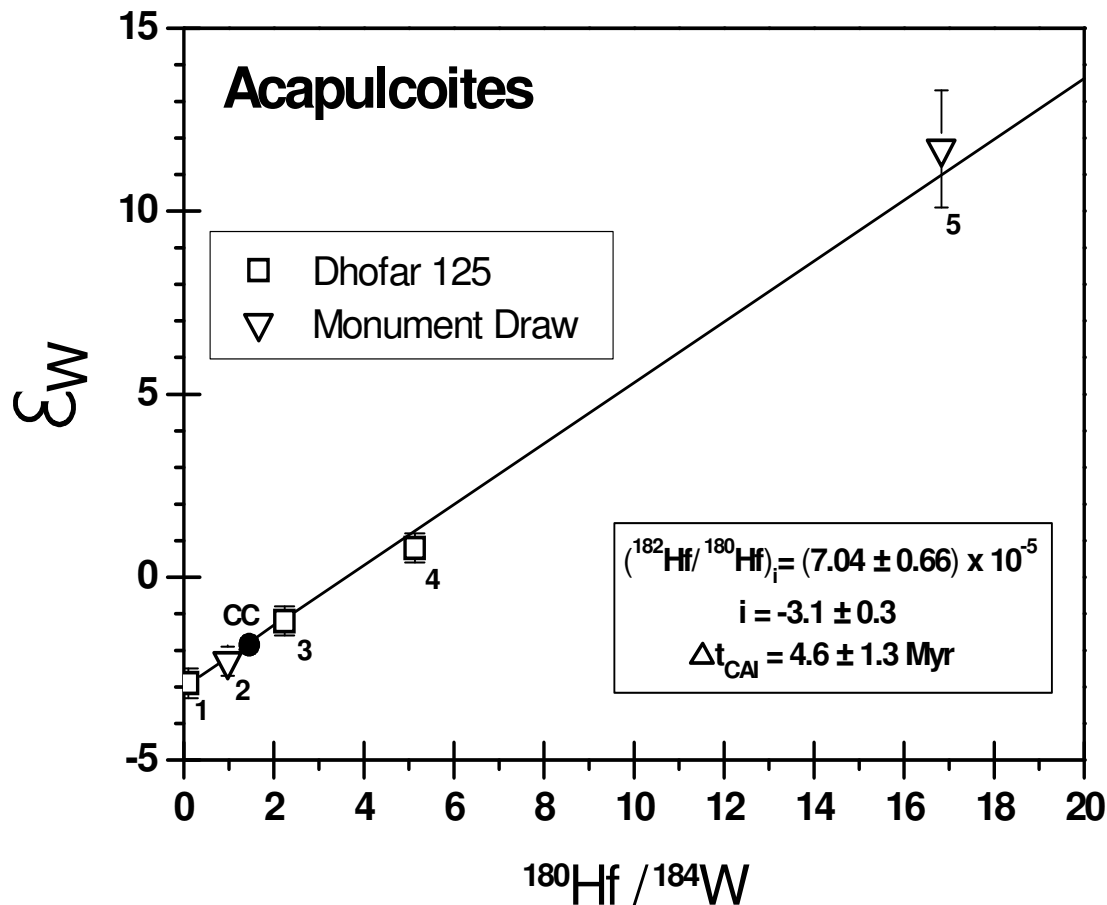
Figure 4.1: εW versus ^{180}Hf/^{184}W for Acapulcoites (MSWD = 1.4). 1 = Dh125-M, 2 = MD-WM, 3 = Dh125-WM, 4 = Dh125-bulk, 5 = MD-NM (MD=Monument Draw), CC = carbonaceous chondrites. The isochron was calculated including all analyzed Acapulcoite samples (model 1 fit from ISOPLOT; Ludwig, 1991). The slope corresponds to a time interval of 4.6 ± 1.3 Myr between Allende CAIs (^{182}Hf/^{180}Hf of 1.01 ± 0.05 x 10^{-4}; Burkhardt et al., 2007) and Acapulcoites.

Samples from Winonaites selected for this study include silicate fractions obtained from the Winona, Mount Morris, Hammadah al Hamra 193 and NWA 4024 meteorites. Additionally, it was possible to extract a pure metal phase from

NWA 4024. Hammadah al Hamra 193 (HaH 193) is a fluoro-edenite bearing winonaite. Winona, the type specimen for this meteorite group as well as Mount Morris are fine-grained rocks with equigranular textures and patches interpreted as partial melt residues (Floss et al., 2003). Hafnium-W data for Winonaites are summarized in Table 2. The W concentration in the metal phase of NWA 4024 is ~0.3 ppm. Tungsten concentrations measured for weakly magnetic fractions vary between 70 and 170 ppb, those for non-magnetic separates between 40 and 80 ppb. A bulk sample measured from NWA 4024 shows nearly chondritic Hf and W concentrations, yielding a typical chondritic Hf/W ratio of ~1.2. The $^{182}W/^{184}W$ measurement of the metal phase from NWA 4024 gave a value of -2.5 ± 0.3 ε-units. This value provides an important constraint on the time of metal-silicate segregation in the Winonaite parent body. Non-magnetic fractions exhibit excesses in ^{182}W up to +2.7 ε-units. The weakly magnetic fraction of HaH 193 shows, within uncertainty, the same ^{182}W signature of -2.4 ± 0.5 ε-units as the metal in NWA 4024, even though its Hf/W ratio is nearly chondritic. In the εW versus $^{180}Hf/^{184}W$ space, most analyzed separates show the expected increase of ^{182}W excesses with increasing Hf/W ratios. Six of the eight separates from HaH 193, Mount Morris, Winona and NWA 4024 define a linear array with a slope corresponding to an initial $^{182}Hf/^{180}Hf$ of (3.27 ± 0.69) x 10^{-5} and an initial $^{182}W/^{184}W$ ratio of -2.9 ± 0.4 ε-units (Fig. 4.2). Two separates from Winona (WM-1) and Mount Morris (NM) lie above this isochron. An internal isochron for Winona (neglecting the outlier separate WM-1) yields an initial $^{182}Hf/^{180}Hf$ of (3.26 ± 0.39) x 10^{-5}, indistinguishable from the combined isochron. The slope corresponds to a time-interval of 14.5 ± 2.8 Myr after CAIs and an absolute age of 4554.0 ± 2.9 Myr, using the same initial $^{182}Hf/^{180}Hf$ ratios of (1.01 ± 0.05) x 10^{-4} for Allende CAIs (Burkhardt et al., 2007) and the same absolute Pb-Pb age for CAIs of 4568.5 ± 0.5 Myr (Bouvier et al., 2007) as before. The value for

carbonaceous chondrites (εW value at -1.9 $\pm$ 0.1; Kleine et al., 2004) does not plot on the combined Winonaite-isochron.

Meteorite	separate	^{182}W/^{184}W [6/4]$\pm2\sigma$	εW [6/4]$\pm2\sigma$	W [ppm]	Hf [ppm]	^{180}Hf/^{184}W $\pm2\sigma$
HaH 193	NM	0.864524 $\pm$ 43	-1.8 $\pm$ 0.5	0.0414	0.1279	3.7121 $\pm$ 185
	WM	0.864472 $\pm$ 43	-2.4 $\pm$ 0.5	0.1701	0.1398	0.9704 $\pm$ 49
Mount Morris	bulk	0.864689 $\pm$ 43	0.1 $\pm$ 0.5	0.0823	0.0271	0 .3891 $\pm$ 19
Winona	WM-1	0.864913 $\pm$ 215	2.7 $\pm$ 2.7	0.0702	0.0554	0.9321 $\pm$ 280
	WM-2	0.864455 $\pm$ 43	-2.6 $\pm$ 0.5	0.1485	0.0423	0.3358 $\pm$ 17
	NM	0.864732 $\pm$ 50	0.6 $\pm$ 0.6	0.0420	0.3135	8.8180 $\pm$ 352
NWA 4024	M	0.864464 $\pm$ 35	-2.5 $\pm$ 0.3	0.2679	0.0096	0.0423 $\pm$ 2
	bulk	0.864455 $\pm$ 50	-2.6 $\pm$ 0.6	0.1445	0.1532	1.2516 $\pm$ 63

Table 4.2: NM = non-magnetic fraction, WM = weakly magnetic fraction; M = metal; bulk = whole rock. 1 and 2 denote different fractions of the same meteorite. The εW values of each isotope measurement are expressed as the deviations in parts per 10,000 relative to the terrestrial standard value of 0.864680. Uncertainties refers to the last significant digits.
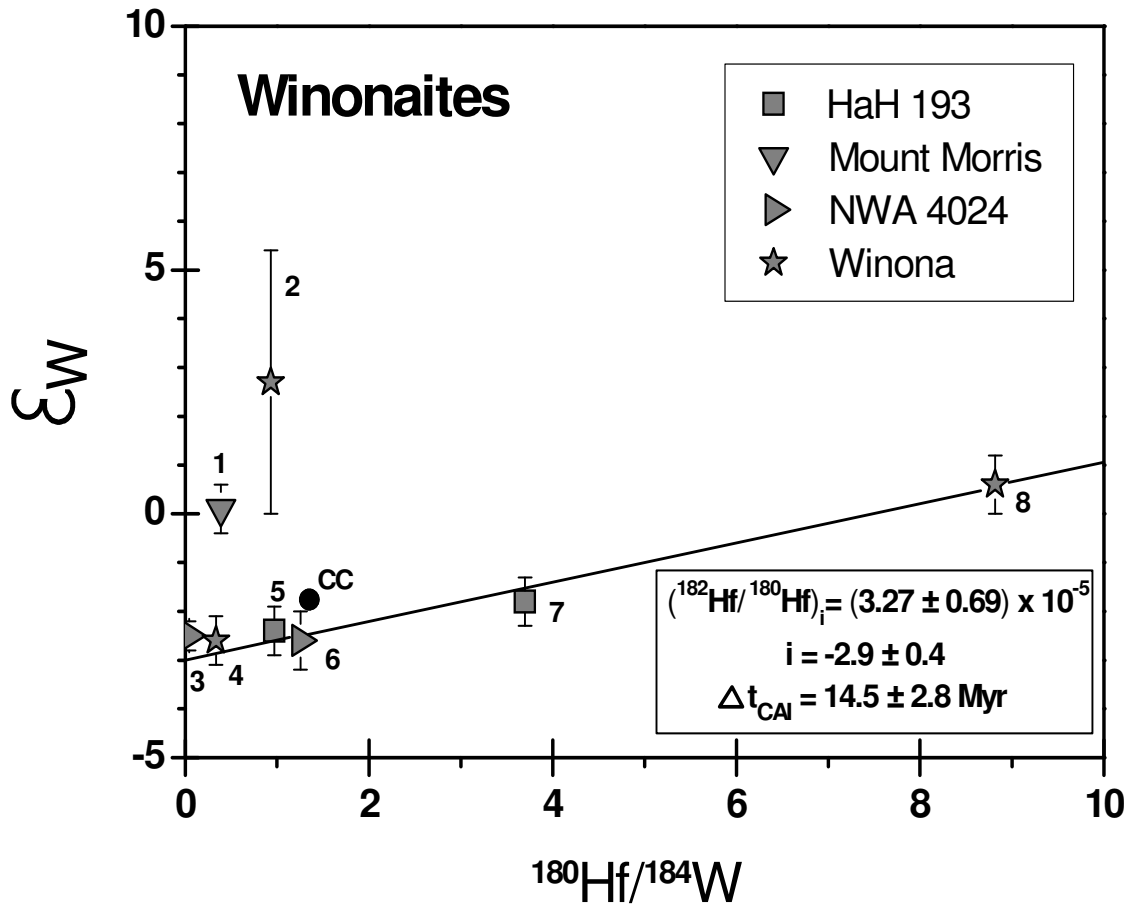
Figure 4.2: εW versus $^{180}Hf/^{184}W$ for Acapulcoites (MSWD = 0.97). 1 = MM-bulk, 2 = Win-WM1, 3 = NWA4024-M, 4 = Win-WM2, 5 = HaH193-WM, 6 = NWA4024-bulk, 7 = HaH193-NM, 8 = Win-NM (MM=Mount Morris, Win = Winona, HaH193 = Hammadah al Hamra 193, CC = carbonaceous chondrites). The isochron was calculated including all analyzed samples except samples 1 and 2 (model 1 fit from ISOPLOT; Ludwig, 1991). The slope corresponds to a time interval of 14.5 ± 2.8 Myr between Allende CAIs ($^{182}Hf/^{180}Hf$ of 1.01 ± 0.05 x 10^{-4}; Burkhardt et al., 2007) and winonaites.

4.4   Discussion

The Acapulcoite parent body

A linear trend defined by the six data-points of separates from Monument Draw and Dhofar 125 is interpreted as an isochron, yielding an age of 4.6 ± 1.3 Myr after solar system formation (relative to CAIs), within uncertainties indistinguishable from the model age calculated from the intercept of the the isochron (3.5 ± 3.3 Myr relative to CAIs). The Acapulco isochron defines an age that indicates cooling below the Hf-W blocking temperature. That all points lie on the isochron within error limits suggests that the system was not disturbed after the first cooling below the blocking temperature. A point defined by carbonaceous chondrites plots on the combined isochron, indicating that the Acapulcoite parent body had a chondritic composition, i.e., a chondritic Hf/W ratio.

Comparing age differences obtained for Acapulcoites using different chronometers with different blocking temperatures allows the deduction of cooling rates for acapulcoites. Figure 4.4 indicates an exponential cooling curve for the Acapulcoite parent body, showing an effective heat loss with cooling rates of ~100°C/Myr in the high temperature interval (700-400°C) and cooling rates of about 10°C/Myr in the low temperature interval (<400°C). This is in agreement with earlier estimates (Zipfel et al., 1995). A previously proposed model for the evolution of the ordinary chondrites is an onion-shell-layered model, which involves different cooling rates for rocks from varying burial depths in an internally heated parent body (Herndon et al., 1977; Trieloff et al., 2003). The slowest cooling rates are expected in the center of the asteroid, near surface regions cool much faster. As Figure 4.3 reveals, the exponential cooling curve

deduced for Acapulcoites is similar to that observed for the H4-chondrite Ste. Marguerite, but significantly steeper than that observed for the equilibrated H6-chondrite Kernouve. This is a clear indication that Acapulcoites cannot be derived from the H-chondrite parent body, as Acapulcoites have seen higher equilibration temperatures than H6 chondrites but cooled faster than equilibrated H-chondrites. A different parent body of H-chondrites and acapulcoites is also required from oxygen isotopes (Clayton and Mayeda 1996). Acapulcoites must be derived from a smaller parent body which was heated to higher temperatures than ordinary chondrites. This would imply higher ^{26}Al-contents. One should therefore expect that Acapulcoites are older than ordinary chondrites, assuming a uniform distribution of ^{26}Al. However, this assumption is unlikely, because a Hf-W age for the H4-chondrite Ste. Marguerite is significantly older (2.2 ± 1.2 Myr; Kleine et al., 2002) than that obtained for the Acapulcoites (4.6 ± 1.4 Myr after CAIs; this study). Either ^{26}Al was not homogeneously distributed in the solar system or other heat sources, such as impacts must be invoked to produce the required re-distribution of Hf and W isotopes.
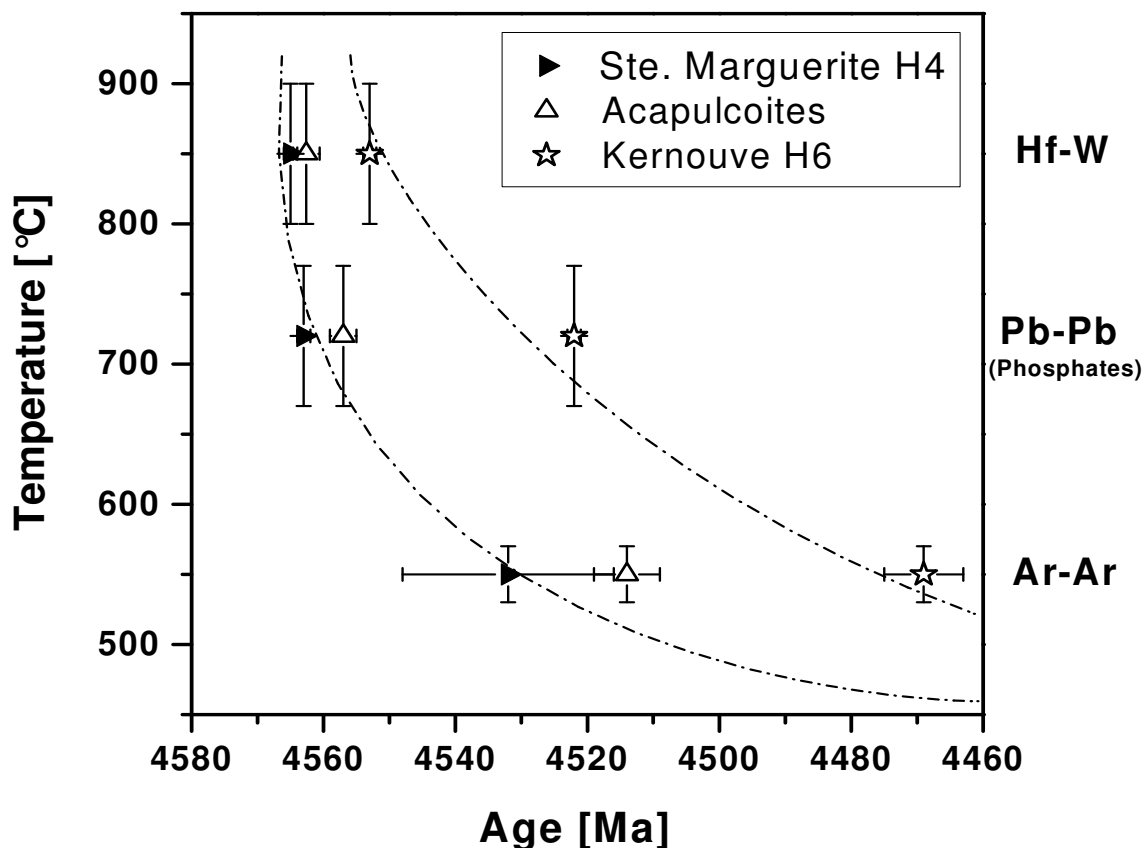
Figure 4.3: Cooling curves for H-chondrites and Acapulcoites. Hf-W ages are from Kleine et al., 2002 (Ste Marguerite), Kleine et al., 2006 (Kernouve). Pb-Pb and Ar-Ar ages for chondrites as well as blocking temperatures from Trieloff et al., 2001 and Trieloff et al., 2003 for Acapulcoites. A Pb-Pb age for Acapulco phosphates is taken from Zipfel et al., 1995. Blocking temperature for Hf-W from Kleine et al., 2005.

The Winonaite parent body

A linear regression fitted through six out of eight data-points is interpreted as a combined isochron, yielding an age 14.5 ± 2.8 Myr after solar system formation (relative to CAIs). This age is apparently to young to be related to an

internal heat-source. It is therefore valid to assume that this age represents an impact controlled event. A point for carbonaceous chondrites (Kleine et al., 2002) plots close but off the combined Winonaite-isochron (Fig. 4.2). Therefore the precursor material of the Winonaites seems to be not related to this chondrite group. Despite their low Hf/W ratios two of the analyzed metal-rich separates from Winona and Mount Morris show radiogenic ^{182}W values and also do not plot on the isochron defined by all other sample splits. A possible explanation for these unexpectedly radiogenic values could be a late stage formation of metals from a silicate reservoir that already accumulated radiogenic W. Hence, there is evidence for two generations of metals in winonaites. The metals plotting on the isochron constitute first stage metal formed during initial metal-silicate segregation, whereas two radiogenic metal-rich separates from Winona and Mount Morris constitute second-stage metal. The time for metal-silicate segregation is assumed to be given by the age of the combined Winonaite isochron and the ^{182}W composition of a discrete metal-chunk from NWA 4024 (-2.5 ± 0.3 ε-units). Contemporaneously or after initial metal-silicate segregation, tiny first stage metal inclusions in the winonaites (with an ε^{182}W signature of ~ -2.5) may acquired radiogenic W during diffusion from the initially more radiogenic silicates, thereby forming second stage metal generations, exhibiting different radiogenic W compositions. In an alternate scenario second-stage metals formed in situ via reduction of Fe^{II+}. The highly reduced compositions of the Winonaites, together with the presence of second stage metals in other achondrites (e.g. eucrites; Kleine et al. 2005) tentatively suggests a second episode of metal procession.

Plotting the respective blocking temperatures for the Hf-W and Ar-Ar chronometers against available age data allows the deduction of cooling curves for winonaites (Fig. 4.4). Taking the age of the combined Winonaite isochron as

a starting point (the last W exchange between metal and silicate during progressive cooling of the Winonaite parent body) it is possible to identify individual cooling paths for different winonaites. The apparently old Ar-Ar age for Pontlyfni (4.529 ± 0.013 Myr; Benedix et al., 1998) indicates fast and more or less constant cooling within the parent body (~100°/Myr in the 800-400°C interval), possibly due to a shallow burial depth. Contrastingly, Winona and Mount Morris have significantly younger Ar-Ar ages of ~4.51 Ga and ~4.40 Ga (Benedix et al,. 1998), indicating a common and more exponential cooling path for this specimens. This most likely is an evidence for a deeper burial depth for Mount Morris and Winona within the Winonaite parent body compared to Pontlyfni.
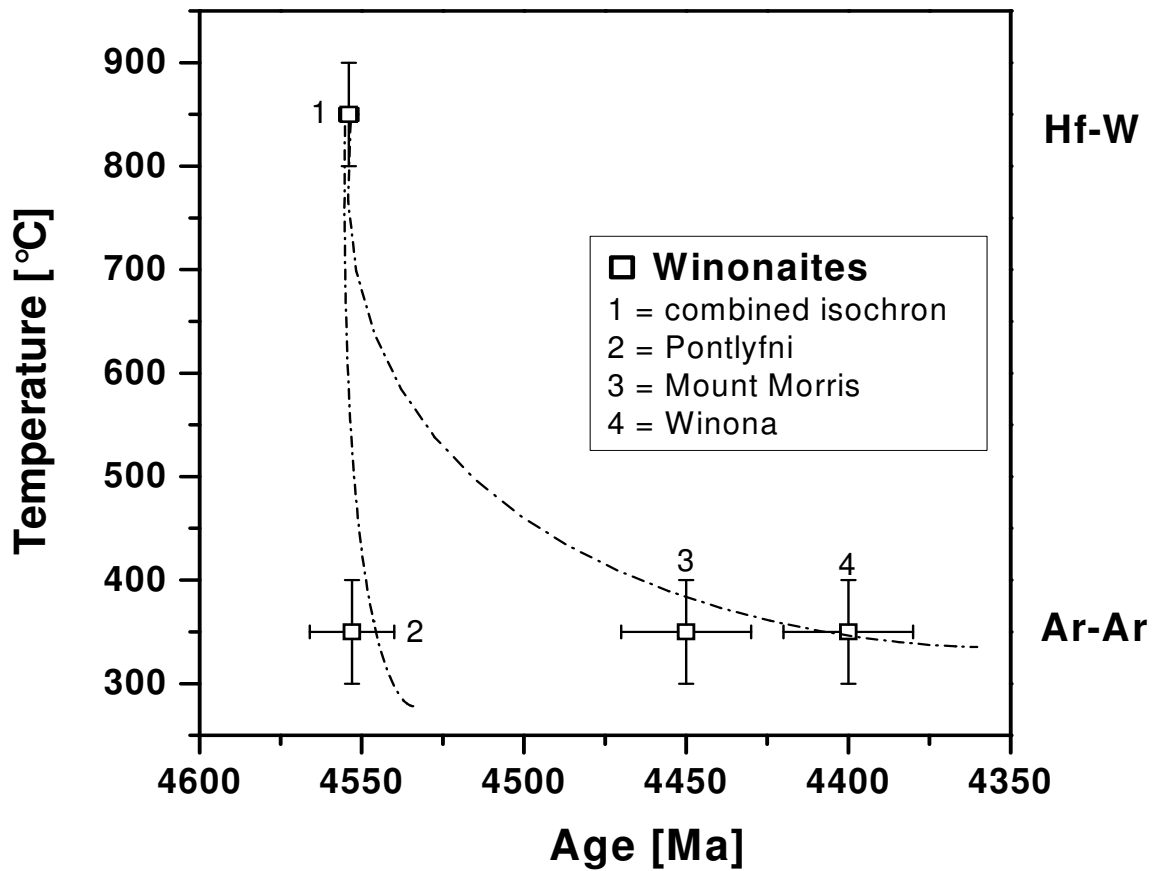
Figure 4.4: Cooling curves for Winonaites. 1 = this study, 2 - 4 = Benedix et al., 1998. Blocking temperature for Hf-W from Kleine et al., 2005. Average blocking temperature for K-Ar from Vogel et al., 2008.

It was argued earlier that winonaites and IAB iron meteorites are related to each other and probably originate from the same parent body. Given this assumption, the age information obtained for the winonaites preferably represents a discrete impact related thermal event in the surface region of a common Winonaite/IAB parent asteroid. The metamorphic event at 14.5 ± 2.8 Myr after CAIs (combined Winonaite isochron) could then be related to the "El Taco event" at 11.3 ± 2.3 Myr after CAIs (see Chapter 3). After accretion, an internal heating source (most probably ^{26}Al) caused incomplete differentiation of the

Winonaite/IAB parent body as described in Chapter 3. During the early stages of parent body cooling, the temperature passes through the blocking temperature of the I-Xe and Hf-W systems (Fig. 4.5). If a more or less constant cooling rate is assumed during the 1000-700°C interval, an average rate of ~100°C/Myr is obtained. On the other hand, measured Ar-Ar ages for IAB silicates (Vogel et al., 2008) and most Winonaites (Benedix et al., 1998) are younger by 50 to 150 Myr compared to the I-Xe and Hf-W ages. This implies a significantly slower cooling rate of ~5°/Myr in the 700-400°C interval. This is consistent with previous estimates for metallographic cooling rates of IAB iron meteorites that lie in the range of 1-10°/Myr (Rasmussen, 1989), 30-70°/Myr (Herpfer et al., 1994) and 1-15°/Myr (Meiborn et al., 1995). Rb-Sr and Sm-Nd age data for IAB silicates fit well in the cooling trend for most winonaites and therefore confirm a common cooling path for most IAB silicates and winonaites. An Ar-Ar age obtained for Pontlyfni (Benedix et al., 1998) and an age for Caddo County gives a significantly older age compared to Mount Morris and Winona (Benedix et al., 1998), most likely indicating that at least some Winonaites and IABs experienced a faster cooling history, probably correlating with a shallower burial depth. According to the Benedix et al., 2000 formation model for the Winonaite/IAB parent body, a catastrophic impact destroyed the parent asteroid, which than re-established as a rubble pile. Based on Ar-Ar age data for IAB silicates, Vogel et al., 2008 placed this disruption and reassembly event between 4500-4450 Myr. The contrasting cooling rates could then represent the pre-impact (fast cooling; ~100°/Myr) and post-impact (slow cooling; ~5°/Myr) histories.
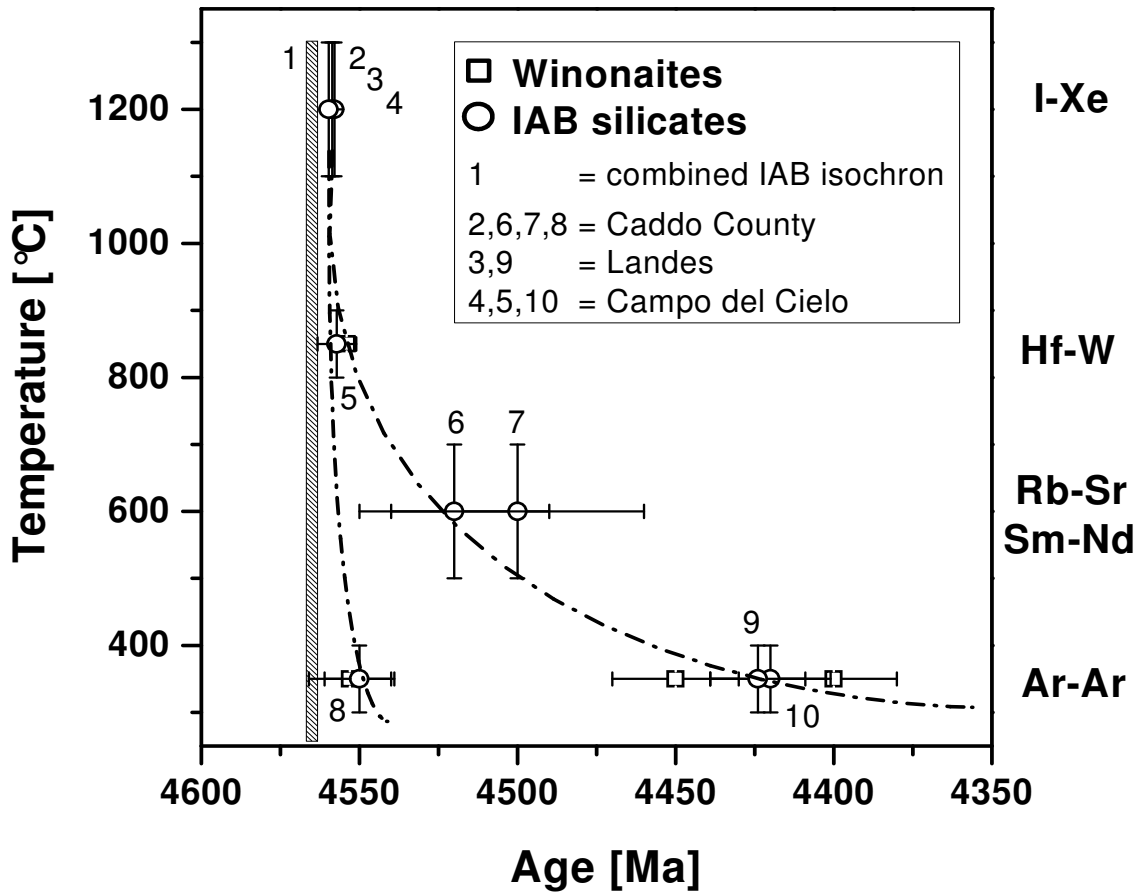
Figure 4.5: Cooling curves for a common Winonaite/IAB parent body. 1,5 = this study, 2 = Takeda et al., 2000, 3 = Niemeyer 1979a, 4 = Podosek 1970, 6,7 = Liu et al., 2002, 8-10 = Vogel et al. 2008. Blocking temperatures for Hf-W from Kleine et al., 2005, for K-Ar from Vogel et al., 2008. Those for I-Xe, Rb-Sr and Sm-Nd are only approximate (see Bogard et al., 2005).

4.5   Conclusions

The timing of accretion and differentiation of asteroidal bodies in the early solar system is essential for a complete understanding of asteroid-forming processes. In this study, we applied the extinct Hf-W chronometer to winonaites and acapulcoites because this radionuclide-system provides a high time-resolution for early solar system processes (e.g. metal segregation, silicate differentiation and metamorphism). Building on previous work, we established a broader model, describing the timing of the beginning of asteroidal differentiation during the first few million years of solar system history.

The enhanced Hf-W dataset in Figure 4.6 tentatively suggests that most parent bodies of achondritc meteorites accreted and differentiated contemporaneously or shortly after the formation of chondrites. On the other hand the W isotope composition of magmatic iron meteorites provide unequivoval evidence of metal segregation in the solar system within the first ~1.5 Myr (Schersten et al., 2006), shortly before chondrite formation. Therefore it is very unlikely to assume that the undifferentiated chondrites are the precursor material of the magmatic iron meteorites (e.g. Kleine et al. 2004). There is also no temporal link between all of the achondrite groups analyzed so far and magmatic iron meteorites. The fact that all analyzed achondrites formed contemporaneously with or shortly after the chondrite genesis, clearly evidences that silicate complementaries of the earliest segregated irons are missing (assuming that combined whole rock isochrones for differentiated silicate groups obtained so far are primary and have not been thermally resetted).
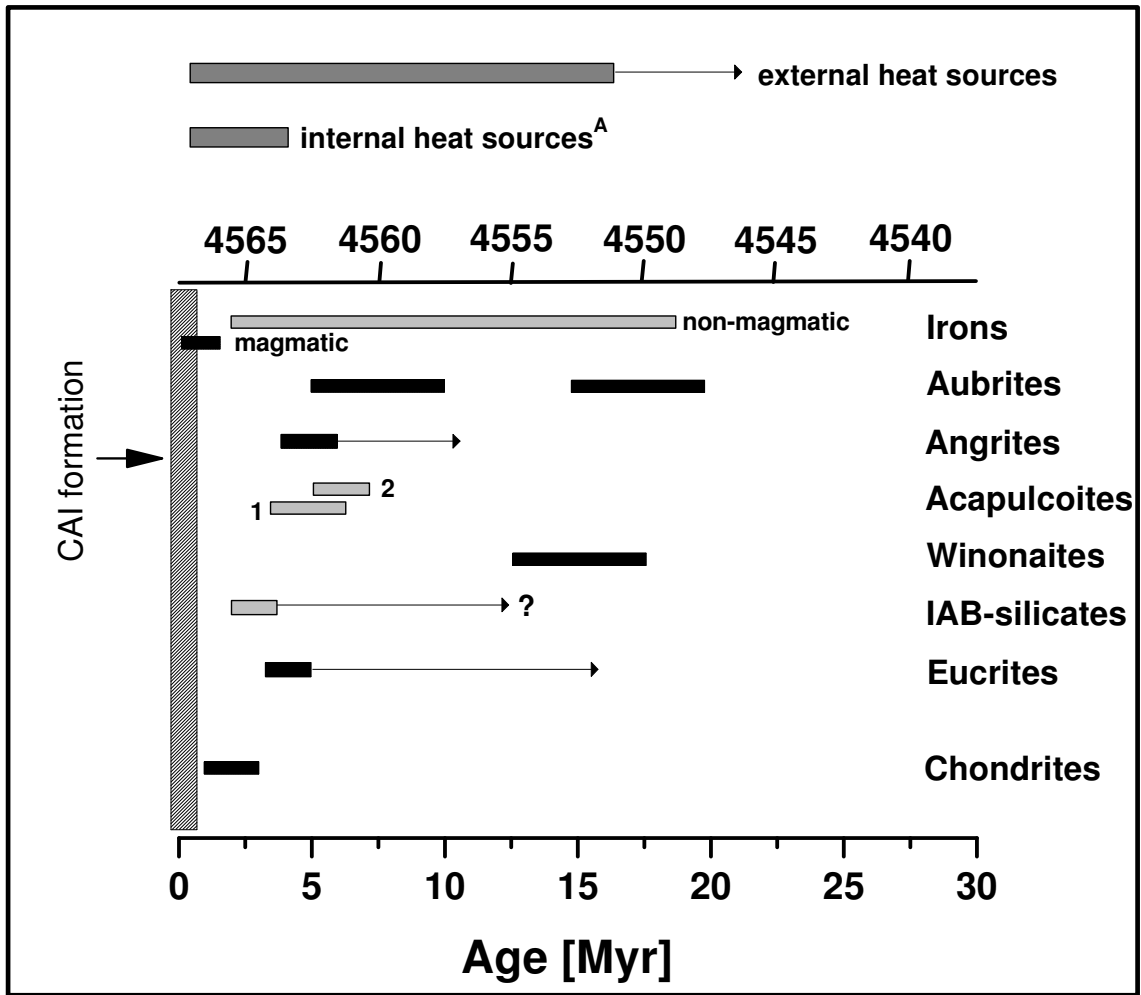
Figure 4.6: Comparison of asteroidal differentiation processes as inferred from Hf-W chronometry. 1 = data from this study; 2 = data from Touboul et al., 2007

Chapter 5

Summary and conclusions

Summary and conclusions

The aim of this thesis was to investigate differentiation processes (metal-silicate segregation, silicate differentiation and metamorphism) in the parent bodies of three different achondritic meteorite groups:

1) The IAB iron meteorite parent body

The earliest stages of the evolution of the IAB parent body are characterized by three events that occurred more or less contemporaneously within the first ~6 Myr of solar system history and are probably triggered by an internal heat source:

- A limit on the timescales involved in metal segregation on the IAB parent body were obtained from a weighted average of the ε^{182}W values for seven metal phases (-3.1 ± 0.2 ε-units), corresponding to the time of 4565.0 ± 2.3 Myr (3.5 ± 2.3 Myr relative to CAIs)

- A combined silicate isochron defined by three bulk inclusions from different IAB specimens yields an age of 4565.6 ± 2.7 Myr (2.9 ± 2.2 Myr relative to CAIs), corresponding to the time of silicate differentiation on the IAB parent body

- Partial melting of silicates on the IAB parent body is likely to have occurred at 4563.6 ± 2.6 Myr (4.9 ± 2.0 Myr relative to CAIs), as indicated by an internal Caddo County isochron

A prolonged history of thermal metamorphism on the IAB parent body is indicated by three events that occurred more or less contemporaneously ~12 Myr after the start of the solar system and that probably can be attributed to a single impact event:

- A second episode of metal segregation on the IAB parent body is indicated by the $\varepsilon^{182}W$ signature of metal from the Mundrabilla meteorite (~ -2.6), which corresponds to a time of ~4558 Myr (~11 Myr relative to CAIs)

- Three separates from a single El Taco inclusion define an internal silicate isochron, corresponding to a time of 4557.2 ± 3.1 Myr (11.3 ± 2.3 Myr relative to CAI formation). This most likely indicates a short re-heating event

- A regression line defined by two Lueders separates yields a maximum age that postdates the formation of CAIs by ~12 Myr

2) The Winonaite parent body

- A linear regression fitted through six out of eight winonaite separates is interpreted as a combined isochron, yielding an age of 4554.1 ± 3.8 Myr (14.5 ± 2.8 Myr relative to CAI formation), apparently too young to be related to an internal heat-source

- Assuming that winonaites and IAB iron meteorites originate from the same parent body, the age information obtained for the winonaites preferably represents a discrete impact related thermal event in the surface region of the common Winonaite/IAB parent asteroid (most likely related to the Mundrabilla-, El Taco- and Lueders- ages)

3) The Acapulcoite parent body

    - Five Acapulcoite separates define a linear array with a slope corresponding to an absolute age of 4563.9 ± 1.4 Myr (4.6 ± 1.3 Myr relative to CAI formation)

    - An exponential cooling curve deduced for Acapulcoites suggests that this meteorite group must be derived from a smaller asteroid than the H-chondrite parent body

    - Acapulcoites are younger than the H4-chondrite Ste. Marguerite. Therefore impact events must be invoked to produce the required re-distribution of Hf and W isotopes (or, alternatively, ^{26}Al was not homogeneously distributed in the early solar system)

A comparison with Hf-W data compiled from the literature shows that asteroidal differentiation on the Winonaite/IAB iron meteorite and Acapulcoite parent body occurred well after the formation of most magmatic iron meteorites and contemporaneously with or shortly after the accretion of known chondrite parent bodies, lending further support for a revised solar system chronology where chondrites cannot be the precursor material of differentiated asteroids.

References

Allegre C.J., Birck J.L., Fourcade S., Semet M.P. (1975), ^{87}Rb-^{87}Sr age of Juvinas basaltic achondrite and early igneous activity in the solar system, *Science* **187**, 436-438

Amelin Y., Krot A. N., Hutcheon I.D., Ulyanov A.A. (2002), Lead isotopic ages of chondrules and calcium-aluminium rich inclusions, *Science* **297,** 1678-1683

Amelin Y., Wadhwa M., Lugmair G. (2006), Pb-isotopic dating of meteorites using 202Pb-205Pb double spike: comparison with other hogh resolution chronometers, *Lunar Planet. Sci.* XXXVII, #1970

Amelin Y., Irving A.J. (2007), Seven million years of evolution on the Angrite parent body, *Chronol. of Met.* 1347, 20-21

Amelin Y. (2008), U-Pb ages of angrites, *Geochim. Cosmochim. Acta* **72**, 221-232

Baker J., Bizzarro M., Wittig N., Conelly J., Haack H., Early planetesimal melting from an age of 4.5662 Gyr for differentiated meteorites, *Nature* **436**, 1127-1131

Benedix G.K., McCoy T.J., Keil K., Bogard D.D., Garrison D.H., A petrologic and isotopic study of winonaites: evidence for early partial melting, brecciation and metamorphism, *Geochim. Cosmochim. Acta* **62**, 2553-2553

Benedix G.K., McCoy T.J., Keil K., Love S.G. (2000), A petrologic study of the IAB iron meteorites: Constraints on the formation of the IAB-Winonaite parent body, *Geochim. Cosmochim. Acta* **35**, 1127-1141

Benedix G.K., Lauretta D.S., McCoy T.J. (2005), Thermodynamic constraints on the formation conditions of winonaites and silicate-bearing IAB irons, *Geochim. Cosmochim. Acta* **69**, 5123-5131

Bild R.W. (1977), Silicates in group IAB irons and a relation to the anomalous stones Winona and Mt. Morris, *Geochim. Cosmochim. Acta* **41**, 1439-1456

Bizzarro M., Baker J.A., Haack H. (2004), Mg isotope evidence for contemporaneous formation of chondrule and refractory inclusions, *Nature* **431**, 275-278

Bizzarro M., Baker J.A., Haack H., Lundgaard K.L. (2005), Rapid timescales for accretion and melting of differentiated planetesimals inferred from ^{26}Al-^{26}Mg chronometry, *Astrophysical Journal* **632**, 41-44

Bogard D.D., Garrison D.H., Takeda H. (2005), Ar-Ar and I-Xe ages and the thermal history of IAB meteorites, *Meteoritics* **40**, 207-224

Bouvier A., Blichert-Toft J., Moynier F., Vervoort J.D., Albarede F. (2007) Pb-Pb dating constraints on the accretion and cooling history of chondrites, *Geochim. Cosmochim. Acta* **71**, 1583-1604

Bunch T.E., Keil K., Huss G.I. (1972), The Landes meteorite, *Meteoritics* **7**, 31

Burkhardt C., Kleine T., Palme H., Bourdon B., Zipfel J., Friedrich J., Ebel D. (2007), ^{182}Hf-^{182}W chronometry of CAIs and tähe age of the solar system, *70th Metsoc*, 5189

Burnett D. S., Wasserburg G. J. (1967), ^{87}Rb-^{87}Sr ages of silicate inclusions in iron meteorites, *Earth Planet. Sci. Lett.* **2**, 397-408

Carlson R.W., Hauri E.H. (2001), Extending the ^{107}Pd-^{107}Ag chronometer to low Pd/Ag meteorites with multicollector plasma-ionization mass spectrometry, *Geochim. Cosmochim. Acta* **65**, 1839-1848

Casanova I. (1992), Osbornite and the Distribution of Titanium in Enstatite meteorites *Meteoritics* **27**, 208

Chen J.H., Wasserburg G.J. (1990), The isotopic composition of Ag in metorites and the presence of [107]Pd in protoplanets, *Geochim. Cosmochim. Acta* **54**, 1729-1743

Choi B.G., Ouyang X., Wasson J.T. (1995), Classification and origin of IAB and IIICD iron meteorites, *Geochim. Cosmochim. Acta* **59**, 593-612

Clayton R.N., Mayeda T.K. (1996) Oxygen isotope studies of achondrites, *Geochim. Cosmochim. Acta* **60**, 1999-2017

Cook D.L., Walker R.J., Horan M.F., Wasson J.T., Morgan J.W. (2004), Pt-Re-Os systematics of group IIAB and IIIAB iron meteorites, *Geochim. Cosmochim. Acta* **68**, 1413-1431

Fittipaldo M.M., Jones R.H., Shearer C.K. (2005), Thermal histories of angrite meteorites: Trace element partitioning among silicate minerals in Angra dos Reis, Lewis Cliff 86010, and experimental analogs, *Meteoritics* **40**, 573

Floran R.J. (1978), Impact melt model for the formation of immiscible silicate and metallic liquids in the Simoudium, Pinnaroo and Hainholz mesosiderites, *Meteoritics* **13**, 461

Floss C., Crozaz, G., McCay G., Mikouchi T., Killgore M. (2003), Petrogenesis of angrites, *Geochim. Cosmochim. Acta* **67**, 4775-4789

Gaffey M.J., Burbine T.H., Piatek J.L., Jennifer L., Reed K.L., Chaky D.A., Bell J.F., Brown R.H. (1993), Mineralogical variations within the S-type asteroid class, *Icarus* **106**, 573

Ghosh A., McSween H.Y. (1998), A thermal model for the differentiation of asteroid 4 Vesta, based on radiogenic heating, *Icarus* **134**, 187-206

Göpel C., Manhes G., Allegre C.J. (1994), U-Pb systematics of phosphates from equilibrated ordinary chondrites, *Earth Planet. Sci. Lett.* 1**21**, 153-171

Greshake A, Clayton R.N., Mayeda T.K. (2001), Dhofar 125: a new Acapulcoite from Oman, *Lunar Planet. Sci.* **XXXII**, 1325

Haack H, Scott E.R.D. (1993), Chemical fractionations in group IIIAB iron meteorites – Origin by dendritic crystallization of an asteroidal core, *Geochim. Cosmochim. Acta* **57**, 3457-3472

Herndon J.M., Herndon M.A. (1977), Aluminum-26 as a planetoid heat source in the early solar system, *Meteoritics* **12**, 459-465

Herpfer M.A., Larimer J.W., Goldstein J.I. (1994), A comparison of metallographic cooling rate methods used in meteorites, *Geochim. Cosmochim. Acta* **58**, 1353

Hewins R.H. (1983), Impact versus internal origins for mesosiderites, *Lunar Planet. Sci.* **XIV**, B257

Hewins R.H., Newsom H.E. (1988), Igneous activity in the early solar system, Univ. of Arizona Press, 73-101

Hidaka H., Yoneda S., Marti K. (2006), Regolith history of the aubritic meteorite parent body revealed by neutron capture effects on Sm and Gd isotopes, *Geochim. Cosmochim. Acta* **70**, 3449-3456

Horan M.F., Smoliar M.I., Walker R.J. (1998), ^{182}W and ^{187}Re-^{187}Os systematics of iron meteorites: Chronology for melting, differentiation and crystallization in asteroids, *Geochim. Cosmochim. Acta* **62**, 545-554

Irving A.J., Kuehner S.M, Rumble, D., Bunch T.E., Wittke J.H. (2005), Unique Angrite NWA 2999: The case for samples from Mercury, *Americ. Geophys. Union* , P51A-0898

Jones J.H., Palme H. (2000), in Origin of the Earth and Moon, R. M. Canup, K. Righter, Eds. *(Univ. Arizona Press, Tucson, AZ)*, 197–216.

Keil K. (1989), Enstatite meteorites and their parent bodies, *Meteoritics* **24**, 195-208

Kelly W.R., Larimer J.W. (1977), Chemical fractionations in meteorites. VIII – Iron meteorites and the cosmochemical history of the metal phase, *Geochim. Cosmochim. Acta* **41**, 93-111

Kleine T., Münker C., Mezger K., Palme H. (2002), Rapid accretion and early core formation in asteroids and the terrestrial planets from Hf-W chronometry, *Nature* **418**, 952-955

Kleine T., Mezger K., Münker C., Palme H., Bischoff A. (2004), ^{182}Hf-^{182}W isotope systematics of chondrites, eucrites and martian meteorites: Chronology of core formation and mantle differentiation in Vesta and Mars, *Geochim. Cosmochim. Acta* **68**, 2935-2946

Kleine T., Mezger K., Palme H., Scherer E., Münker C. (2005a), Early core formation in asteroids and late accretion of chondrite parent bodies: Evidence from ^{182}Hf-^{182}W in CAIs, metal rich chondrites and iron meteorites, *Geochim. Cosmochim. Acta* **69**, 5805-5818

Kleine T., Mezger K., Palme H., Scherer E., Münker C. (2005b), The W isotope composition of eucrite metals – Constraints on the timing and cause of thermal metamorphism of basaltic eucrites, *Earth Planet. Sci. Lett.* **231**, 41-52

Kleine T., Halliday A. N., Palme H., Mezger, K., Markowski A., Touboul M. (2006), Hf-W Ages for the Accretion of Ordinary Chondrite Parent Bodies, *Meteoritics & Planet. Sci.,* **41**, 5299

Kleine T., Bourdon B., Burkhardt C., Irving, A.J. (2008), Hf-W Chronometry of Angrites: Constraints on the Absolute Age of CAIs and Planetesimal Accretion Timescales, *Lunar Planet. Sci.* **XXXIX**, 1391

Kracher A. (1982), Crystallization of a S-saturated Fe, Ni-melt, and the origin of iron meteorite groups IAB and IIICD, *Geophysical Research Letters* **9**, 412-415

Kuehner S.M., Irving A. J., Bunch T. E., Wittke J. H., Hupe G. M. (2006), Coronas and Symplectites in Plutonic Angrite NWA 2999 and Implications for Mercury as the Angrite Parent Body, *Lunar Planet. Sci.* **XXXVII**, 1344

Lee D.C. (2006), A tungsten and molybdenum isotopic study of lodranite GRA95209 and acapulcoite NWA725, and their implications to the early evolution history in the parent body of lodranites and acapulcoites, *Geochim. Cosmochim. Acta* **70,** A347

Lee D.C., Halliday A.N. (1997), Core formation on Mars and differentiated asteroids, *Nature* **388**, 854-857

Lesher C.E. (1990), Decoupling of chemical and isotopic exchange during magma mixing, *Nature* **344**, 235-237

Leya I., Wieler R., Halliday A.N. (2003), The influence of cosmic-ray production on extinct nuclide systems, *Geochim. Cosmochim. Acta* **67,** 529-541

Liu Y.Z., Nyquist L.E., Wiesmann H., Reese Y., Shih C.Y., Takeda H. (2002), Rb-Sr and Sm-Nd ages of plagioclase-diopside-rich material in Caddo County IAB iron meteorite, *Lunar Planet. Sci.* **XXXIII**, 1233

Lorenzetti S., Eugster O., Busemann H., Marti K., Burbine T. H., McCoy T. (2003), History and origin of aubrites, *Geochim. Cosmochim. Acta* **67,** 557-571

Ludwig K. (1991) ISOPLOT: a plotting and regression program for radiogenic isotope data. Version 2.53. *Open File Report* 91–0445. USGS.

Lugmair G.W., Galer S.J.G. (1992), Age and isotopic relationships among the angrites Lewis Cliff 86010 and Angra DOS Reis, *Geochim. Cosmochim. Acta* **56,** 1673-1694

Lugmair G.W., Shukolyukov A. (1998) Early solar system timescales according to 53Mn-53Cr systematics, *Geochim. Cosmochim. Acta* **62,** 2863-2886

Luzius-Lange D., Palme H. (1985), Origin of silicate inclusions in the Landes meteorite, *Meteoritics* **20**, 701

Markowski A., Quitté G., Kleine T., Halliday A.N. (2006), Tungsten isotopic compositions of iron meteorites: Chronological constraints vs. cosmogenic effects, *Earth Planet. Sci. Lett.* **242**, 1-15

Markowski A., Quitté G., Kleine T., Halliday A.N., Bizzarro M., Irving A.J. (2007), Hafnium tungsten chronometry of angrites and the earliest evolution of planetary objects, *Earth Planet. Sci. Lett.* **262**, 214-229

Masarik J. (1997), Contribution of neutron-capture reactions to observed tungsten isotopic ratios, *Earth Planet. Sci. Lett.* **152**, 181-185

McCoy T.J., Ehlmann A.J., Benedix G.K., Keil K., Wasson J.T. (1996), The Lueders, Texas, IAB iron meteorite with silicate inclusions, *Meteoritics & Planetary Science* **31**, 419-422

Meibom A., Haack H., Jensen, S. K., Ulff-Moller F., Rasmussen K. L. (1995), Metallographic Cooling Rates of IAB Iron Meteorites, *Meteoritics* **30**, 544

Merk R., Breuer D., Spohn T., Numerical Modeling of ^{26}Al-Induced Radioactive Melting of Asteroids Considering Accretion, *Icarus* **159**, 183-191

Mikouchi T., McKay G. (2000), Mineralogical Investigation of D'Orbigny: A New Angrite Showing Close Affinities to Asuka 881371, Sahara 99555, and Lewis Cliff 87051, *Lunar Planet. Sci.***XXXII**, 1876

Mikouchi T., McKay G., Le L. (2001), A new angrite Sahara 99555: Mineralogical comparison with Angra dos Reis, Lewis Cliff 86010, Lewis

Cliff 87051, and Asuka 881371 angrites, *Antarctic Meteorites* **XXV**, 74-76

Münker C., Weyer S., Scherer E., Mezger K. (2001) Separation of high field strength elements (Nb, Ta, Zr, Hf) and Lu from rock samples for MC-ICPMS measurements. *Geochem. Geophys. Geosyst.* **2,** 2001GC000183.

Newsom H.E., Sims K.W., Noll P.D., Jaeger W.L., Maehr S.A., Beserra T. B. (1996), The depletion of tungsten in the bulk silicate earth: Constraints on core formation, *Geochimica et Cosmochimica Acta* **60**, 1155-1169

Niemeyer S. (1979a), I-Xe dating of silicate and troilite from IAB iron meteorites, *Geochim. Cosmochim. Acta* **43**, 843-860

Niemeyer S. (1979b), ^{40}Ar-^{39}Ar dating of inclusions from IAB iron meteorites, *Geochim. Cosmochim. Acta* **43**, 1829-1840

Nyquist L.E., Bansal B., Wiesmann H. (1994), Neodymium, strontium and chromium isotopic studies of the LEW86010 and Angra DOS Reis meteorites and the chronology of the angrite parent body, *Meteoritics* **29**, 872-885

Palme H., Rammensee W. (1981), The significance of W in planetary differentiation processes: Evidence from new data on eucrites, *Proc. Lunar Planet. Sci.* **12B**, 949-964

Palme H., Hutcheon I.D., Kennedy A.K., Sheng Y.J., Spettel B. (1991), Trace element distribution in minerals from a silicate inclusion in the Caddo IAB iron meteorite, *Lunar Planet. Sci.* **XXII**, 1015

Petaev, M. I., Jacobsen S.B. (2004), Differentiation of metal-rich meteoritic parent bodies: I. Measurements of PGEs, Re, Mo, W, and Au in meteoritic Fe-Ni metal, *Meteoritics & Planet. Sci.* **39**, 1685-1697

Petitat, M., Kleine, T., Touboul M., Bourdon B., Wieler R. (2008), Hf-W Chronometry of Aubrites and the Evolution of Planetary Bodies, *Lunar Planet. Sci.* **XXXIX**, 2164

Podosek F. A. (1970), Dating of meteorites by the high temperature release of iodine correlated ^{129}Xe, *Geochim. Cosmochim. Acta* **34**, 341-366

Polnau E., Lugmair G.W. (2001), Mn-Cr Isotope Systematics in the Two Ordinary Chondrites Richardton (H5) and Ste. Marguerite (H4), *Lunar Planet. Sci.* **XXXII**, 1527

Qin L., Dauphas N., Wadhwa M., Janney P. E. (2006), High Precision W Isotope Measurements of Iron meteorites, *Meteoritics & Planet. Sci.* **41**, 5267

Quitté G., Birck J. L., Allègre C. J. (2000), Chronology of Basaltic Achondrites, Irons, and Stony-Iron Meteorites as Inferred by Hafnium-Tungsten Systematics, *Meteoritics & Planet. Sci.* **35**, A131

Quitté G., Birck J.L., Allegre C.J. (2004), Stony-iron meteorites: History of the metal phase according to tungsten isotopes, *Geochim. Cosmochim. Acta* **69**, 1321-1332

Quitté G., Birck J.L. (2004), Tungsten isotopes in eucrites revisited and the initial ^{182}Hf/^{180}Hf of the solar system based on iron meteorite data, *Earth Planet. Sci. Lett.* **219**, 201-207

Quitté, G., Latkoczy, C., Halliday, A. N., Schönbächler, M., Günther, D. (2005), Iron-60 in the Eucrite Parent Body and the Initial ^{60}Fe/^{56}Fe of the Solar System, *Lunar Planet. Sci.* XXXVI, 1827

Rasmussen K.L. (1989), Cooling rates of IIIAB iron meteorites, *Icarus* **80**, 315-325

Scherstén A., Elliot T., Hawkesworth C., Russel S., Masarik J. (2006), Hf-W evidence for rapid differentiation of iron meteorite parent bodies, *Geochim. Cosmochim. Acta* **241**, 530-542

Schoenberg R., Kamber B.S., Collerson K.D., Eugster O. (2002), *Geochim. Cosmochim. Acta* **66**, 3151-3160

Schulz T., Münker C., Mezger K., Palme H. (2007), The tungsten isotope composition of winonaites – Evidence for late stage equilibration on the Winonaite parent body, *Lunar Planet. Sci.* **XXXVIII**, 1760

Shen J.J., Papanastassiou D.A., Wasserburg G.J. (1996), Precise Re-Os determinations and systematics of iron meteorites, *Geochim. Cosmochim. Acta* **60**, 2887-2900

Shukolyukov A., Lugmair G.W. (1993), Live iron-60 in the early solar system, *Science* **259**, 1138-1142

Shukolyukov A., Lugmair G.W. (2004), Manganese-chromium isotope systematicsof enstatite meteorites, *Geochim. Cosmochim. Acta* **68**, 2875-2888

Smoliar M.I., Walker R.J., Morgan J.W. (1996), Re-Os ages of group IIA, IIIA, IVA, and IVB iron meteorites, *Science* **271**, 1099-1102

Srinivasan G., Goswami J.N., Bhandari N. (1999), 26Al in Eucrite Piplia Kalan : plausible heat source and formation chronology, *Science* **284**, 5418

Stewart B., Papanastassiou D.A., Wasserburg G.J. (1996), Sm-Nd systematics of a silicate inclusion in the Caddo IAB iron meteorite, *Earth Planet. Sci. Lett.* **143**, 1-12

Sugiura N., Hoshino. H. (2003), Mn-Cr chronology of five IIIAB iron meteorites, *Meteoritics & Planetary Science* **38**, 117-144

Takeda H., Baba T., Saiki K., Otsuki M., Ebihara M. (1993), A Plagioclase-Augite Inclusion in Caddo County: Low-Temperature Melt of Primitive Achondrites, *Meteoritics & Planetary Science* **28**, 447

Takeda H., Otsuki M., Yamaguchi A., Miyamoto M., Otsuki M., Tomobuchi M., Hiroi T. (1994), Inhomogenous distribution of materials in lodranites-acapulcoites and IAB irons and and their common formation processes, *Lunar Planet. Sci.* **XX**, 1375

Takeda H. (2000), Mineralogy, petrology, chemistry, and ^{39}Ar-^{40}Ar and exposure ages of the Caddo County IAB iron: evidence for early partial melt segregation of a gabbro area rich in plagioclase-diopside, *Geochim. Cosmochim. Acta* **64**, 1673-1694

Taylor T.J. (1992), Core formation in asteroids, *Journal of Geophs. Research* **97**, 717-726

Taylor T.J., Keil K., McCoy T., Haack H., Scott E.R.D. (1993), Asteroid differentiation – pyroclastic volcanism to magma oceans, *Meteoritics* **28**, 34-52

Touboul M., Kleine T., Bourdon B., Irving A.J., Zipfel J. (2007), Hf-W evidence for rapid accretion and fast cooling of the Acapulcoite parent body, *Lunar Planet. Sci.* **XXXVIII**, 2317

Trieloff M. Jessberger E.K., Fieni C. (2001), Comment on ^{40}Ar-^{39}Ar age of plagioclase from Acapulco meteorite and the problem of systematic errors in cosmochronology, *Earth Planet. Sci. Lett.* **190**, 267-269

Trieloff M., Jessberger E.K., Herrwerth I., Hopp J., Fieni C., Ghelis M., Bourot D.M., Pellas P. (2003), Structure and thermal history of the H-chondrite parent asteroidrevealed by thermochronometry, *Nature* **422**, 502-506

Urey H.C. (1955), The cosmic abundances of Potassium, Uranium and Thorium and the heat balances of the Earth, Moon and Mars, *Proceed. Of the Nat. Academy of Sci. of Americ.* **41**, 127-144

van Orman J.A., Kleine T., Bourdon B. (2008), Closure temperature of the ^{182}Hf-^{182}W system in chondrites: a model, *Lunar Planet. Sci.* **XXXIX**, 1015

Vockenhuber C., Oberli F., Bichler M., Ahmad I., Quitté G., Meier M., Halliday A.N., Lee D.C., Kutschera W., Steier P., Gehrke R.J., Helmer R.G. (2004), New half-live measurement of ^{182}Hf; Improved chronometer for the early solar system, *Phys. Rev. Lett.* **93**, 172-501

Vogel N., Renne P.R. (2008), ^{40}Ar-^{39}Ar dating of plagioclase grain size separates from silicate inclusions in IAB iron meteorites and implications for the thermochronological evolution of the IAB parent body, *Geochim. Cosmochim. Acta* **72**, 1231-1255

Wadhwa M., Lugmair G.W. (1996), Age of the eucrite caldera from convergence of long-lived and short-lived chronometers, *Geochim. Cosmochim. Acta* **60**, 4889-4893

Wadhwa M., Amelin Y., Bogdanovski O., Shukolyukov A., Lugmair G.W. (2005), High precision relative and absolute ages for Asuka 881394, a unique and ancient basalt, *Lunar Planet. Sci.* **XXXVI**, 2126

Wasson J.T. (1972), Parent-body models for the formation of iron meteorites, *Proc. Intl. Geol. Cong.* **24**, 161-168

Wasson J.T., Willis J., Wai C.M., Kracher A. (1980), Origin of iron meteorite groups IAB and IIICD, *Z. Naturforsch.* **35a**, 781-795

Wasson J.T, Richardson J.W. (2001), Fractionation trends among IVA iron meteorites: contrasts with IIIAB trends, *Geochim. Cosmochim. Acta* **65**, 951-970

Wasson J.T., Kallemeyn G.W. (2002), The IAB iron-meteorite complex: A group, five subgroups, numerous grouplets, closely related, mainly formed by crystal segregation in rapidly cooling melts, *Geochim. Cosmochim. Acta* **66**, 2445-2473

Wlotzka F., Jarosewich E., Mineralogical and chemical composition of silicate inclusions in the El Taco, Campo del Cielo, iron meteorite, *Smithsonian Contrib. Earth Sci.* **19**, 104-125

Yin Q.Z., Jacobsen S.B.Yamashita K., Blichert-Toft J., Telouk P., Albarede F. (2002), Ashort timescale for terrestrial planet formation from Hf-W chronometry of meteorites, *Nature* **418**, 949-952

Yin Q.Z., Jacobsen S.B. (2003), The initial ^{182}W/^{183}W and ^{182}Hf/^{180}Hf of the solar system and a consistend chronology with Pb-Pb ages, *Lunar Planet. Sci. XXXIV*, 1857

Zipfel J., Palme H., Kennedy A.K., Hutcheon I.D. (1995), Chemical composition and origin of the Acapulco meteorite, *Geochim. Cosmochim. Acta* **59**, 3607-3627

Danksagung

Curriculum Vitae

Name:	Toni Schulz
Born:	21.06.1975 in Dinslaken, Germany
Nationality:	German
Marital status:	single
Address:	Sebastianstr. 28/30
	53145 Bonn
	Germany
e-mail:	toni.schulz@o2online.de

1981 - 1984	primary school
1984 - 1990	secondary school
1990 - 1994	Abitur (Gottfried-Wilhelm Leibniz Gesamtschule Duisburg)
1994 - 1996	extended voluntary social year in the Tannenhof psychiatry in Remscheid

Scientific career:

1997 - 2004	Study of Mineralogy and Chemistry (no degree) at the Albertus-Magnus Universität zu Köln
2004	Diploma in Mineralogy:

- Herkunftsanalytische Bestimmung von Wüstenmeteoriten
  (Classification of desert meteorites)

2005 - 2008	PhD thesis:

- Differentiation of asteroids in the early solar

  system from Hf-W systematics

Ich versichere, dass ich die von mir vorgelegte Dissertation selbständig angefertigt, die benutzten Quellen und Hilfsmittel vollständig angegeben und die Stellen der Arbeit – einschließlich Tabellen, Karten und Abbildungen –, die anderen Werken im Wortlaut oder dem Sinn nach entnommen sind, in jedem Einzelfall als Entlehnung kenntlich gemacht habe; dass diese Dissertation noch keiner anderen Fakultät oder Universität zur Prüfung vorgelegen hat; dass sie – abgesehen von unten angegebenen Teilpublikationen – noch nicht veröffentlicht worden ist sowie, dass ich eine solche Veröffentlichung vor Abschluss des Promotionsverfahrens nicht vornehmen werde. Die Bestimmungen der Promotionsordnung sind mir bekannt. Die von mir vorgelegte Dissertation ist von Prof. Herbert Palme betreut worden.

Toni Schulz